UNIVERSITÀ DI PARMA

UNIVERSITA' DEGLI STUDI DI PARMA

DOTTORATO DI RICERCA IN

Scienze Medico-Veterinarie

CICLO XXXVII

***In vitro* and *in vivo* assessment of thiosemicarbazones against *Toxoplasma gondii* infection**

Coordinatore:
Chiar.mo Prof. Gaetano Donofrio

UNIVERSITÀ DI PARMA Firmato digitalmente da Gaetano Donofrio Data: 09.01.2025 12:36:39 CET

Tutor:
Chiar.ma Prof.ssa Laura Helen Kramer

UNIVERSITÀ DI PARMA Firmato digitalmente da Laura Helen Kramer Data: 09.01.2025 13:55:13 CET

Dottoranda: Manuela Semeraro

Anni Accademici 2021/2022 – 2023/2024

Table of contents

1 Abstract 6

2 Introduction 9

***2.1 Biology of* Toxoplasma gondii** 9

2.1.1 Classification 9

2.1.2 Structure and life cycle 10

2.1.2.1 Life cycle in the definitive host: the cat 12

2.1.2.2 Life cycle in the intermediate hosts 13

2.2 Toxoplasmosis: sources of infection 14

2.2.1 Infection through tissue cysts 14

2.2.2 Infection through oocysts 15

2.2.3 Infection through tachyzoites 16

2.3 Population structure of *T. gondii* 16

2.3.1 Genotypes, their geographic distribution and virulence 17

2.4 Virulence factors of *T. gondii* and host-parasite relationship 18

2.4.1 Virulence factors 18

2.4.2 The immune response to *T. gondii* and immuno-prophylaxis 19

2.4.3 Alterations in host signaling and immune evasion 21

2.5 Toxoplasmosis in animals and humans 21

2.5.1 Infection in domestic animals 21

2.5.2 Infection in wild animals 22

2.5.3 Toxoplasmosis in humans 23

2.5.3a Toxoplasma gondii and human health: pathogenesis 23

2.5.3b Congenital toxoplasmosis 24

2.6 Challenges and limitations of current toxoplasmosis treatments 25

2.7 Novel treatments against toxoplasmosis 27

2.7.1 Calcium-dependent protein kinase inhibitors, endochin-like quinolone and natural compounds 27

2.7.2 Thiosemicarbazones and their metal complexes 29

2.8 Mechanisms of drug resistance in *T. gondii* 30

2.9 Techniques commonly used for drug screening 31

2.9.1 Cell cytotoxicity assays *in vitro* 31

2.9.2 *In vitro* efficacy assessment of drugs on *T. gondii* 32

2.9.2a Morphology assay: Diff-Quick May Grunwald and Giemsa staining 33

2.9.2b Assay using reporter strains: T. gondii β-gal assay 33

2.9.2c Real-time Polymerase Chain Reaction 33
2.9.3 Tools to investigate drug mode of action and potential targets 34
2.9.4 Immune and embryonic toxicity assessment of the compounds 35
2.9.4a Evaluation of the effect of the compounds on the stimulation of the host immune cells 35
2.9.4b Evaluation of the toxicity on embryonic stages of fish 36
2.9.5 *In vivo* efficacy assessment of drugs on *T. gondii* 36
3 *In vitro* and *in vivo* assessment of thiosemicarbazones against *Toxoplasma gondii* infection 38
4 Materials and Methods 39
4.1 Host cells and parasites 39
4.1.1 Cell maintenance 39
4.1.2 Cell counting and seeding 39
4.1.3 Parasite maintenance 40
4.2 Compounds 40
4.2a Copper complexes and their thiosemicarbazone ligands 41
4.2b Gold complexes and their thiosemicarbazone ligands 42
***4.3 In vitro* toxicity evaluation of thiosemicarbazones on host cells** 42
4.3.1. Alamar Blue assay 42
4.4 *In vitro* efficacy assessment of thiosemicarbazones on *Toxoplasma gondii* 43
4.4.1 Diff-Quick May Grunwald – Giemsa staining 43
4.4.2 *T. gondii* β-galactosidase viability assay 44
4.4.3 Viability assay of *T. gondii* wild-type (WT) and clones "adapted" to the treatment 45
4.5 Discovering the mechanism of action of the drugs 45
4.5.1 Embedding samples for Transmission Electron Microscopy (TEM) 45
4.5.2 Tetramethylrhodamine Ethyl Ester (TMRE) assay 47
4.5.3 Long-term *in vitro* treatment 47
4.5.4 Differential Affinity Chromatography (DAC) 49
4.5.5 Proteomics 50
4.6 Evaluation of the effect of thiosemicarbazones on host immune cells and evaluation of the toxicity in a model organism 53
4.6.1 Assessment of viability of murine splenocytes after treatment with C3 and C4 *in vitro* (AlamarBlue) 53
4.6.2 Effects of C3 and C4 on early zebrafish (*Danio rerio*) embryo development 54
4.7 *In vivo* efficacy of the compounds in the murine model of cerebral toxoplasmosis 55
4.7.1 Drug stock preparation 55

4.7.2 Thiosemicarbazones efficacy assessment in CD1 mice orally infected with TgShSp1 oocysts 56
4.7.2a DNA extraction from mice organs 56
4.7.2b Parasite load quantification by Real-time PCR (529 bp gene detection) 57
4.7.2c Histopathology of mice brains 57
4.*7.3* Assessment of susceptibility of murine splenocytes to C3 and C4 *in vivo*: measurement of viability and proliferation 58
5. Results 58
5.1 Toxicity of thiosemicarbazones on host cells *in vitro* 58
5.1a AlamarBlue assay with copper complexes and their thiosemicarbazone ligands 58
5.1b AlamarBlue assay with gold complexes and their thiosemicarbazone ligands 59
5.2 *In vitro* efficacy of thiosemicarbazones on *T. gondii* 60
5.2a Efficacy of copper complexes and their thiosemicarbazone ligands on *T. gondii* using β-galactosidase assay 60
5.2b Efficacy of gold complexes on *T. gondii* using β-galactosidase assay 61
5.2c Efficacy of gold complexes and their thiosemicarbazone ligands on *T. gondii* ME49 wild-type and adapted clones to the treatment 63
5.3 Mechanism of action of C3 and C4 compounds 64
5.3a TEM results 64
5.3b TMRE Results 68
5.3c DAC results 69
5.3d Long term treatments and generation of clones of drug adapted *T. gondii* tachyzoites 73
5.3e Proteomic analysis analysis of *T. gondii* ME49 clones recovered after *in vitro* adaptation to C3 and C4 74
5.4 Effect C3 and C4 on the stimulation of the host immune cells and evaluation of the toxicity in a model organism 78
5.4a Assessment of viability of murine splenocytes after treatment with C3 and C4 *in vitro* 78
5.4b Effects of C3 and C4 on early zebrafish embryo development 79
5.5 *In vivo* efficacy of the compounds in a murine model of cerebral toxoplasmosis 81
5.5a Parasite load quantification by Real-time PCR 81
5.5b Histopathology of mice brains 82
5.6 Viability and proliferation of murine splenocytes after treatment with C3 and C4 *in vivo* 84
5.6.1 Measurement of viability and proliferation after treatment *in vivo* 84
5.6.2 Measurement of viability and proliferation after infection and treatment *in vivo* 85
6. Discussion 86
7. References 95
8. Websites 113

9. Appendix..... 115
10. Aknowledgement..... 117

1 Abstract

Toxoplasma gondii is a globally widespread apicomplexan parasite, with domestic cats (or felines in general) as definitive hosts and many warm-blooded animals, including humans, as intermediate hosts. The parasite has three infectious stages: tachyzoites, bradyzoites and oocysts. After infection (usually through ingestion of tissue cysts containing bradyzoites), cats shed oocysts in the environment which sporulate and become infectious after several days. Intermediate hosts can be infected through the ingestion of food or water contaminated with sporulated oocysts or by ingestion of tissue cysts.

T. gondii infections are common in humans, livestock, and companion animals, but clinical disease is rare. Over 80% of immunocompetent individuals, especially in Europe and North America, experience no symptoms. In the remaining cases, mild symptoms like fever and lymphadenopathy may occur. However, in immunocompromised individuals, toxoplasmosis often results from the reactivation of a chronic infection and can be life-threatening. The primary organs affected by *T. gondii* include the brain (toxoplasmic encephalitis), heart (myocarditis), lungs (pulmonary toxoplasmosis), eyes and pancreas. Congenital toxoplasmosis is another significant concern, occurring in pregnant women, where the severity of outcomes depends on the stage of pregnancy during maternal infection.

Treatment options for toxoplasmosis are limited, with the folate pathway being the primary target of anti-*Toxoplasma* drugs, such as pyrimethamine and sulfadiazine. Other drugs, such as atovaquone, spiramycin, azithromycin, and clindamycin are also used as second-line drugs.

Unfortunately, current treatment regimens often cause side effects such as myelotoxicity (e.g., leukopenia and thrombocytopenia), rash, nausea, or vomiting, which can necessitate discontinuing therapy or, more commonly, lead to poor patient compliance. In addition, a key challenge in treating *T. gondii* infections is that, while existing drugs can control acute toxoplasmosis, no approved therapy is available to eliminate the tissue cysts that cause chronic infections and the risk reactivation.

For this reason, new compounds have been recently optimized and tested to develop new therapies that address all these issues. Thiosemicarbazones (TSCs) are organosulfur compounds which have been shown to exhibit very good activity against *T. gondii*.

The present thesis has focused on evaluating the activity of three gold(III) complexes with salicyl-TSC ligands against *T. gondii in vitro* and *in vivo*. Among the compounds, one gold complex (C3) and its corresponding salicyl-TSC ligand (C4) demonstrated promising inhibition constants *in vitro* against the parasite (nanomolar range: C3 IC_{50} = 100 nM; C4 IC_{50} = 30 nM) and were selected for further analyses. Interestingly, after several days of *in vitro* treatment, *T. gondii* tachyzoites quickly adapted to these

compounds, suggesting that the inhibitory effects of C3 and C4 were transient. To explore the mode of action of the drugs and the mechanisms behind the adaptation to the treatment, differential affinity chromatography coupled with mass spectrometry and proteomics (DAC-MS-proteomics) was employed. Initially, DAC-MS-proteomics was used to identify *T. gondii* tachyzoite proteins that interact with C3 and C4. Subsequently, DAC-MS-proteomics was carried out to compare the protein expression profiles of six *T. gondii* tachyzoite clones adapted to C3 and C4 treatment with those of non-adapted tachyzoites.

DAC results suggested that C3 and C4 may interfere with protein biosynthesis and that adaptation to the treatment may be associated with the upregulated expression of tachyzoite transmembrane proteins and transporters, suggesting that the *in vitro* drug tolerance in *T. gondii* might be due to reversible, non-drug specific stress-responses mediated by phenotypic plasticity.

Furthermore, the potential side effects of the compounds were investigated, especially regarding their impact on the immune system and embryonic development. Since neither compound exhibited any immunosuppressive effects on murine splenocytes, *in vivo* experiments were performed in a murine model of cerebral toxoplasmosis. However, the congenital murine model of toxoplasmosis was excluded from further studies due to the toxicity observed in the zebrafish embryo development model. *In vivo* efficacy of the compounds in the murine model of cerebral toxoplasmosis was evaluated by performing Real-time PCR on DNA extracted from the organs (brain, heart, and eyes) of mice after euthanasia. The analysis targeted the 529 bp gene of *T. gondii*, comparing parasite loads between infected, untreated mice and those treated with C3 and C4 compounds.

The results from quantification of the parasite burden after *in vivo* treatments showed that neither compound was effective in reducing parasite burdens in the brain and eyes, while there is a statistically significant decrease of parasite burden in the heart after C4 treatment.

This lack of efficacy in the brain and in the eyes is likely due to the inability of these compounds, like many other drugs tested for toxoplasmosis treatment, to cross the blood-brain barrier (BBB). Further studies should explore alternative routes of administration, which may enhance the compounds' activity, and investigate their pharmacokinetics to assess how they are metabolized. This would help determine whether dosage adjustments are feasible. Another possibility could be testing these compounds in combination with standard therapies like sulfadiazine or pyrimethamine to potentially improve treatment outcomes.

In summary, *T. gondii,* the parasite responsible for toxoplasmosis, continues to cause significant challenges in treatment. Current therapies manage acute infection but have limitations, including

incomplete parasite elimination and harmful side effects. Recent research focuses on developing new compounds, such as thiosemicarbazones and small molecules, which show promise in laboratory studies. These new drugs could offer better efficacy, reduced toxicity, and broader action, addressing the shortcomings of current treatments. This underlines the importance and continued necessity of studies like this to drive the discovery of more effective treatment options.

2 Introduction

2.1 Biology of Toxoplasma gondii

2.1.1 Classification

Toxoplasma gondii is a globally widespread apicomplexan parasite, with felines, particularly domestic cats, serving as definitive hosts, while a wide range of warm-blooded animals, including humans, act as intermediate hosts.

The taxonomic classification of *T. gondii* is reported in Table 1.

Table 1. Taxonomic classification of *T. gondii* (Dubey, 2021a).

Phylum	Apicomplexa	Levine, 1970
Class	Sporozoasida	Leukart, 1879
Subclass	Coccidiasina	Leukart, 1879
Order	Eimeriorina	Leger, 1911
Family	Toxoplasmatidae	Biocca, 1956
Genus	*Toxoplasma*	Nicolle and Manceaux, 1909
Species	*Toxoplasma gondii*	Nicolle and Manceaux, 1909

T. gondii is the only existing species, named "gondii" because it was isolated for the first time from the African rodent *Ctenodactylus gundi*. The life cycle of *T. gondii* was described for the first time in 1970 (Dubey and Frenkel, 1972). In that year, *T. gondii*, a parasite previously known as able to parasitize extra-intestinal tissues of virtually all warm-blooded hosts, was found to also be an intestinal coccidian of cats and to have an *Isospora- like* oocyst. This finding was a breakthrough in medical and veterinary science and led to the discovery of several new taxa of economically important *Toxoplasma*-like parasites (i.e. *Neospora caninum*, *Sarcocystis* spp.) and the description of their life cycles.

Historically, *T. gondii* probably originated as a coccidian parasite of cats with a fecal-oral cycle. With domestication, it adapted its transmission by several modes, including transmission by carnivorism, and transplacentally. There are three infectious stages of *T. gondii*: the tachyzoites, the bradyzoites, and oocysts, all linked in a complex life cycle (Dubey, 2021a) (Figure 1).

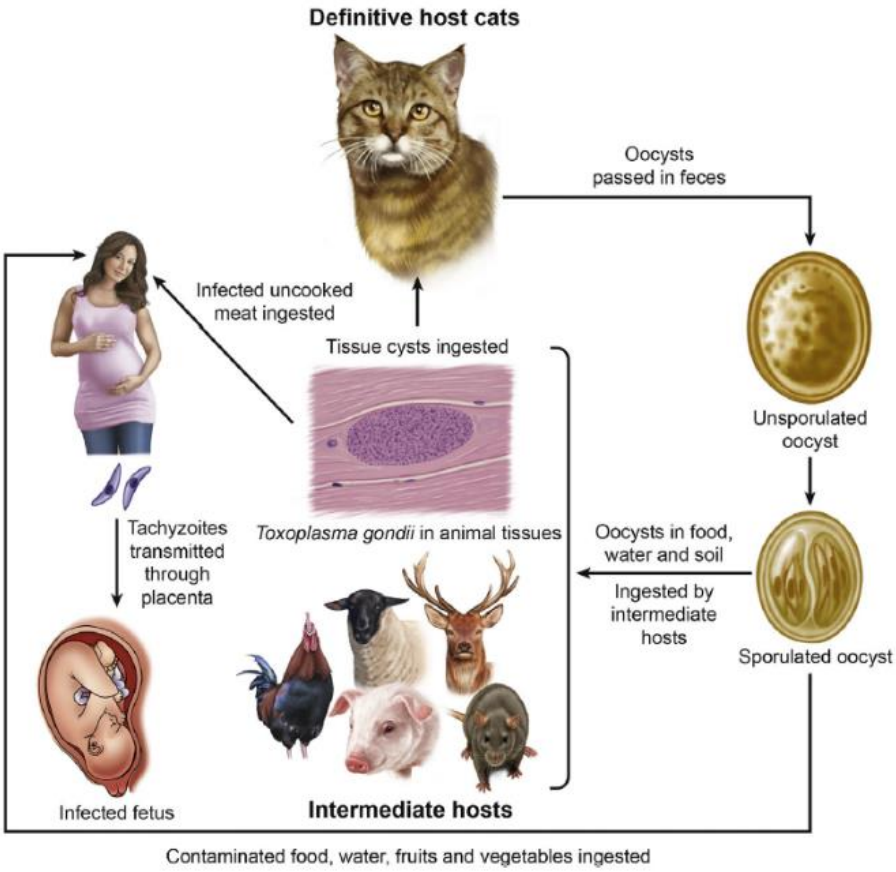

Figure 1. Life cycle of *T. gondii* (Taken from: Lindsay and Dubey, 2020).

2.1.2 Structure and life cycle

Tachyzoites (táchos = *speed* in Greek) represent the proliferative and rapid stage of the parasite. It is crescent-shaped, having a size of approximately 2 × 6 µm, with a pointed anterior (conoidal) end and rounded posterior end. The tachyzoite has a complex structure comprised of several organelles and inclusion bodies including a pellicle (outer covering), cytoskeleton or inner membrane complex (IMC), subpellicular microtubules, apical rings, polar rings, a conoid, secretory organelles (rhoptries, micronemes, dense granules), a mitochondrion, a Golgi complex, ribosomes, rough and smooth endoplasmic reticula, nucleus and an apicoplast.

The nucleus is usually situated toward the central area of the tachyzoite. It consists of a nuclear envelope with pores, clumps of chromatin and a centrally located nucleolus. The mitochondrion is branched, nearly as long as the whole tachyzoite and has bulbous cristae (Dubey, 2021a).

Tachyzoite motility is driven through the actin-myosin motor complex anchored to the IMC and with this system the parasite penetrates host cells. The mechanical events involved in zoite attachment and penetration include (i) gliding of the zoite; (ii) probing of the host cell with the zoite's conoidal tip; (iii)

indenting the host cell plasmalemma; (iv) forming a moving junction that moves posteriorly along the zoite as it penetrates the host cell; and (v) partially exocytosing micronemes, rhoptries and dense granules (Dubey, 2021a).

T. gondii can penetrate many different nucleated cell types from a wide range of hosts, indicating that the biochemical receptors involved in attachment and penetration are probably common to most animal cells. Following penetration of the host cell, tachyzoites are quickly surrounded by a membrane derived from the host-cell plasmalemma that becomes the parasitophorous vacuole membrane (PVM). Inside the cells, tachyzoites start to divide by endodyogeny, an asexual process of reproduction in which two progeny form within the parent parasite. Tachyzoites continue to proliferate inside the cells till their rupture, that allows the infection of other cells. After many divisions and after the activation of the host immune response, tachyzoites convert into a slowly replicating stage, called bradyzoite (brady = *slow* in Greek), that form intracellular tissue cysts. Inside the cyst, the parasites remain alive, viable and replicate slowly. If the host's immune defenses are compromised for any reason, the parasites begin to replicate more aggressively, eventually leading to cyst rupture. This allows the infectious bradyzoites to escape, enter the circulatory system, transform into tachyzoites and infect other cells and tissues, causing necrosis and organ damage.

Tissue cysts can have different sizes, depending on the age of the parasites: young tissue cysts may be 5 µm in diameter and contain only two bradyzoites, while older ones may contain thousands. The tissue cyst wall is elastic and less than 0.5 µm thick and it contains chitin-like polysaccharides and glycoproteins. Bradyzoites have only some differences in the structure from the tachyzoites, since the nucleus is situated toward the posterior end, while in the tachyzoite is more centrally located. In addition, bradyzoites are less susceptible to destruction by proteolytic enzymes compared to tachyzoites (Dubey, 2021a).

Experimental infections have shown that after inoculation, tissue cysts begin to form after three days. Their location is dependent on the host: in fact, cysts have been found in lungs, liver and kidneys, but are more prevalent in muscular and neural tissues, including the brain, eye, skeletal and cardiac muscle (Dubey, 2021a).

2.1.2.1 Life cycle in the definitive host: the cat

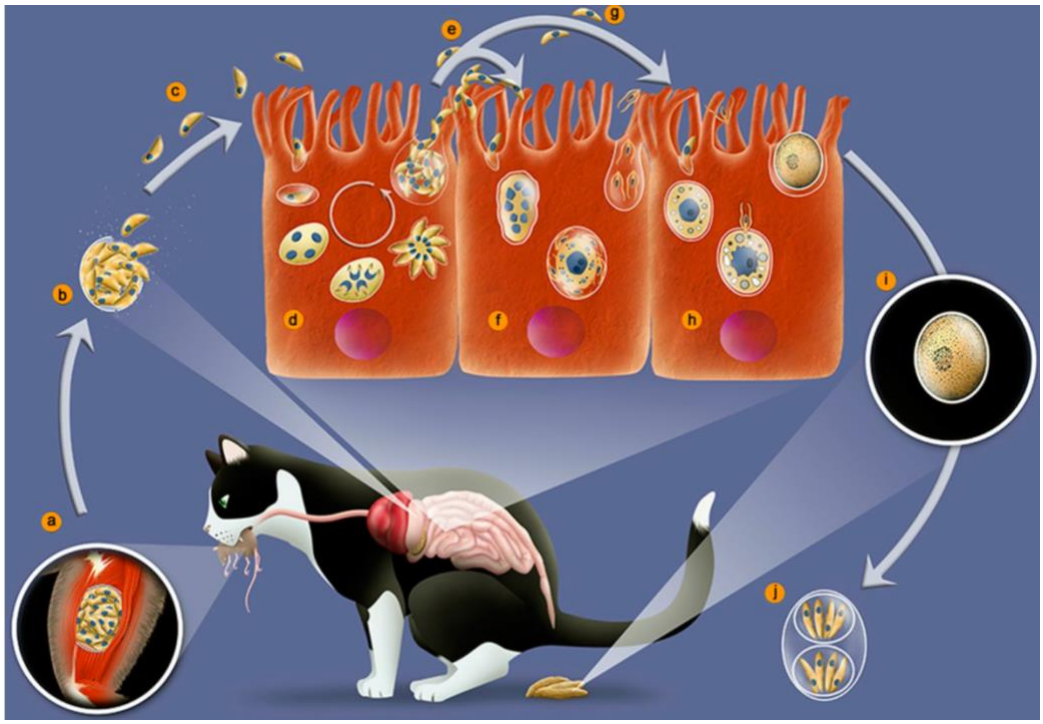

Figure 2. Life-cycle of *T. gondii* in cat. **a)** Ingestion of prey containing tissue cysts. **b)** The cyst wall is digested in the stomach and intestines, liberating bradyzoites. **c)** Bradyzoites invade epithelial cells of the intestine. **d)** In the enterocytes bradyzoites divide by schizogony giving rise to merozoites. **e)** Merozoites differentiate into microgamonts, or macrogametes **(f)**. **g)** Fertilization gives rise to an unsporulated oocyst excreted with cat feces **(h)**. **i)** Sporulation occurs and generates two sporocysts with four sporozoites each **(j)** (Taken from: Attias et al., 2020).

After ingestion of bradyzoites or oocysts, cats can shed oocysts in the environment. Prepatent periods and frequency of oocyst excretion vary according to the stage of *T. gondii* ingested. Prepatent periods are 3-10 days after ingesting tissue cysts and are more than 18 days after ingesting oocysts, irrespective of the dose. On the other hand, the prepatent period after ingesting tachyzoites may vary. Fewer than 50% of cats shed oocysts after ingesting tachyzoites or oocysts, whereas nearly all cats shed oocysts after ingesting tissue cysts (Dubey, 2021a). Tachyzoites, indeed, are very rarely infectious for cats.

After reaching the stomach, the tissue cyst wall is disintegrated by proteolytic enzymes, releasing bradyzoites into the intestine. There, they convert to tachyzoites and begin replicating through multiple generations via both asexual (schizogony) and sexual (gametogony) reproduction (Figure 2).

The zygote is enclosed in a protective wall containing cytoplasm and a large central nucleus. The infected epithelial cells then disintegrate, releasing the oocysts into the intestinal lumen, which are excreted into the environment via feces. The oocysts measuring 10 x 12 µm are shed as non-infectious, they need to sporulate. Sporulation requires 1–5 days, depending on external environmental conditions

like temperature, humidity and oxygenation. Sporulated oocysts contain two sporocysts, each containing four sporozoites formed by endodyogeny, resulting in each oocyst containing eight sporozoites (Dubey, 2021a).

2.1.2.2 Life cycle in the intermediate hosts

Toxoplasma gondii is usually transmitted to intermediate hosts through the ingestion of sporulated oocysts found in contaminated food or water or by ingestion of tissue cysts.

In case of the ingestion of sporulated oocysts, sporozoites excyst, penetrate enterocytes and goblet cells of intestinal epithelium and traverse to the lamina propria. Several studies have suggested that cell traversal of sporozoites to the lamina propria takes place within 6-12 hours post-infection (p.i.) and is driven by the production and release of several dense granule proteins (GRA)s (Dubey, 1997; Tartarelli et al., 2020; Speer and Dubey, 1998). Twelve hours post-infection, sporozoites have divided into two tachyzoites and by six days p.i., bradyzoites and tissue cysts are formed (Dubey, 2021a).

The parasite may spread first to mesenteric lymph nodes and then to distant organs by invasion of lymphatic system and blood and can multiply in virtually any cell in the body.

All extracellular forms of the parasite are directly affected by host immune response, but intracellular forms are not. In fact, immunity does not eradicate infection and tissue cysts can persist for several years after acute infection, potentially for all the life of the subject (Hill and Dubey, 2014).

In immunocompromised patients, bradyzoites can reconvert into replicating tachyzoites, thereby reactivating the infection and potentially causing serious tissue damage in critical organs (Augusto et al., 2021). Pathogenicity of *T. gondii* is determined by the virulence of the strain and the susceptibility of the host species. *T. gondii* strains may vary in their pathogenicity in each host. Certain strains of mice are more susceptible than others and the severity of infection in individual mice within the same strain may vary. Mice of any age are susceptible to clinical *T. gondii* infection. However, adult rats do not become ill, while young rats can die of toxoplasmosis. Adult dogs, like adult rats, are resistant, whereas puppies are fully susceptible to clinical toxoplasmosis. Certain species are genetically resistant to clinical toxoplasmosis. Cattle and horses are among the hosts more resistant to clinical toxoplasmosis, whereas certain marsupials and New World monkeys are highly susceptible to *T. gondii* infection (Hill et al., 2005).

2.2 Toxoplasmosis: sources of infection

As mentioned above, intermediate hosts, including humans, can be infected *via* different pathways. These include (i) ingestion of water, vegetables and fruits contaminated with viable sporulated oocysts, shed in the feces by cats (Figure 3d); (ii) ingestion of raw or undercooked meat containing viable tissue cysts (Figure 3f); (iii) congenital transmission from the mother through the placenta (Figure 3h); (iv) blood transfusion; (v) organ transplantation, where the organs may contain cysts or tachyzoites (Figure 3j). Oocysts can also survive in oysters and mussels retaining its infectivity. Ingestion of non- pasteurized milk or milk products is a potential (but uncommon) source of transmission, especially goat milk (Attias et al., 2020).

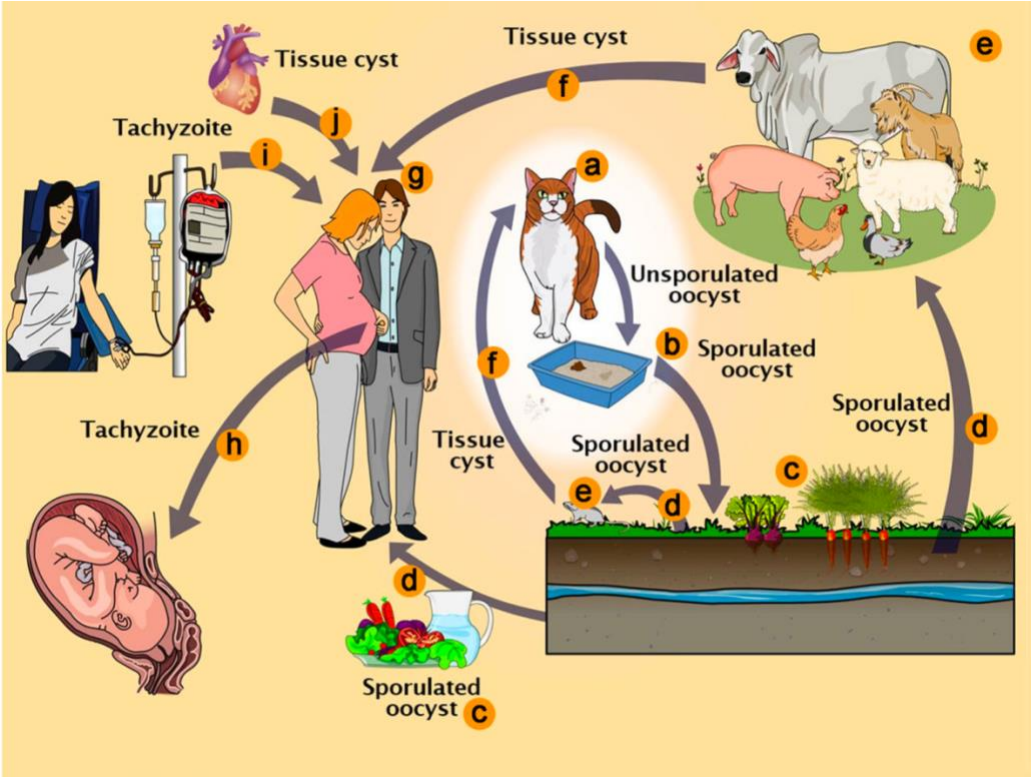

Figure 3. *T. gondii* pathways of transmission. **a)** Feline definitive host (cat). **b)** Unsporulated oocysts in cat feces. **c)** Food contaminated with sporulated oocysts. **d)** Oocysts may be ingested by intermediate hosts *via* water or raw vegetables. **e)** Intermediate hosts (e.g. cattle, sheep, poultry and swine). **f)** Ingestion of tissue cysts in uncooked meat. **g)** Intermediate hosts (humans). **h)** Tachyzoites transmitted through the placenta to the fetus. **i)** Transmission by blood transfusion and organ transplant (**j**). (Taken from: Attias et al., 2020).

2.2.1 Infection through tissue cysts

Tissue cysts play a crucial role in the life cycle of *T. gondii*, as they represent the parasite's dormant stage, awaiting consumption by animals, including humans. In Europe, consuming undercooked

infected meat is a significant risk factor, accounting for 30–63% of infections (Cook et al., 2000; Tenter, 2009). Based on the proportion of different meats consumed, their likelihood of being eaten raw or undercooked, and the susceptibility of various animal species to *T. gondii*, meat from pigs and small ruminants is considered the primary source of human infection (farm-to-fork food chain). Meat from wildlife, horses, poultry, and cattle are less common sources (Gabriël et al., 2023).

Tissue cysts have been found to persist in edible tissues of live animals for months. There are numerous reports tracing toxoplasmosis to the consumption of infected meat, and some serological surveys incriminate meat more strongly than cats as a source of human infection. The prevalence of *T. gondii* infection is greater in abattoir workers and in people who handle raw meat than in the general population.

2.2.2 Infection through oocysts

Based on experimental studies, the commonly reported duration of oocyst shedding is approximately 1–2 weeks after initial infection, during which cats can excrete a variable number of oocysts, going from 3 to 810 million oocysts (occasionally, none) per cat infection (Dubey & Frenkel, 1972; Torrey & Yolken, 2013). These need between one and five days to become infective for other hosts, depending on temperature, humidity and oxygenation, which explains why the direct contact with cats is not thought to be a major risk for human infection. Unsporulated oocysts lose the ability to sporulate and to become infective, after freezing at −6°C for seven days or after exposure to 37°C for one day. Once sporulated they remain viable in a moist environment for more than a year. Under laboratory conditions, they resist at 4°C for up to 54 months. They survive freezing at −10°C for 106 days and heating at 35°C and 40°C for 32 days and 9 days, respectively. However, they are killed within 1–2 min by heating at 55–60°C (when cooking vegetables for example). They are also highly impermeable and very resistant to disinfectants (Dumètre and Dardé, 2003). All these characteristics make oocysts very resistant and durable, explaining why they are found in water and in soil, from where they reach vegetables and fruits, finally infect humans and intermediate hosts. Oocyst ingestion constitutes a significant proportion of *T. gondii* infections and the water-borne route of infection is one of the most common routes of transmission of toxoplasmosis in humans, mainly in countries with precarious infrastructure for water and sewage treatment. A significant number of outbreaks have been described in Brazil, for example, with water or contaminated produce implicated as the common source of exposure (Pinto-Ferreira et al., 2019).

Water contamination with *T. gondii* oocysts can also lead to the presence of the parasite in edible shellfish, such as *Mytilus* spp., which are commonly consumed in many Mediterranean countries. This leads to a significant health concern. A recent survey conducted in Sardinia (Italy), confirmed the presence of various parasites, including *T. gondii*, in mussels, further raising awareness about this issue (Tedde et al., 2019).

2.2.3 Infection through tachyzoites

The tachyzoite form of the parasite is not able to survive without a host and it is easily destroyed by gastric secretions. Despite that, tachyzoites can be transmitted through vertical transmission from the mother to the fetus, causing congenital toxoplasmosis. After infection with *T. gondii*, parasitemia occurs and tachyzoites can invade the placenta if the woman is pregnant. Nearly half of fetuses whose mothers become infected during pregnancy escape *T. gondii* infection. The stage of gestation at the time of mother's infection may determine the transmission of *T. gondii* to fetus. In general, the transmission is more efficient in the later term of gestation, mostly related to the anatomy and immune factors. For example, the thickness of the placenta varies with gestation; in early pregnancy, placental barrier of humans is 50–100 μm thick and progressively decreases to 2.5–5 μm at the end of pregnancy, allowing tachyzoites to more easily invade trophoblasts by the end of the gestational course (Błaszkowska and Góralska, 2014). Transplacental transmission of *T. gondii* infection generally occurs when a woman becomes infected for the first time during pregnancy. Rarely, congenital transmission occurs in women infected just before pregnancy or during chronic infection. Transplacental infection can lead to a wide variety of manifestations in the fetus and infant including spontaneous abortion, stillbirth; it can also cause severe disease in live infant, but most children are asymptomatic at birth (see paragraph **2.5.3b** about congenital toxoplasmosis) (Dubey et al., 2021).

Other but less common/rare routes of tachyzoite transmission include transfusion of packed leukocytes or by organs' transplantation (for example from an infected donor into an immunocompromised recipient) and ingestion of raw contaminated milk (human or goat) (Dubey, 2021a).

2.3 Population structure of *T. gondii*

The parasite is characterized by a clonal population structure and the genotypes are historically divided into types I, II, III. This distinction was originally made based on the different virulence patterns observed in mice. Despite the presence of a sexual stage in the life cycle of the parasite and a worldwide distribution, the population structure, in isolates genotyped and sequenced in United States and

Europe, appears highly clonal with low genetic diversity. However, multi-locus and multi-chromosome genotyping of isolates from other continents have revealed a much more complex population structure. Most isolates in South America, Africa or Asia do not fit into the three major lineages and they are also considered the more virulent, responsible for important outbreaks and severe cases of ocular toxoplasmosis in humans (Carme et al., 2009; de-la-Torre et al., 2013).

2.3.1 Genotypes, their geographic distribution and virulence

Using the microsatellites (MS), geographic differences were found among 275 isolates, with some isolates confined to Brazil whereas others were worldwide in distribution (Lehmann et al., 2006) .

From Northern to Southern Europe the population structure of *T. gondii* is highly clonal, with a predominance of strains belonging to the type II lineage. Type II and III predominate in Europe and atypical strains have been rarely isolated. In North America the population structure is very similar to that one described for Europe, but also a fourth clonal lineage (haplogroup 12) and atypical strains isolated both from domestic and wild animals showed an important prevalence (Dubey et al., 2011).

The identification of atypical strains is clinically and epidemiologically significant, as these strains are often linked to severe disease outcomes. Contamination by non-European strains can occur through residence abroad or consumption of imported meat. High-resolution analyses are needed to identify the genotype more prevalent in different areas: MS are the most used and are amplified by PCR. A single-multiplex-PCR using 15 MS markers located on 11 different chromosomes of *T. gondii* was developed and led to the identification of atypical isolates that were characterized by a different mix of alleles of haplogroups 1 to 3 and by additional atypical alleles at some loci. The detection of these atypical alleles brought to discover atypical strains in South America (1, 14, 15) (Ajzenberg et al., 2010).

In Brazil in particular numerous studies have highlighted the presence of atypical and new strains isolated from animals and from healthy humans with acute toxoplasmosis. Some of these strains are more prevalent and widely distributed in Brazil: BrI (*Toxoplasma* database (ToxoDB) #6), BrII (#11), BrIII (#8), and BrIV (#17) (Brito et al., 2023).

Looking at African countries less information is available, and most samples identified and genotyped (118/141) were from Egypt. Overall, types III and II variant were the dominant (Mercier et al., 2010). In Asia, the most common genotype found is ToxoDB#9 (Chinese 1), at least in China, while clonal types I, II and II variants, and III have also been found (Shwab et al., 2014; Almeria and Dubey, 2021).

Experimental virulence is defined by the mouse reaction after the inoculation of the parasite intraperitoneally. Type I isolates are highly virulent, leading to the death of mice in less than 10 days

after the inoculation of less than 10 tachyzoites; while type II and III are considered avirulent strains, allowing survival after the inoculation of more than 10^3 tachyzoites. The virulent strains display several characteristics that may explain the rapid dissemination and virulence. Type I strains are
more rapid in destroying a cell monolayer than type II or III because they multiply rapidly and show a lower rate of tachyzoite-to-bradyzoite interconversion (Saeij et al., 2006).

2.4 Virulence factors of *T. gondii* and host-parasite relationship

2.4.1 Virulence factors

To invade host cells *T. gondii* uses a vast repertoire of effector proteins housed primarily in two secretory organelles, the rhoptries and dense granules. The rhoptry organelle effectors (ROPs) are secreted by the parasite into the host cytosol during or immediately prior to invasion by an as-yet-undefined mechanism (Rastogi et al., 2020). The few ROPs that have been characterized to date include virulence factors that disrupt immune clearance mechanisms, remodel the host's cortical actin cytoskeleton at the point of parasite penetration and coopt the signal transducer and activator of transcription proteins (STATs) STAT3 and STAT6 pathways.

In contrast, the dense granule effectors (GRAs) are thought to be secreted later during the invasion process and mostly after the parasite has invaded the host cell (Rastogi et al., 2020). ROP18 and ROP5 were identified as the major factors of virulence of *T. gondii,* secreted from the parasite into the host cell during invasion where they colocalize to the surface of the parasitophorous vacuole. In addition, ROP18 is an active serine/threonine (S/T) protein kinase that contributes to differences in pathogenesis between the three types of strains, since it has been demonstrated that the expression of the type I allele of ROP18 in the non- virulent type III background is sufficient for conferring acute virulence of *T. gondii* (Saeij et al., 2006; Taylor et al., 2006; Behnke et al., 2015). ROP5 plays also an important role in the pathogenesis, considering that is an inactive member of protein kinase family that controls virulence by blocking interferon gamma (IFN-γ) - mediated clearance in activated macrophages. It can also regulate the active protein kinase ROP18, which normally prevents clearance of the parasite in interferon-activated macrophages phosphorylating host immunity related GTPases (IRGs). Additionally, ROP5 has other functions indicating that it plays a general role in governing virulence factors that block immunity (Behnke et al., 2015).

Another rhoptry protein, ROP16, was identified as playing a role in altering host gene transcription by comparing the differences in host gene expression induced by various parasite strains. These studies

led to a focus on genes involved in interleukin IL-4 and IL-6 responses and implicated changes in the activity of the transcription factors STAT3 and STAT6 (Saeij et al., 2007). Although all three strains initially induce STAT3 and STAT6 activity, only the type I or III strains (which share the same ROP16 variant, ROP16I/III) sustain this response. Prolonged STAT3/6 activation by ROP16I/III down-regulates the induction of IL-12, thus limiting the protective T helper (TH1) cytokine responses (Saeij et al., 2007), which might lead to less inflammation, reduced pathology and enhanced parasite survival.

Another virulence factor is GRA15, which is a crucial effector of type II strains of *T. gondii* that is closely associated with host immune modulation by suppressing the indoleamine 2,3-dioxygenase-1 (IDO1)-dependent immune response in human neurons. Recent studies showed that GRA15 also inhibits IFN-γ-induced IDO1- dependent antiparasitic immune responses in human cells, suggesting a novel therapeutic strategy for human toxoplasmosis by blocking nitric oxide (NO) or IL-1β production (Cai et al., 2020).

2.4.2 The immune response to *T. gondii* and immuno-prophylaxis

The immune response to *T. gondii* is complex and involves both the innate and adaptive immune systems. Upon initial infection, the innate immune response is triggered to control the rapid replication of the tachyzoite form of the parasite.

Innate immune response includes dendritic cells (DC) and macrophages, that play an essential role in recognizing the parasite via pattern recognition receptors (PRRs) such as tool-like receptors (TLRs).

In addition, cytokines such as interleukin-12 (IL-12) are produces by human neutrophils and monocytes in response to *T. gondii* (Schlüter et al., 2001; Aldebert et al., 2007).

At this point IL-12 induces the production of interferon-gamma (IFN-γ), a key mediator of immunity in humans and mice (Cerávolo et al., 1999; Lima and Lodoen, 2019) that initiates protective type 1 immunity (Lüder, 2024).

In addition to activating T cell-mediated immunity, IFN-γ functions autonomously within cells to control intracellular parasites. For example, IFN-γ increases tryptophan degradation in human fibroblasts, inhibiting parasite replication (Pfefferkorn, 1984).

Another IFN-γ- dependent mechanism of resistance in humans and mice involves guanylate binding proteins (GBPs), which are recruited to the parasitophorous vacuole membrane and cause vacuolar membrane disruption and parasite clearance. Human GBP1 restricts replication of type II *T. gondii* in epithelial cells without targeting the parasitophorous vacuole, suggesting that GBPs can participate in host defense without causing classical vacuolar membrane disruption (Lima and Lodoen, 2019).

Although innate immune responses to *T. gondii* have been examined in detail, how these processes lead to the stimulation of adaptive immunity, including the ability of DC to access antigens for priming of CD4+ and CD8+ T cells, are less well understood. Moreover, infection of host cells is associated with reduced expression of major histocompatibility complex (MHC) molecules (Lüder et al., 1998). Despite these mechanisms of avoidance, infection with type II strains of *T. gondii* leads to the activation and expansion of DCs and a strong CD8+ T cell response, while infection with virulent type I strains induces a weaker response (Tait et al., 2010).

While infection or vaccination with avirulent strains of *T. gondii* generally induces life-long immunity, using these strains for human vaccination is not recommended due to risks, especially to pregnant women, of a possible reactivation of tissue cysts that may eventually developed. Vaccines made from killed *T. gondii* have proven to be ineffective, offering only marginal protection. Similarly, attempts to attenuate *T. gondii* through irradiation have not been practical, as the parasite remains virulent even at high doses. Vaccination using mutant strains is also not feasible due to the risk of reversion to virulence.

In sheep, a live attenuated vaccine using a cyst-less strain of *T. gondii* S48 has been successful in reducing abortion and neonatal mortality in lambs, and a commercial version is available (Toxovax®, MSD) (Buxton and Innes, 1995).

Recently, a prophylactic vaccine has been tested in French zoos where lethal *T. gondii* infection occurred annually in squirrel monkeys (*Saimiri sciureus*) (Ducournau et al., 2023). The vaccine is based on inactivated *T. gondii*, associated with lipidated maltodextrin-based nanoparticles (NPL). It was administered twice nasally at one-month intervals, followed by a 3rd heterologous nasal/subcutaneous boost at 6 months. No death has occurred among vaccinated animals in the participating zoos since the first administration, thanks to a memory Th1 immune response induced (Fasquelle et al., 2023).

No effective vaccine for humans has been developed to date.

Ideally, the solution of the environmental contamination with sporulated oocysts, and indirectly for toxoplasmosis, could be the creation of a vaccine for cats. Several attempts have been done, starting from an infection with non-oocyst-producing strains, or with an oral live vaccine using bradyzoites of the mutant strain T-263. In this case, the mutant T-263 strains was effective in preventing oocyst excretion (Mateus-Pinilla et al. 1999), but its commercial production was discontinued due to its short shelf-life, high cost and lack of demand and the mechanism by which it prevented oocyst shedding is still unclear. A more recent genetically engineered mutant, HAP2KO, has been developed (Ramakrishnan et al., 2019) which initially led to the production of abnormal, non-sporulating oocysts

in cats, and subsequently rendered the cats immune to oocyst excretion. Another study found that the ablation of AAH genes reduced infection rates in cats, lowered oocyst yields, and decreased sporulation (Wang et al., 2017). Attempts to develop vaccines using killed *T. gondii* or recombinant proteins have been unsuccessful in preventing oocyst shedding after challenge with tissue cysts. Similarly, efforts to immunize cats with crude or recombinant rhoptry proteins via rectal or nasal routes have failed to prevent oocyst excretion (Zulpo et al., 2012, 2017).

2.4.3 Alterations in host signaling and immune evasion

The three dominant clonal lineages of *T. gondii* (types I, II, III) notably differ in their effects on host cells. Type I and III, but not type II strains activate STAT3 and STAT6 in human and mouse cells, thereby down-regulating IL-12 (Lima and Lodoen, 2019).

Another major signaling cascade dysregulated by *T. gondii* is the NF-κB pathway, which leads to the production of pro-inflammatory cytokines involved in host immunity. In infected HFFs, type I *T. gondii* limits NF-κB activation by reducing p65/RelA phosphorylation and translocation to the nucleus (Shapira et al., 2005). Type I *T. gondii* also inhibits LPS- induced IL-1β production in primary human neutrophils, and this effect is associated with inhibition of NF-κB signaling. In *T. gondii*-infected neutrophils, IκBα degradation and p65/RelA phosphorylation are reduced, as are transcripts for IL-1β and the inflammasome sensor NLRP3. *T. gondii* also inhibits caspase-1 cleavage and activation in infected neutrophils (Lima et al., 2018), but not in infected human monocytes (Gov et al., 2013, 2017), representing different human cell type-specific mechanisms of IL-1β regulation.

2.5 Toxoplasmosis in animals and humans

2.5.1 Infection in domestic animals

Toxoplasma gondii infections are common in humans, livestock and in companion animals but clinical disease is relatively rare. Differences in virulence of *T. gondii* strains and the host immune system's conditions are key factors in pathogenesis of clinical toxoplasmosis. Infection in cats continues to be a public health and veterinary concern, since they are the only hosts that can excrete the environmentally resistant oocysts (Dubey et al., 2020). Cats of any age or any breed and either sex can die of toxoplasmosis. Fortunately, reports of clinical toxoplasmosis in cats are sporadic. Domestic dogs may also be infected with *T. gondii*; however, clinical infection is less common than subclinical disease

(Dubey, 2009; Hill and Dubey, 2013). When manifested, clinical signs may affect respiratory, neuromuscular, or gastrointestinal systems and can prove fatal (Dubey, 2009).

Toxoplasmosis is common in sheep, goats, pigs and chickens; however, cattle and horses are notably resistant to the disease. In sheep, congenital infection is a leading cause of stillbirth and preterm lamb loss. Lambs that are born infected and survive usually exhibit normal growth, but they still represent a public health risk if their infected meat is consumed (Dubey, 2009). Toxoplasmosis can also occur in adult goats and the disease is more severe than in sheep. Congenital infection results in loss of kids before or after birth. Pigs may become infected with *T. gondii* by consumption of oocysts, congenitally by tachyzoite transplacental transmission and through consumption of meat containing *T. gondii* bradyzoite tissue cysts (i.e rodents). Although adult pigs rarely show clinical signs, the meat of infected pigs can act as a source of human infection (Aguirre et al., 2019).

2.5.2 Infection in wild animals

Toxoplasmosis is a global disease found in all habitats and regions, from the Arctic to the tropics in terrestrial, aquatic, and marine settings affecting all homeotherms (Sibley, 2003).

Several serosurveys document high levels of exposure to *T. gondii* in circumpolar bear species. Zarnke et al. (1997) examined sera from 892 grizzly bears (*Ursus arctos*) in Alaska by the modified agglutination test (MAT) and detected antibodies in 220 (24.7%). The bears were captured from north-western, southern, and eastern interior Alaska and seroprevalence was highest in the northwestern bears. Geographic differences in prevalence are likely accounted for by differences in feeding ecology rather than exposure to oocysts, given the absence of both lynx and domestic cats at the northwestern collection sites (Zarnke et al., 1997; Elmore et al., 2012).

Infection in marine mammals is geographically and taxonomically widespread, driven by land-to-sea coastal oocyst pollution linked to oocysts from storm water runoff (Cole et al., 2000; Rengifo-Herrera et al., 2012). The endangered southern sea otter (*Enhydra lutris nereis*), exposed through the consumption of invertebrate prey (Johnson et al., 2009), serves as a sentinel of the land-to-sea flow of *T. gondii* oocysts originating from runoff carrying infected domestic or wild felid fecal matter (Conrad et al., 2005).

Recent studies reported the presence of *T. gondii* in wild boars or red deers in Germany (Bier et al., 2020), which are of significant interest to hunters, as well as in wild boars (43% of positive) (Gazzonis et al., 2018) and free-ranging pigs (95 % of positive) (Bacci et al., 2015) in Italy.

2.5.3 Toxoplasmosis in humans

Approximately 30% of the human population is infected with *T. gondii*. In most people, symptoms (when present) are mild and mimic other ailments such as flu, Lyme disease, Q fever, hematological alterations and mumps (Dubey, 2021b).

The prevalence varies between countries: low seroprevalence (10-30%) in North America, South Eastern Asia, Northern Europe and Sahelian countries of Africa; moderate seroprevalence (30 to 50%) in Central and Southern Europe; high seroprevalence (50-80%) from Colombia and Brazil and in tropical African countries (Robert-Gangneux and Dardé, 2012; Cañón-Franco et al., 2014; Mose et al., 2020).

Climate factors such as temperature and humidity influence the resistance of oocysts and consequently can influence infection levels. High prevalence is classically recorded in tropical countries (warm and humid) and lower ones in arid or colder countries. Other factors such as economic, social and cultural habits can explain the wide variations in human seroprevalence (dietary habits, methods of cooking meat, hand washing, water quality, risk knowledge associated with food consumption) (Vismarra et al., 2022).

In the United States, toxoplasmosis was identified as the second leading cause of foodborne illness-related deaths and fourth leading cause of foodborne illness-related hospitalizations (an estimated 327 deaths, and 4428 hospitalizations annually) (Scallan et al., 2011; Gao et al., 2016; CDC Toxoplasmosis 2024). Globally, the WHO reported that foodborne toxoplasmosis reached a rate of 149 cases/100,000 citizens while in Europe the estimation of foodborne toxoplasmosis is still complicated to evaluate because there are no EU regulations concerning the surveillance and monitoring of *T. gondii* in animals and food. Therefore, the available and reported information relies on national legislation and whether the countries have a mandatory reporting system following the detection of *T. gondii*. Moreover, the cases of congenital toxoplasmosis in the EU are strongly biased by the high number of cases reported from France, which has accounted for 75.1% to 82.7% of overall EU cases in 2017–2021 (Available at: WHO, 2024; EFSA-ECDC report, 2023).

2.5.3a *Toxoplasma gondii* and human health: pathogenesis

Most horizontal transmissions to humans are caused either by the ingestion of tissue cysts in infected meat or by the ingestion of soil, water, or food contaminated with sporulated oocysts derived from the environment or, less frequently, directly from feline feces.

Primary acquired infection is asymptomatic in more than 80% of cases of immunocompetent subjects in European countries or North America (Dunay et al., 2018). As mentioned above, some patients may

experience fever or cervical lymphadenopathy, sometimes associated with myalgia, asthenia, or other nonspecific clinical signs. (Robert-Gangneux and Dardé, 2012).

In contrast to *T. gondii* infection in immunocompetent individuals, toxoplasmosis can be life-threatening in immunocompromised patients, regardless of virulence, though the host's immune background remains crucial. In these individuals, toxoplasmosis almost always happens because of reactivation of chronic infection. The CNS is the site most typically affected by re-infection. Clinical presentation of toxoplasmic encephalitis varies from a subacute gradual process evolving over weeks to an acute confusional state, with or without focal neurological deficits, evolving over days. Toxoplasmosis in immunocompromised patients can also present as chorioretinitis, pneumonitis, or multiorgan involvement presenting with acute respiratory failure and haemodynamic abnormalities like septic shock. *Toxoplasma* pneumonia seems to be more frequent in recipients of bone-marrow transplants and in patients with AIDS (Dunay et al., 2018).

In addition, recent data indicate that chronic *T. gondii* infection (tissue cysts) may predispose to neurological diseases due to alterations in neuronal architecture, neurochemistry, and behavior (Carter, 2013; Kazemi Arababadi et al., 2024). Several studies have explored the connection between *T. gondii* infection and conditions such as schizophrenia, epilepsy, depression, bipolar disorder, dysphoria, Alzheimer's disease, Parkinson's disease, and obsessive-compulsive disorder (OCD). However, the evidence regarding *T. gondii*'s role in these neurological and neurobehavioral disorders remains varied and inconclusive and needs more detailed study (Virus et al., 2021).

2.5.3b Congenital toxoplasmosis

When primary infection is acquired by a pregnant woman, tachyzoites can colonize placental tissues during the dissemination process and from there can gain access to the fetal compartment in about 30% of cases. The frequency of vertical transmission increases with the gestational age at maternal infection. At the beginning of pregnancy, the transplacental passage of tachyzoites is a rare event, but the consequences for the offspring are heavy (Robert-Gangneux and Dardé, 2012).

Transplacental infection can lead to a wide variety of manifestations in the fetus and infant including spontaneous abortion, stillbirth; it can also cause severe disease in live infant, but most children are asymptomatic at birth. Most severe cases of prenatally acquired toxoplasmosis were reported first with the predominant manifestation of encephalomyelitis. Moreover, ocular symptoms are the most common signs of congenital toxoplasmosis (Dubey et al., 2021).

However, a high incidence and severity of ocular toxoplasmosis in immunocompetent subjects and in congenitally infected babies, caused mainly by atypical strains, have been reported from Africa, Brazil and Colombia (Gilbert et al., 2008; Huang et al., 2012, 2018).

The prevalence of ocular toxoplasmosis varies from less than 1% to approximately 18% of persons, depending on geographical location. For the majority, ocular toxoplasmosis involves the posterior eye and is characterized by recurrent necrotizing retinitis, with frequent extension of the inflammation and tissue destruction into the choroid, which encapsulates the retina (Smith et al., 2021).

2.6 Challenges and limitations of current toxoplasmosis treatments

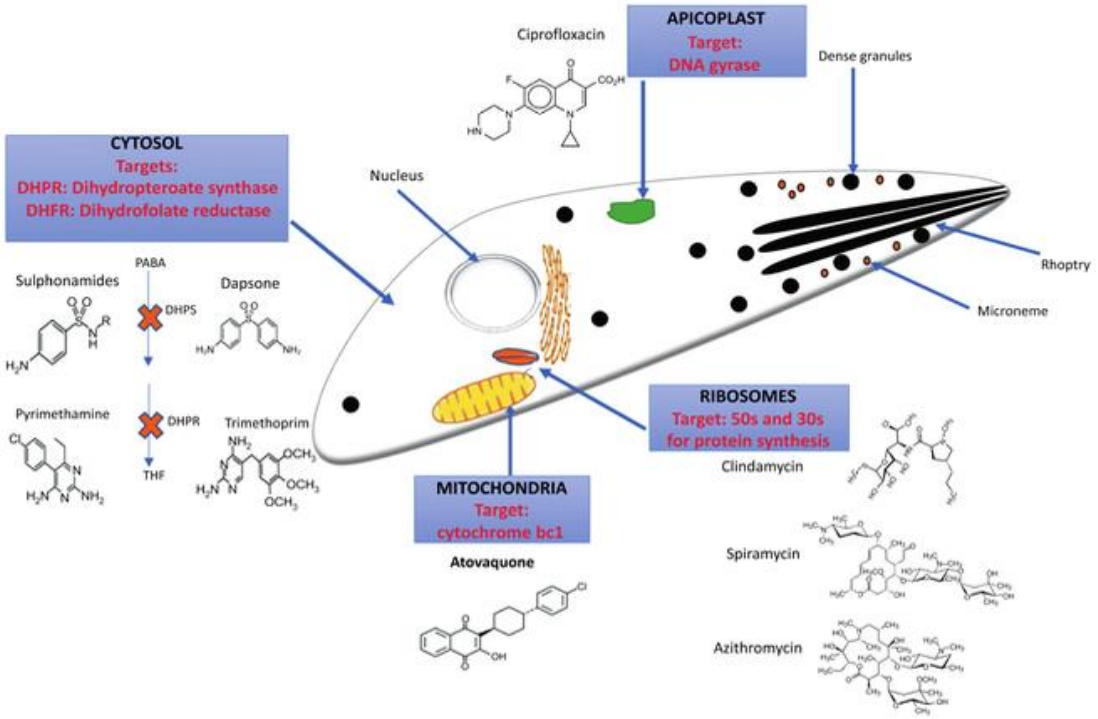

Figure 4. Currently available drugs, their chemical structures, and targets on *T. gondii* (Taken from: Abdullahi et al., 2020).

Figure 4 reports currently available drugs for treatment of toxoplasmosis, their chemical structures, and targets on *T. gondii*.

Treatment options for toxoplasmosis are limited, with the folate pathway being the primary target of anti-*Toxoplasma* drugs. This pathway, essential for DNA synthesis, involves the enzymes dihydrofolate reductase (DHFR) and dihydropteroate synthetase (DHPS), which are inhibited by current chemotherapy agents. Pyrimethamine (PYR) and sulfadiazine (SDZ) are the primary drugs used for the treatment of acute toxoplasmosis: PYR targets the parasite's DHFR, while SDZ inhibits the DHPS. However, they are unable to distinguish between the parasite's enzymes and those of the human host.

In addition, when taken alone they do not have full efficacy and must be used in combination regimens, blocking DHFR and DHPS synergically. Other treatment regimens include trimethoprim (another DHFR inhibitor), in combination with sulfamethoxazole and atovaquone either alone or in combination with sulfadiazine (Dunay et al., 2018).

Pyrimethamine is an antiparasitic drug commonly used to treat toxoplasmosis but also malaria (White et al., 2014). Sulfadiazine and trimethoprim are broad-spectrum antibiotics primarily effective against gram-positive bacteria. Sulfadiazine, a sulfonamide antibiotic, inhibits bacterial folic acid synthesis, similarly to how pyrimethamine acts on parasites. Trimethoprim, on the other hand, is commonly paired with sulfamethoxazole to form a combination known as co-trimoxazole, a treatment widely used for bacterial infections such as urinary tract infections, pneumonia, and certain gastrointestinal infections. Both sulfadiazine and trimethoprim target the bacterial folic acid pathway, making them highly effective against a variety of bacterial pathogens. (Available at "MSD MANUAL: trimethoprim and sulfamethoxazole" by Werth, *PharmD, University of Washington School of Pharmacy Reviewed May 2024)*. In addition, these two drugs are widely used in combination as prophylaxis for toxoplasmosis treatment, especially in HIV infected individuals.

Other drugs, such as atovaquone, spiramycin, azithromycin, and clindamycin are also used to treat *T. gondii* infection as second-line drugs. The second-line drugs are used individually or in combination with either pyrimethamine or sulfadiazine. Spiramycin is used in pregnant women as a prophylaxis to prevent fetal infection but is ineffective for the treatment for an established fetal infection, since it barely crosses the placental barrier (Robert-Gangneux, 2014). Spiramycin, along with other antibiotics used in the treatment of toxoplasmosis such as clindamycin and azithromycin, targets ribosomal proteins, thereby inhibiting protein synthesis in the parasite. These antibiotics interfere with the parasite's ability to produce essential proteins, disrupting its growth and replication. Despite their efficacy, these drugs primarily act on the acute phase of infection and do not eliminate tissue cysts, underscoring the need for more comprehensive treatment strategies (Dunay et al., 2018). Another antibiotic, ciprofloxacin, targets the DNA gyrase complex in the apicoplast, affecting DNA replication (Martins-Duarte et al., 2015).

Another common drug target against apicomplexa parasites, including *T. gondii* (Alday and Doggett, 2017), is the cytochrome bc1 complex. Inhibitors binding to the Qo and Qi sites of the complex disrupt the electron transport chain. Atovaquone is the only cytochrome bc1 inhibitor currently used in clinical practice and it is a therapeutic and prophylactic agent used against the protozoan *Pneumocystis carinii*, although it was originally developed as an antimalarial (Meshnick et al., 2001). Like other

naphthoquinones, it binds to the Qo site of the complex. Its effectiveness in reducing *T. gondii* tissue cyst burden has been shown both when used alone (Ferguson et al., 1994) and in combination with clindamycin (Djurkovic-Djakovic et al., 2002). However, mutations in the cytochrome b binding site can lead to resistance, limiting its broader use.

Only a limited number of parasite targets have been identified as sites of action for drugs against T. gondii. Furthermore, many of these targets are also present in the human host, and treatment can lead to significant adverse effects (Abdullahi et al., 2020). Indeed, current treatment regimens often cause side effects such as myelotoxicity (e.g., leukopenia and thrombocytopenia), rash, nausea, or vomiting, which can necessitate discontinuing therapy or, more commonly, lead to poor patient compliance. This is a serious drawback, as patients (congenitally infected neonates, immunocompromised patients) usually need prolonged treatments (Porter et al., 1992; Konstantinovic et al., 2019). Another major challenge in treating *T. gondii* infections is that, while several existing drugs can effectively manage acute toxoplasmosis, there is currently no approved therapy capable of eliminating the tissue cysts responsible for chronic infections and potential reactivation.

Unlike many other apicomplexans, *T. gondii* can cross the blood-brain barrier (BBB) and establish a persistent infection with the drug-resistant bradyzoite stage. The ideal treatment for toxoplasmosis would need to be effective against both the actively replicating tachyzoite and the quiescent bradyzoite stages and to achieve therapeutic concentrations in the systemic circulation, brain, and eyes, targeting the organs where the parasite persists.

2.7 Novel treatments against toxoplasmosis

2.7.1 Calcium-dependent protein kinase inhibitors, endochin-like quinolone and natural compounds

Ongoing research into new treatments has yielded promising preclinical compounds specifically aimed at toxoplasmosis (Alday and Doggett, 2017). New compounds have been optimized, such as calcium-dependent protein kinase 1 (CDPK1) inhibitors (Rutaganira et al., 2017) and endochin-like quinolone (ELQ) (Doggett et al., 2012), both of which show promising potential as leads for developing new therapies targeting both the acute and latent stages of *T. gondii* infection.

The CDPK1 inhibitors are particularly interesting because *T. gondii* CDPK1 is crucial for the parasite's gliding motility, host-cell invasion and egress and, importantly, it differs from human kinases (Lourido et al., 2010).

Among promising TgCDPK1 inhibitors, pyrazolo-pyrimidine (PP)-based compounds that belong to the class of bumped kinase inhibitors (BKI)s have been shown to be highly efficacious against different apicomplexan parasites *in vitro* (Van Voorhis et al., 2017) and in laboratory animal models (Lourido et al., 2013; Alday and Doggett, 2017). BKI 1294 demonstrated high efficacy against acute toxoplasmosis in mice (Doggett et al., 2014). However, concerns have been raised about its potential cardiotoxicity due to inhibition of the human Ether-à-go-go-Related Gene (hERG) ion channel (Ojo et al., 2014). Despite the potential toxicity for humans, a study on sheep infected with *T. gondii* during pregnancy found that BKI1294 was safe and successfully prevented vertical transmission of the parasite (Sánchez-Sánchez et al., 2019). Vidadala et al., (2016) optimized a new compound (compound 32) with modifications in the main PP scaffold that retained favorable BKI 1294 properties but lacked the hERG inhibitory activity. This compound significantly reduced the parasite burden in a murine model of acute *T. gondii* infection. Moreover, it was able to penetrate the CNS where it significantly reduced the brain cyst burden (by 88.7%) when administered five weeks after infection (Konstantinovic et al., 2019). A more recent alternative to BKI 1294 is BKI 1748, which has also proven effective against congenital toxoplasmosis in sheep. Unlike BKI 1294, BKI 1748 does not exhibit toxicity toward hERG K+ channels, thus mitigating the cardiovascular risks associated with BKI 1294 treatment (Sánchez-Sánchez et al., 2024).

Unlike naphthoquinones, which bind to the Qo site of the cytochrome bc1 complex, another class of compounds is the ELQs, which are thought to bind to the Qi site. From a library of these compounds, ELQ-271 and ELQ-316 were selected for further study and demonstrated low IC_{50} values. These compounds were significantly more effective than atovaquone in a murine model of acute toxoplasmosis, reducing brain cysts by 88% in mice treated five weeks post-infection with the ME49 strain (Doggett et al., 2012). Since atovaquone and ELQs target different sites (Qo and Qi) of the bc1 complex, their combination has been proposed to act synergistically, potentially preventing resistance development (Alday and Doggett, 2017).

Another interesting compound, ELQ-300, in its prodrug form ELQ-331, was recently accepted as a preclinical candidate by the Medicines for Malaria Venture for potential use in malaria prevention and treatment (Frueh et al., 2017).

Guanabenz, an FDA-approved drug for the treatment of hypertension, protected mice against lethal acute infection and significantly reduced the number of brain cysts in chronically infected mice due to its excellent passage through the BBB (Benmerzouga et al., 2015). Guanabenz shows potential for repurposing as an antiparasitic drug in humans, with the distinctive ability to reduce tissue cysts in the

brain, targeting *T. gondii* eukaryotic initiation factor-2alpha (TgIF2alpha) which plays a key role in controlling translation and is used by the parasite to modulate gene expression during its developmental stages (Narasimhan et al., 2008).

Other compounds currently being studied are plant-derived substances, such as artemisinin, a sesquiterpene lactone used as an antimalarial (Loo et al., 2017) that is derived from *Artemisia annua*, an herb traditionally used in Chinese medicine. Recent data indicate that artemisinin and its derivatives also show activity against *T. gondii* (Dunay et al., 2009; Deng et al., 2020) and target the parasite's metabolism, likely by generating reactive oxygen species (ROS) that damage vital proteins and enzymes (Rosenberg et al., 2019).

While they show potential, the effectiveness of different derivatives varies, suggesting possible differences in their mechanisms of action or the parasite's ability to absorb the drugs. Artemisinin-based treatments are being explored as alternative or adjunct therapies for toxoplasmosis, especially in drug-resistant or severe cases. However, further studies are needed to fully understand their potential in combating *T. gondii*.

In summary, while some novel treatments for toxoplasmosis still present toxicity concerns due to their effects on human targets, there are also promising compounds that have progressed to experimental testing in preclinical studies in animals, such as mice and sheep. These advancements highlight the potential for safer, more effective therapies in the future, with some compounds, like ELQs and newer BKIs, showing efficacy against *T. gondii* and other apicomplexan parasites, and moving closer to clinical trials.

2.7.2 Thiosemicarbazones and their metal complexes

Thiosemicarbazones (TSCs) are organosulfur compounds known for their antimicrobial and anticancer properties (Beraldo and Gambino, 2004; Pelosi, 2010; Khan et al., 2022; Scaccaglia et al., 2022). Two specific TSC iron chelators, Dp44mT and DpC, belonging to the di-2-pyridylketone thiosemicarbazone (DpT) class, have demonstrated significant efficacy against cancer cells both *in vitro* and *in vivo*. These compounds are believed to accumulate in lysosomes, generating reactive oxygen species (ROS) and inducing apoptosis (Krchniakova et al., 2022). Since 2005, over fifty TSC derivatives have been tested for activity against *T. gondii in vitro*, with several showing promising results against the proliferative tachyzoite stage (de Aquino et al., 2008; Gomes et al., 2013; Dzitko et al., 2014; Ansari et al., 2020; Bekier et al., 2021). One study on 4-arylthiosemicarbazides suggested that the TSC scaffold targets *T. gondii* tyrosine metabolism by inhibiting tyrosine hydroxylase, which in turn inhibits tachyzoite

proliferation *in vitro* (Bekier et al., 2021). In addition, the biological properties of semicarbazones and thiosemicarbazones are often related to metal ion coordination, indeed the metal complex can be more active than the free ligand and some side effects may decrease upon complexation or the complex can exhibit bioactivities which are not shown by the free ligand (Beraldo and Gambino, 2004). For example, gold-based complexes have attracted significant interest for treating *T. gondii* infections. A notable example is auranofin, an FDA-approved drug for rheumatoid arthritis (Faa et al., 2017), which has been repurposed as an antibacterial agent (Liu et al., 2022) and that has demonstrated high efficacy against *T. gondii*, both *in vitro* and in an experimental model of acute toxoplasmosis (Andrade et al., 2014). Gold(III) complexes featuring pyridine, porphyrin, phosphines, and thiosemicarbazone (TSC) ligands have been synthesized (Dominelli et al., 2018; Almeida et al., 2022). These complexes are thought to target cysteine- or seleno-cysteine-containing enzymes, such as thioredoxin reductase, phosphatases, and cathepsin, all of which are present in *T. gondii* (Dou and Carruthers, 2011; Xue et al., 2017).

2.8 Mechanisms of drug resistance in *T. gondii*

Mechanisms of drug resistance or lower susceptibility have been reported for several drugs used to treat *T. gondii* infection. *T. gondii* possesses remarkable adaptive potential, making it inherently "resistant" to various treatments. However, the precise mechanisms underlying its resistance or adaptation have yet to be fully elucidated (Kropf et al., 2012).

Drug-resistant mutants have been generated *in vitro* through mutagenesis under drug pressure for sulfonamides (Pfefferkorn et al., 1992), pyrimethamine (Reynolds et al., 2001) and atovaquone (Mcfadden et al., 2000). However, only six strains of *T. gondii* resistant to SDZ were found in clinical cases between 2013 and 2017. A potential cause of concern is the slight recent increase in SDZ resistance of Brazilian *T. gondii* strains obtained from livestock and human newborns with congenital toxoplasmosis between 2016 and 2017 (Montazeri et al., 2018). The relationship between genotype and drug susceptibility is not well understood, however, results from one study comparing *in vitro* susceptibilities of *T. gondii* strains from genotypes I, II, and III, suggested that type II and III strains were approximately 40 times more susceptible to pyrimethamine than the type I RH strain (Reynolds et al., 2001).

2.9 Techniques commonly used for drug screening

2.9.1 Cell cytotoxicity assays *in vitro*

Cell cytotoxicity and proliferation assays are commonly employed in drug screening to determine whether compounds affect cell proliferation or exhibit direct cytotoxic effects. It is crucial that the host cells remain unaffected by the compounds being tested on the parasite, as this ensures that any observed effects are specific to the parasite and not due to host cell toxicity.

Different methods are available to detect cytotoxic and cytostatic effects of different compounds and assess cellular viability. These methods are based on the detection of various cellular functions, including cell membrane permeability, dye uptake, metabolic activity, enzyme release, cell adherence, ATP production, co-enzyme production, DNA synthesis, and nucleotide uptake activity (Adan et al., 2016). The most used are the metabolic cell proliferation assays like the 3-(4,5-dimethylthiazol-2-yl)-2,5-diphenyl-2H-tetrazolium bromide (MTT), Alamar Blue or Resazurin Reduction Assay (RES) and Lactate Dehydrogenase (LDH) assay.

The MTT assay was first described by Mosmann (1983) as an alternative to radioisotopes (Mosmann, 1983). It is based on the conversion of MTT into insoluble formazan crystals by mitochondrial NAD(P)H-dependent oxidoreductase enzymes in living cells (Figure 5). This assay helps determine the number of viable cells by measuring mitochondrial activity, which correlates with the amount of formazan produced. Proliferating cells exhibit a higher rate of MTT conversion, while dead or slowly growing cells show reduced metabolism, resulting in lower MTT reduction. After MTT application, the formazan crystals are solubilized using solutions such as dimethyl sulfoxide (DMSO) or sodium dodecyl sulfate (SDS). The concentration of formazan is then measured using a spectrophotometer at wavelengths between 540 nm and 720 nm. This assay really helps to determine drug effects *in vitro* to make prediction for clinical applications. On the other hand, it is not convenient for follow-up studies *in vitro* since it needs to kill all the cells during protocol. It is also not possible to distinguish cytotoxic and cytostatic agents by this method and results would not be proper when the cell number is low (Adan et al., 2016).

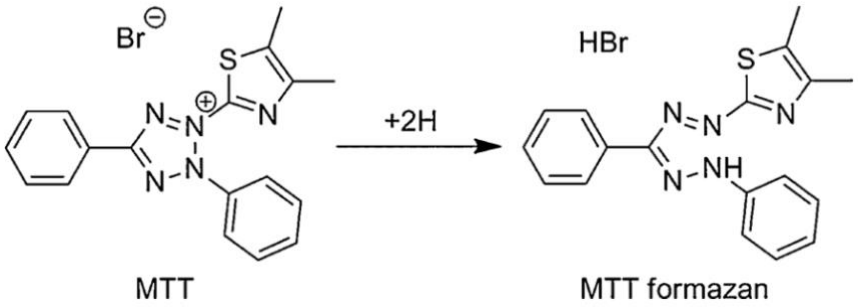

Figure 5. Reduction of MTT bromide to its formazan (Taken from: Ghasemi et al., 2021).

The Alamar Blue assay, also known as resazurin assay, is a non-toxic, cell-permeable dye that serves as a vital indicator of cellular viability. Resazurin was discovered by Weselsky and first used by Pesch and Simmert in 1929 for estimating the bacterial content of milk (Twigg, 1945). Once inside the cell, resazurin is reduced to resorufin, which is pink and highly fluorescent (Figure 6) and reflects the reducing environment within the cytosol. Proliferating cells exhibit a higher rate of resazurin reduction, while dead or damaged cells show lower reduction, making this a useful marker for distinguishing viable cells. The fluorescence produced can be measured at 570 nm and 630 nm. This assay is preferred due to its lower toxicity compared to other assays, allowing for long-term experiments without harming the cells. Resazurin is also non-radioactive, water-soluble, and highly stable in cell culture. However, using resazurin may require extensive experimental optimization, limiting its convenience for rapid assays. Additionally, fluorescence interference can occasionally occur, leading to false results (Adan et al., 2016).

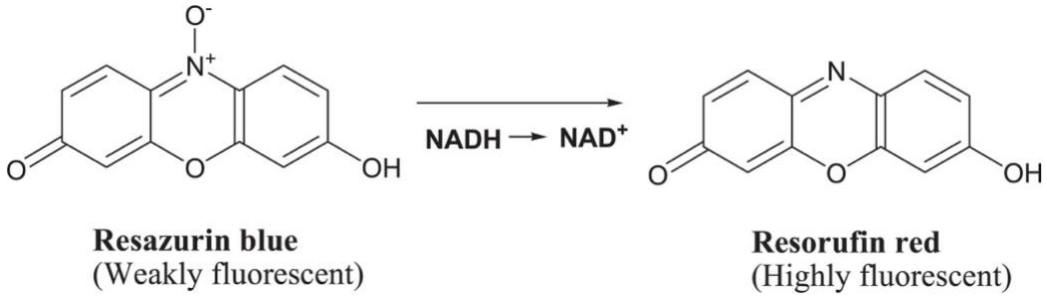

Figure 6 Reduction of resazurin to resorufin (Taken from: Sanjai et al., 2024).

2.9.2 *In vitro* efficacy assessment of drugs on *T. gondii*

To date, various systems are available for *in vitro* drug screening against *T. gondii*, including morphology assays, quantification assays (immunofluorescence, ELISA, qPCR) and assays using reporter strains.

2.9.2a Morphology assay: Diff-Quick May Grunwald and Giemsa staining

The morphological assay is a method used to observe *T. gondii*-infected host cells for drug screening. While it requires minimal technical equipment, it is labor-intensive and demands highly trained personnel to conduct the observations (Jin et al., 2009).

The principle of this assay is based on staining and counting parasitophorous vacuoles formed within an infected monolayer of cells. All assays based on staining can be used with any type of strain or isolate and are therefore highly versatile. A disadvantage is the inherent lack of specificity of these dyes (Müller and Hemphill, 2024). One of the most commonly used stains is Diff-Quick May Grunwald-Giemsa to discriminate between nuclei and cytoplasm.

2.9.2b Assay using reporter strains: *T. gondii* β-gal assay

This assay is based on the use of a reporter strain of *T. gondii* that expresses bacterial β-galactosidase, enabling a high-throughput and nonradioactive screening method for drug testing of viable parasites. The gene reporter was introduced under the control of the strong Surface Antigen 1 (SAG1)-promotor, to obtain a stable expression (McFadden et al., 1997). This allows discrimination between live and dead parasites through a colorimetric assay. This method has become the "gold standard" for measuring parasite growth (Seeber, 2000; Molina et al., 2021; Păunescu et al., 2021; Desiatkina et al., 2022b; Boubaker et al., 2024), offering several advantages, such as the use of a single reagent, chlorophenol red-β-D-galactopyranoside (CPRG). This makes the test simpler and cheaper than an enzyme-linked immunosorbent assay (ELISA) assay, for example, which requires multiple steps and the use of several reagents. In addition, the result is visible to the naked eye and immediate, lending additional convenience and speed to the analysis (McFadden et al., 1997). CPRG is the substrate of the enzyme β-galactosidase, which is initially yellow in color and because of the reaction catalyzed by the enzyme turns red, and its coloration is detectable by spectrophotometric reading.

2.9.2c Real-time Polymerase Chain Reaction

Real-time PCR is commonly used to quantify the parasite load after *in vivo* drug treatment. This technique helps determine the effectiveness of the drug by measuring the reduction in parasite numbers. Real-time PCR is a variation of the standard PCR technique that enables real-time monitoring of the DNA amplification process. PCR itself is a molecular method used to enzymatically generate numerous copies of a specific DNA region for various purposes. Real-time PCR is one of the most powerful molecular tools available today, widely used in biological sciences and medicine due to its quantitative accuracy, sensitivity, and speed. Applications of real-time PCR include gene expression

analysis, mutation detection, pathogens' detection and quantification, identification of genetically modified organisms, allergen detection, microbial degradation monitoring, species identification, and assessing parasite fitness.

Real-time PCR systems use a fluorescent reporter to detect and quantify DNA amplification. They are generally classified into two groups based on the type of fluorescent agent and detection specificity. The first group uses double-stranded DNA intercalating dyes, such as SYBR Green I and EvaGreen, which bind to both specific and non-specific amplicons. SYBR Green I is the most used dye, binding to the minor groove of double-stranded DNA and fluorescing only when bound. The strength of the fluorescence correlates with the amount of double-stranded DNA in the reaction. Its advantages include low cost, convenience, and sensitivity but non-specific amplification, such as primer-dimers, that may occur. A melting curve analysis is recommended to verify the specificity of the amplified products.

The second group of real-time PCR systems uses fluorophores attached to oligonucleotides, detecting a specific sequence of the target DNA. This includes probes like TaqMan, molecular beacons, and scorpion probes. The TaqMan probe is a widely used hydrolysis probe system. It consists of a reporter fluorophore at one end and a quencher at the other. During PCR, the probe hybridizes to the target DNA between the forward and reverse primers. As the DNA polymerase extends the strand, its exonuclease activity cleaves the probe, separating the fluorophore from the quencher. This releases the fluorophore, generating a fluorescence signal directly proportional to the amount of target DNA being amplified, making TaqMan highly specific and reliable for quantification.

In addition, detection and quantification of a house-keeping gene is decisive to perform a good analysis, in case of *T. gondii* one of the most used is the B1 gene (Costa et al., 2000) or the 529 bp.

2.9.3 Tools to investigate drug mode of action and potential targets

Over the past two decades, advancements in the analysis of genomes, transcriptomes, and proteomes have opened new avenues for drug target discovery and led to significant improvements in sensitivity and the ability to process large amounts of data within a reasonable time frame.

Current strategies of target deconvolution include the evaluation of those proteins binding to compounds of interest and the determination of whole-cell proteomes of drug-resistant strains by shotgun mass spectrometry (Müller et al., 2024). Proteomics studies the global expression of proteins that an organism can express and how different proteins interact with each other. When it is coupled to mass spectrometry it is possible to perform high-throughput identification of multiple proteins per

sample (Timp and Timp, 2020). It is very useful for identifying which proteins are differentially expressed in resistant strains compared to wild-type strains of *T. gondii*.

The investigation of *T. gondii* proteins binding to compounds is done using Differential Affinity Chromatography (DAC) coupled with mass spectrometry (MS) based quantitative proteomics of respective eluates, allowing a hypothesis of the potential drug target.

Transmission Electron Microscopy (TEM) and the Tetramethylrhodamine Ethyl Ester (TMRE) assay are further methods for evaluating potential drug targets, in particular providing valuable information on potential effects of the drugs on the mitochondria.

TEM is an ideal tool for studying the internal structures of cells and various biological materials and in this case is used to characterize ultrastructural changes in tachyzoites exposed to the drug treatments.

The TMRE assay is specifically designed to detect potential damage to the mitochondrial membrane potential. It uses a fluorescent dye that can cross the mitochondrial membrane only if the membrane remains unaffected by the compounds being tested (Perry et al., 2011).

2.9.4 Immune and embryonic toxicity assessment of the compounds

Before proceeding with *in vivo* experiments involving these compounds in a model of toxoplasmosis infection, it is crucial to further investigate their potential side effects, especially regarding their impact on the immune system and embryonic development (this is especially important for evaluating the risks associated with congenital toxoplasmosis).

2.9.4a Evaluation of the effect of the compounds on the stimulation of the host immune cells

A key aspect of evaluating the toxicity of these compounds is their interaction with the host immune system. The modulation of immune responses, which involves the regulation of both cellular and humoral components following the administration of drugs or natural compounds, is known as immunomodulation. This process can include immunosuppression, immunostimulation or amplification of various phases of the immune response (Alnuqaydan et al., 2022). It is essential to ensure that any potential new drug does not suppress the host's immune system. This can be assessed through *in vitro* tests by using immune cell stimulators along with the addition of the compound of interest to observe any potential immunosuppressive effects. Common stimulators include concanavalin A (ConA), an antigen-independent mitogen that activates T cells, and lipopolysaccharides (LPS), which activate B cells (Walia et al., 2015).

2.9.4b Evaluation of the toxicity on embryonic stages of fish

Zebrafish (*Danio rerio*) is a widely used model organism for assessing the toxicity of pharmaceuticals and new agents. Zebrafish embryos are easy to manipulate and offer several advantages, such as small size, low maintenance costs and rapid development. The Organisation for Economic Co-operation and Development (OECD) has established a fish embryo toxicity test using the zebrafish model. This assay is an alternative to acute toxicity tests on juvenile and adult fish, specifically designed to evaluate the lethal effects of chemicals on fish during embryonic stages (Anghel et al., 2020).

2.9.5 *In vivo* efficacy assessment of drugs on *T. gondii*

After a drug candidate shows effectiveness in a series of *in vitro* experiments, *in vivo* models are used to further advance drug development. These preclinical studies, often conducted on animals, help assess the drug's safety, efficacy and delivery. Laboratory animals, including mice, rats, rabbits, pigs and nonhuman primates are most often used to study the efficacy of drugs against *T. gondii* infection *in vivo*. Mice are the animals most commonly used to study the efficacy of antiparasitic drugs. Strains of *T. gondii*, which differ genetically, also show high levels of virulence in laboratory mice. Type I strains are acutely virulent and a single viable organism is uniformly lethal in all strains of laboratory mice. By contrast, type II strains display intermediate virulence in laboratory mice and are often used to explore the evolution of the infection. Type III strains are highly avirulent in laboratory, with challenge doses leading to a low level of lethal infection (Wang and Sibley, 2020). Animal models of infection allow determination of the efficacy of antiparasitic drugs by applying diverse readouts; these include survival of infected animals, histopathological changes in affected organs, and/or tachyzoite or cyst loads in various organs, determined using staining techniques, qPCR (see paragraph **2.9.2c**), or sub-inoculation of tissue into naïve mice or cell cultures (Piketty et al., 1990).

In the table 2 are reported the most commonly used strains of *T. gondii* for research.

Table 2. Commonly used strains of *T. gondii* for research (Dubey, 2021a).

T. gondii Strain (Year Isolated)	Source	ATCC No[a] or BRC TOXO N[b]	Genetic Type[c] Type	Haplo-groups	References
RH (1937)	Human, brain, USA	50838	I (ToxoDB #10)	1	1079
GT1 (1978)	Goat, muscle, USA	50853 TgA00004	I (ToxoDB #10)	1	341
PRU (Prugniaud) (1964)	Human, fetal tissues, congenital, France	H–001 TgH00001	II (ToxoDB #3)	2	273
ME 49 (1965)	Sheep, muscle, USA	50840 TgA00001	II (ToxoDB #1)	2	821
PTG (?)	(clone from ME 49)	50841	II (ToxoDB #1)	2	661
Beverley (BEV) (1956)	Rabbit, brain, UK	50854 TgA00002	II (ToxoDB #3)	2	118
VEG (1989)	Human, blood, USA	50861 TgH00005	III (ToxoDB #2)	3	371,971
C (CTG, CEP) (1976)	Cat, oocysts, USA	50842	III (ToxoDB #2)	3	997
NED (1989)	Human, placenta, congenital, France	H–002 Tg00003	III (ToxoDB #2)	3	273
TgCatStk7 (2007)	Cat, St. Kitts		Caribbean 1, (ToxoDB #13)	3	398
TgCatBr1 (2003)	Cat, tissue, Brazil		BrII (ToxoDB #11)	4	387
MAS (1991)	Human, fetal tissues, congenital, France	50870 TgH00006	BrIV (ToxoDB #17)	4	273
RUB (1992)	Human-adult, broncho alveolar fluid, immunocompetent, French Guiana	H–003 TgH00002	Atypical (ToxoDB #98)	5	275
GUY–2002–KOE (2002)	Human-adult, peripheral blood, immunocompetent French Guiana	H–005 TgH18002	Atypical (ToxoDB #60)	5	22,190
FOU (1992)	Human, kidney transplant, Africa	TgH00007	BrI, Africa 1 (ToxoDB #6)	6	274,661
CAST (1989)	Human, AIDS, brain abscess, USA	TgH00008	Atypical (ToxoDB #28)	7	661,813
TgCatBr5 (2003)	Cat, tissue, Brazil	TgA00007	Atypical (ToxoDB #19)	8	387
TgCatBr64 (2003)	Cat, tissue, Brazil		Atypical (ToxoDB #111)	8	984
TgPgUs15 (P89) (1991)	Pig, heart, USA	50879	BrIII (ToxoDB #8)	9	365,1256
GUY001-DOS (2001)	Human, French Guiana		Atypical (ToxoDB #97)	10	190
TgCgCa1 (Cougar) (1998)	Cougar, oocysts, Canada		Atypical (ToxoDB #66)	11	57, 395
ARI (1977)	Human, brain abscess, 10 months after heart transplant, USA		Type 12 (ToxoDB #5)	12	661,813
TgCatPRC2 (2007)	Cat, tissue, China		Chinese 1 (ToxoDB #9)	13	392
GAB2-2007-GAL-DOM2 (2007)	Chicken, tissue, Gabon	TgA105004	Africa 3 (ToxoDB #203)	14	881
TgRsCr1 (2006)	Toucan, Costa Rica		Atypical (ToxoDB #52)	15	400
TgCatEg65 (2009)	Cat, Egypt		Africa 4, (ToxoDB #20)	No data	27, 28, 535
CASTELLS (1993)	Sheep, placenta, Uruguay		Atypical (ToxoDB #15)	16	274

[a] Deposited by Dr. David Sibley.
[b] See http://www.toxobrc.com, courtesy of Drs. Ajzenberg and Dardé. Codes beginning by TgH or TgA are from BRC Toxoplasma.
[c] I thank Drs. Dardé, M.L., Montoya, J., and Su, C. in preparation of this Table.

3 *In vitro* and *in vivo* assessment of thiosemicarbazones against *Toxoplasma gondii* infection

As previously mentioned, treating toxoplasmosis remains a significant challenge. Current therapeutic regimens are associated with serious side effects, including myelotoxicity, which can necessitate treatment discontinuation. In some cases, the adverse effects can be life-threatening. Additionally, existing treatments are unable to eliminate tissue cysts, which are responsible for maintaining chronic infections and pose a risk of reactivation, particularly in immunocompromised individuals. These limitations drive the need to develop novel compounds that can not only reduce toxicity but also effectively target tissue cysts. Recently, several new compounds have been optimized and tested with the aim of overcoming these barriers, offering safer, more comprehensive therapies that address both acute and chronic phases of toxoplasmosis. This advancement holds the potential to significantly improve patient outcomes and prevent reactivation of the disease.

In this study, two promising compounds from the thiosemicarbazone class, C3 and C4, were selected for full characterization. The aim of the present experimental thesis was to:

1. Assess the *in vitro* toxicity of the compounds on host cells and evaluate their efficacy against the parasite *T. gondii*.
2. Investigate the mode of action of these compounds using differential affinity chromatography (DAC) and proteomics techniques.
3. Assess their toxicity on host immune cells (in a murine model) and in a zebrafish embryo development model.
4. Evaluate the efficacy of the compounds *in vivo* in a murine model of cerebral toxoplasmosis.

4 Materials and Methods

4.1 Host cells and parasites

Vero cells and human foreskin fibroblast (HFF) cells were used as host cells for *T. gondii* infection.
HFF were maintained in Dulbecco's modified Eagle medium (DMEM), while Vero cells were cultured in RPMI 1640 medium. Both media were supplemented with phenol red, 10% heat-inactivated and sterile-filtered fetal calf serum (FCS), 50 U/ml penicillin, and 50 µg/ml streptomycin.
For the *in vitro* assessment of the synthetized compounds, we used three *T. gondii* strains: (i) *T. gondii* β-gal-RH (Type I), a genetically modified strain constitutively expressing β-galactosidase (kindly provided by Prof. David Sibley, Washington University, St. Louis, USA), (ii) *T. gondii* RH (Type I) and (iii) *T. gondii* ME49 (type II) strain which were provided by Dr. Furio Spano (Istituto Superiore di Sanità, Roma, Italy).

4.1.1 Cell maintenance

Cultures were kept at 37°C with 5% CO_2 in tissue culture flasks (Sarstedt, Sevelen, Switzerland) and were passed at least once a week, after reaching the confluence. Briefly, after discarding the old media, cells were washed twice with Hanks' Balanced Salt Solution (HBSS) (Gibco-BRL, Zürich, Switzerland) and then detached with 1 mL of Trypsin/EDTA (Gibco-BRL, Zürich, Switzerland), that needs to be incubated at 37°C for at least 5 minutes to be activated. Once cells are detached, media at 10% FBS (should be used at least at the same volume of Trypsin to inactivate it) is used to resuspend them and cells are transferred into new flasks or seeded into 96-well plates.

4.1.2 Cell counting and seeding

To seed 96-well plates, it was necessary to determine the concentration of HFF in 1 mL of suspensions using the Burker's counting chamber. Once known the number of cells/mL it was possible to calculate the volume to collect from the suspension, depending on the concentration of cells that must be seeded in each well. Detachment of cells was done as described above (paragraph 4.1.1). From the cell suspension obtained, serial dilutions (1:10, 1:100, 1:1000) in 100 µl as finale volume, using 90 µl of PBS 1X and 10 µl of cells, were made. At this point cells were counted under the microscope at 10x magnification and afterwards 96-well plates were seeded with 200 µl/well of cell suspension prepared at the concentration of 2.5 x 10^4 and incubated at 37°C/5% CO_2 to reach the confluency.

4.1.3 Parasite maintenance

Parasites were maintained by serial passages in either Vero cells or HFF in their respective media. After discarding the old medium, new medium was added and tachyzoites were collected by removing infected cell layers with a rubber cell scraper. The suspension obtained was filtered through a 25-gauge needle three times to break up the cells and isolate parasites. For the new infection different number of parasites were added to new cells flasks (with both HFF or VERO cells), depending on the need (usually in a T25 flask, a volume of 50 µl or 150 µl of parasite suspension is enough for their maintenance). For experiments where determining the number of parasites needed to infect cells was essential, the parasites were counted using the same protocol as for cell counting (refer to paragraph **4.1.2**), with Trypan blue to enhance contrast.

Figure 7 shows a monolayer of HFF cells infected by *T. gondii* β-gal-RH.

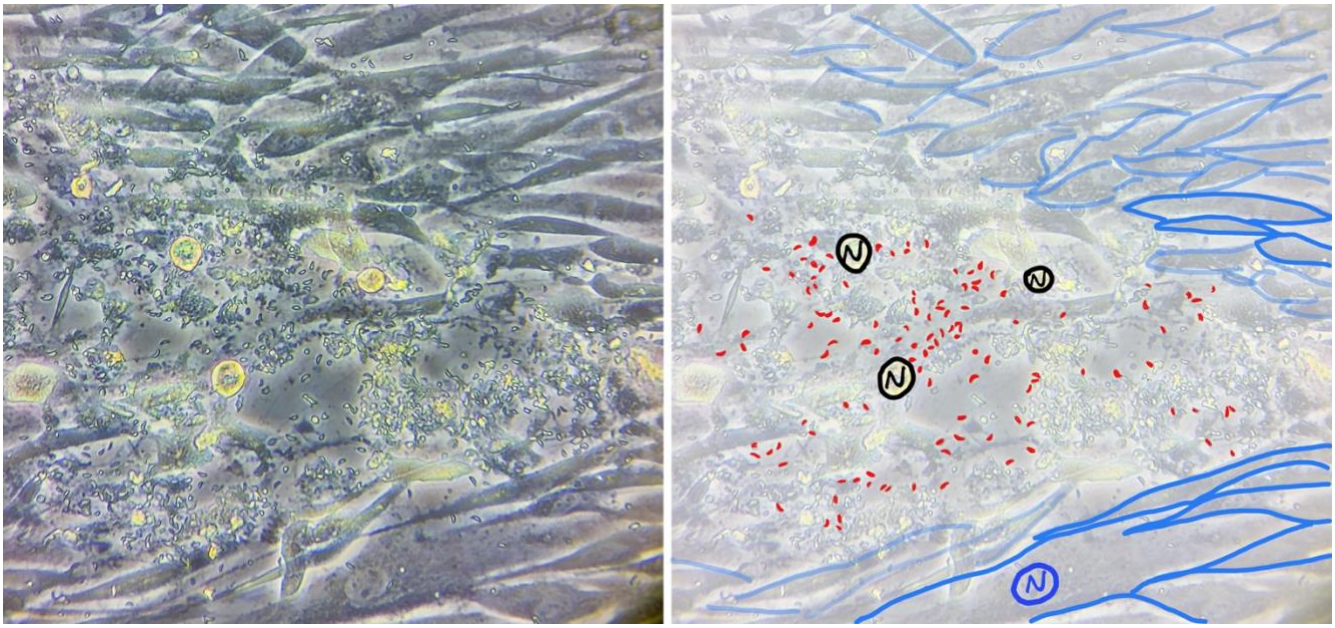

Figure 7. Monolayer of Human Foreskin Fibroblast (HFF) cells infected by *T. gondii* β-gal-RH at 20x magnification.
On the right side of the picture: HFF infected are highlighted in black, HFF non-infected are highlighted in blue and *T. gondii* is colored in red. "N" indicates nucleus of the cells.

4.2 Compounds

Thiosemicarbazone derivatives were selected as coordinating ligands due to their suitability as scaffolds for developing bioactive complexes.

4.2a Copper complexes and their thiosemicarbazone ligands

In this study, we incorporated the pyridoxal moiety into the ligand design, given its vital role in metabolic processes across prokaryotic and eukaryotic cells. Pyridoxal, a key member of the vitamin B6 group, is closely related to pyridoxine, pyridoxamine, and their corresponding 5'-phosphates. In animal tissues, pyridoxal phosphate is the predominant and active form of vitamin B6. Its absorption is controlled by phosphatase-mediated hydrolysis, allowing the non-phosphorylated forms to diffuse passively into cells.

Pyridoxal and pyridoxal 5’-phosphate were subsequently functionalized with thiosemicarbazide. To investigate potential differences in biological activity, we opted for the phosphorylated forms to enhance the compounds' water solubility. Additionally, the presence of two methyl groups on the terminal nitrogen (N4) of MV4 and MV5 increased the ligands' hydrophobicity, providing an opportunity to study the electron-donating effects of these groups on the metal coordination behavior (Scaccaglia et al., 2022). To further boost the biological activity of the ligands, a copper complex was synthesized by adding copper(II) chloride salts to the aqueous ligand solution.

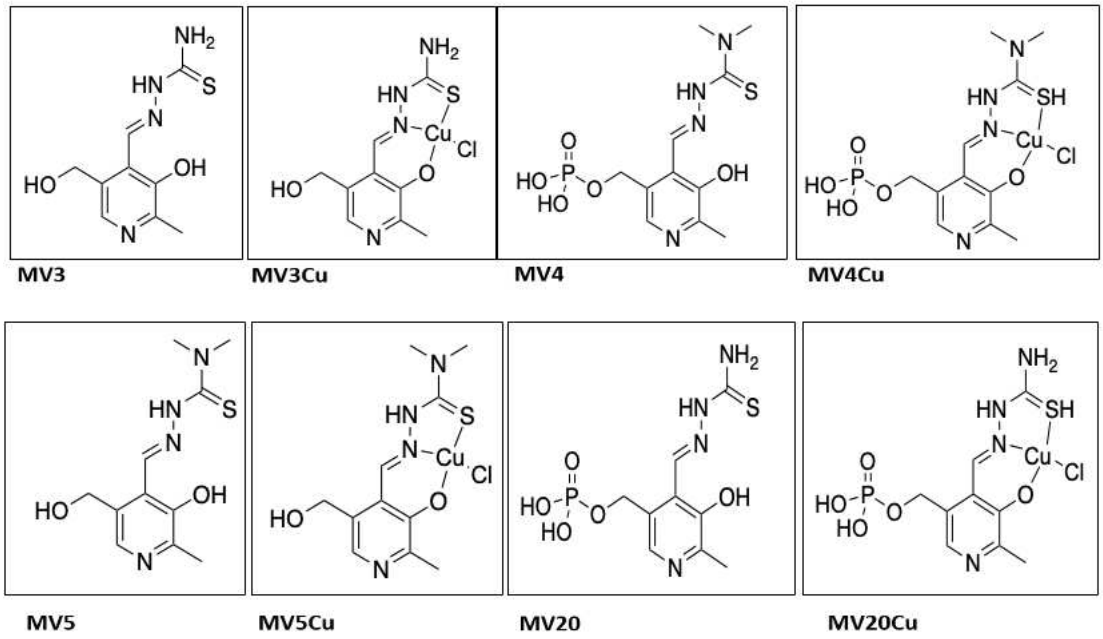

Figure 8. Chemical structures of four copper (Cu) complexes and their thiosemicarbazone ligands. **MV3**: piridoxal thiosemicarbazone, **MV3Cu**: piridoxal thiosemicarbazone copper chloride, **MV4**: pyridoxal-5-phosphate 4,4’dimethyl-3-thiosemicarbazone, **MV4Cu**: pyridoxal-5-phosphate 4,4’dimethyl-3-thiosemicarbazone copper chloride, **MV5:** pyridoxal 4,4’dimethyl-3-thiosemicarbazone, **MV5Cu**: pyridoxal 4,4’dimethyl-3-thiosemicarbazone copper chloride, **MV20**: pyridoxal-5-phosphate thiosemicarbazones, **MV20Cu** pyridoxal-5-phosphate thiosemicarbazones copper chloride.

4.2b Gold complexes and their thiosemicarbazone ligands

Three gold(III) complexes (C1, C2 and C3) and one thiosemicarbazone ligand (C4) (Figure 9) were synthesized according to (Scaccaglia et al., 2024). Briefly, the ligands were synthesized by reacting the corresponding aldehyde with the thiosemicarbazides in an alcoholic solution. The resulting precipitate was filtered and employed in the synthesis of gold (III) compounds through the reaction with $HAuCl_4$. For *in vitro* testing, drug stock solutions were prepared at 20 mM concentration in dimethyl sulfoxide (DMSO) and stored at -20°C.

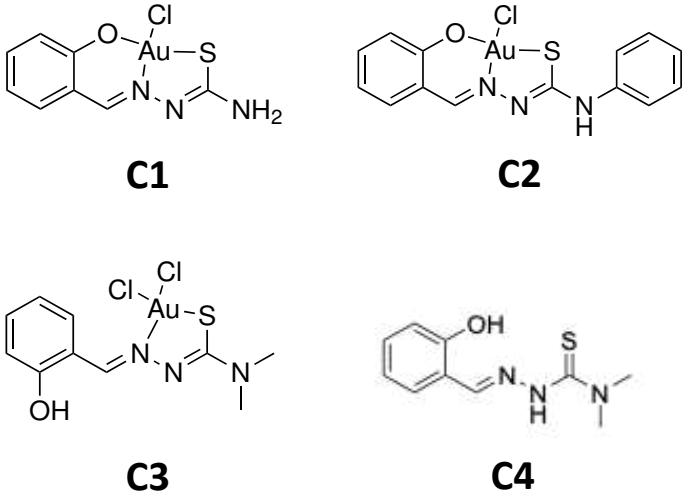

Figure *9.* Chemical structures of three gold(III) complexes and their thiosemicarbazone ligand. **C1**: salicylaldehyde thiosemicarbazone gold(III) chloride, **C2**: salicylaldehyde 4,4-Dimethyl-3-thiosemicarbazide gold(III) dichloride, **C3**: salicylaldehyde 4-phenylthiosemicarbazide gold(III) chloride, and **C4**: salicylaldehyde 4,4-dimethyl-3-thiosemicarbazide.

4.3 In vitro toxicity evaluation of thiosemicarbazones on host cells

For the initial screening of thiosemicarbazones on host cells, two different assays were evaluated to identify the most reliable and effective method. Both the MTT assay and the Alamar Blue assay were tested in parallel. After careful comparison, the Alamar Blue assay was selected as the preferred method due to its superior accuracy, reproducibility and sensitivity in detecting cell viability. This assay provided more consistent results across multiple experiments, making it a more reliable tool for assessing the cytotoxicity of the compounds. The MTT assay, although widely used, showed more variability, leading to its exclusion from further analysis (data not shown).

4.3.1. Alamar Blue assay

Briefly, HFF were seeded in 96-well plates at a density of $5x10^3$ cells/well. Serial dilutions (ratio 1:2) of the compounds were prepared in DMEM complemented with 10% FBS (50 µM-0.8 µM) and added to

HFF cultures with 80% confluency (200 µl/well). Negative controls were prepared using the solvent in which the compounds were dissolved (DMSO).

After culture for 72 h at 37°C/5% CO_2, the medium was discarded and viability of HFF was determined by Alamar Blue Assay.

Briefly, a stock of resazurin concentrated 2g/mL was prepared and stored at 4°C. Cells were washed three times with phosphate saline buffer (PBS) 1X and then resazurin was added to the plates (making a dilution 1:200 from the initial stock [2g/mL] to reach the final concentration of 10 µg/mL per well). Plates fluorescence was read (excitation 530 nm, emission 590 nm wavelength) using a Hidex Sense microplate reader instrument (Hidex, Turku, Finland). The output data were expressed in Relative Fluorescence Unit (RFU) and used to compare the fluorescence intensity detected at the level of the well of the treated samples against the negative controls. Fluorescence-reported values were evaluated through specific steps: initially, two readings were taken, one representing time zero (T0) when the resazurin was added, and a second reading taken approximately three or four hours later (T3h or T4h). This was followed by calculations using Microsoft Excel® software package (Microsoft, Redmond, WA, USA). The first reading was necessary to discard the amount of background fluorescence due to the fluorescent reagent alone. The values obtained from the two readings were subtracted from each other, and from these the respective averages of each group were calculated. This was followed by calculation of the standard deviation and the percent (normalized) fluorescence calculation, which was obtained from a ratio between the mean of the treatments and the mean of the negative control (DMSO), multiplied by 100. In order to minimize the uncertainty, the assay was repeated several times, on different days (at least three times). A calibration line was determined by nonlinear regression considering the mean value of each group compared to the negative control. From there, the half-maximal inhibitory concentration (IC_{50}) value given by the exponential of the intercept of the line was measured. The IC_{50} value corresponded to the minimum concentration of drug capable of inhibiting 50% of the cells.

4.4 *In vitro* efficacy assessment of thiosemicarbazones on *Toxoplasma gondii*

4.4.1 Diff-Quick May Grunwald – Giemsa staining

Vero cells were seeded on glass coverslips at the concentration of $7x10^5$/mL in 6-well plates.

Once confluent, cells were infected with $3.5x10^6$ parasites/mL and simultaneously treated with compounds (MV5 and MV5Cu) prepared in DMEM complemented with 10% FBS at 100 µM and 200 µM in a final volume of 3 mL/well.

After 3 h from the infection, medium was removed, and cells were washed twice with HBSS.

After 24 h or 48 h (different plates were made for different time points), coverslips were washed three times with HBSS e then let to dry. Once dried, glass coverslips were stained with Diff-Quick May Grunwald Giemsa (Bio-Optica, Milano, Italy).

4.4.2 *T. gondii* β-galactosidase viability assay

T. gondii β-gal-RH (Type I) is a genetically modified strain constitutively expressing β-galactosidase under the control of the promoter SAG1 (constitutive promoter). Susceptibility of *T. gondii* β-gal to the tested compounds was assessed by determining IC_{50} values based on β- galactosidase assay, as described by (Păunescu et al., 2021). Briefly, HFF ($5x10^3$/well) were seeded into 96-well plates and once confluent, serial dilutions (ratio 1:2) of compounds (10 µM to $1x10^{-5}$ µM) were prepared in DMEM complemented with 10% FBS and added either 5 min prior to infection of host cells (IC_{50} in pre-infection *in vitro* model) or 3 h after infection (IC_{50} in post-infection *in vitro* model, for C3 and C4). Negative controls were prepared using the solvent in which the compounds were dissolved (DMSO).

Compounds were added at a volume of 100 µl per well, along with 100 µl per well of parasites at a concentration of 10^4/mL (resulting in 10^3 parasites per well). After 72 h of culture at 37°C, 5% CO_2, cultures were washed once with 200 µl/well of PBS 1X. Subsequently 90 µl per well of Triton-X at 0.05% were added to the plates to obtain cell lysis and exposure of β-galactosidase enzyme. Ten µl of 5 mM chlorophenol red-β-D-galactopyranoside (CPRG) were added and plates were measured at 570 nm absorbance.

Absorbance intensity detected in treated samples was compared to negative controls. The values referring to absorbance are evaluated through specific steps. Initially several readings were taken: at T0 to remove the background of the reaction and other readings to follow its progress. The last reading was taken when the production of the colored compound was visible and the reaction was saturated (usually in maximum 30 minutes). The values obtained from the two readings were subtracted from each other, and from these, the respective averages of each group were calculated. This was followed by calculation of the standard deviation and the calculation of percentage (normalized) absorbance, which was obtained from a ratio between the mean of the treatments and the mean of the negative control (DMSO), multiplied by 100. A calibration line was then created by nonlinear regression

considering the mean value of each group compared to the negative control. From there, the IC_{50} value given by the exponential of the intercept of the line was measured. The IC_{50} value corresponds to the minimum concentration of drug capable of inhibiting 50% of the cells.

4.4.3 Viability assay of *T. gondii* wild-type (WT) and clones "adapted" to the treatment

To determine IC_{50} values of C3 and C4 adapted clones to the treatment and WT-*T. gondii* ME49 tachyzoites, confluent HFF monolayers grown in 24-well plates were treated with drugs diluted in DMEM complemented with 10% FBS at concentrations ranging from 4 x 10^{-3} to 2 µM.

Parasites previously frozen after long term-treatment (see paragraph **4.5.3**) were then thawed and used to infect the cells. An amount of 2 ×10^3 freshly purified tachyzoites was used in a total volume of one mL (drug + tachyzoites). After five days of culture at the classical conditions, the culture medium of each well was collected and centrifuged at 2000 *x* g for 10 min, supernatants were discarded and pellets collected. The pellets from the supernatants and the corresponding lysates from the wells were combined in Eppendorf tubes and DNA was extracted using the Nucleospin Rapid lyse according to the manufacturer's instructions. Quantification of tachyzoite numbers was done using *T. gondii*-specific quantitative TaqMan Real-time PCR as described in paragraph **4.7.2b** (Hänggeli et al., 2022). Assays were performed in triplicates and IC_{50} values were calculated using the logit-log algorithm and are indicated with 95% confidence intervals (Semeraro et al., 2024).

In parallel, MICs for C3- and C4 adapted- and WT *T. gondii* ME49 were determined using HFF monolayers grown in 96-well-plates inoculated with 10^3 freshly purified tachyzoites, by applying serial two-fold dilutions of the compounds starting at 50 µM as previously reported. After five days, 96-well plates were examined under the microscope and MIC values were given as first concentration at which rosettes were visible (Müller et al., 2023).

4.5 Discovering the mechanism of action of the drugs

4.5.1 Embedding samples for Transmission Electron Microscopy (TEM)

TEM was conducted as described before (Anghel et al., 2021; Müller et al., 2023).

Briefly, confluent HFF in T25 flasks were inoculated with 1x10^6 *T. gondii* ME49 tachyzoites. At 24 h post-infection, C3 or C4 were added at 1 µM, whereas negative control cultures received complemented DMEM containing 0.005% DMSO (solvent control). As a positive control for visualization of drug-

induced alterations, cultures were treated with 1 µM DB745 (Kropf et al., 2012). Samples were embedded at different time points (6, 12, 24 and 48 h). For fixation, specimens were washed twice with 8 mL of sodium cacodylate solution 0.1 M pH 7.3 and then 8 mL of cacodylate buffer containing 2% glutaraldehyde were added and incubated for 10 minutes at room temperature (RT). Fixed cells were then gently scraped from the flasks and transferred into 15 mL falcon tubes. Samples were centrifuged at 1200 rpm, 4°C for 10 minutes and were fixed for 2 h at RT or overnight (ON) at 4°C. After the incubation another centrifugation at the same conditions but for 5 minutes was performed and supernatant was discarded.

Following several washes in cacodylate buffer (with centrifugation at 1800 rpm at 4°C for 5 minutes) to remove glutaraldehyde, specimens were post-fixed in 500 µl of 2% osmium tetroxide in cacodylate buffer for 1-2 h, RT. Samples were centrifuged in the same conditions as mentioned above, the supernatant was discarded and then washed three times with 5 mL of H_2O (centrifugation in the same condition described before). At the last wash samples were resuspended in 1 mL of H_2O and transferred into 1.5 mL Eppendorf tubes.

This step was followed by stepwise dehydration in a graded series of 1 mL of ethanol (30%, 50%, 70%, 90% and three times with ethanol 100%). Centrifugation after each concentration step was done at 10.000 rpm for 1 min at 20°C. They were finally embedded resuspending the pellet in Epon-182 resin, incubated at 37°C in the water bath for at least 30 minutes to a maximum of 2 h and then centrifuged for 15 min, at maximum speed at 24°C. The tube was then rotated 180° in the centrifuge to prevent the pellet from sticking to one side of the tube, and it was spun down for another 15 minutes at full speed. This step was repeated twice, always ensuring that the tube was filled to the top with resin.

The total incubation time at 37°C should be at least 2.5 h. Finally, centrifugation was performed at full speed for about 30 minutes or longer. The resin was allowed to infiltrate for 24-48 h at RT. Polymerization of the resin was carried out at 60°C. Ultrathin sections (80 nm) were cut using an ultramicrotome (Reichert and Jung, Vienna, Austria) and placed onto 200 mesh formvar-carbon-coated nickel grids (Plano GmbH, Marburg, Germany), stained with Uranyless® and lead citrate (both from Electron Microscopy Sciences, Hatfield PA, USA). Imaging was performed on a FEI Morgagni TEM equipped with a Morada digital camera system (12 Megapixel) operating at 80 kV (Anghel et al., 2021; Müller et al., 2023).

4.5.2 Tetramethylrhodamine Ethyl Ester (TMRE) assay

To assess whether C3 and C4 could interfere with the mitochondrial membrane potential (MMP), TMRE assays were conducted in host cells and/or parasites. Briefly, 5×10^5 HFF were seeded into T25 culture flasks in DMEM supplemented with 10% FBS and maintained for 72 h to reach ~ 80% confluency. HFF monolayers were left either non-infected or were infected with 2 x 10^5 *T. gondii* ME49 tachyzoites. After 48 h, the medium in both infected and non-infected flasks was replaced with either medium containing 0.5 µM C3 or C4, or with medium containing 0.05% DMSO for non-treated controls. As positive controls, the mitochondrial uncouplers carbonyl cyanide 4-(trifluoromethoxy) phenylhydrazone (FCCP) and carbonyl cyanide m-chlorophenylhydrazone (CCCP) were applied at a concentration of 80 and 50 µM, respectively. Pyrimethamine (PYR) was applied at 0.5 µM as a negative control drug that does not affect the MMP.

The HFF monolayers, infected and non-infected, were treated with C3, C4 or PYR for 3.5 h, while FCCP and CCCP were added 10 minutes before the end of the treatment. Untreated cultures served as positive control (100% TMRE uptake). After treatment, cells were washed three times with HBSS, incubated with TMRE (500 nM) for 30 minutes and washed five times with HBSS. Finally, 3 mL of HBSS was added to each T25 flask and cells were removed with a cell scraper and passed through a G25 needle. The resulting lysates were filtered through 3.0-micron polycarbonate membranes and distributed into 96-well plates (100 µl/well). Fluorescence was measured using a Hidex Sense microplate reader instrument (Hidex, Turku, Finland) with the excitation wavelength 544/20 nm and emitted light collected at 590/20 nm. Value from wells belonging to the same experimental condition were summed and the mean TMRE uptake in each condition was calculated from three biological replicates. Results are shown as mean of TMRE uptake in each condition plus/minus standard deviation and statistical significance was calculated using Student's T-test ($p \leq 0.05$) (Semeraro et al., 2024).

4.5.3 Long-term *in vitro* treatment

To determine whether C3 and C4 exert parasiticidal or parasitostatic activity, a long-term treatment experiment was conducted, lasting up to 20 days, with fresh medium containing the compounds added every three days. In brief, HFF grown T25 culture flasks were infected with 2 x 10^5 *T. gondii* ME49 tachyzoites and treatments with 0.5 µM of either C3 or C4 were initiated at 3.5 h post-infection. Negative controls were HFF infected and maintained in medium 0.0025% DMSO. The drugs were removed at various time points (days 3, 6, 9, 12, 16 and 21) and were replaced with fresh DMEM- 10%

FBS. Cultures were observed daily by light microscopy to monitor plaque formation (area of lysis). Since tachyzoites resumed full proliferation in the presence or absence of both drugs, we proceed to generate *in vitro* adapted *T. gondii* clones.

To do this, HFF monolayers in T25 flasks were infected with 2 x 10^5 *T. gondii* ME49 tachyzoites and treatments (0.5 µM C3 or C4) were initiated at 3.5 h post-infection. The media containing C3 or C4 was renewed on day 3. After six days of treatment, the drug-containing medium was replaced with drug-free medium and cultures were maintained for four additional days until plaque formation was evident. On day 10, infected monolayers were washed with PBS 1X, tachyzoites were collected, counted and cloned by limiting dilution (0.2 tachyzoites/0.2 ml medium) in HFF monolayers grown in 96-well plates. After eight-ten days culture at 37°C, 5% CO_2, wells were inspected by light microscopy and cells from those containing a single plaque were transferred into a fresh T25 flask to infect and proliferate within HFF monolayers. The resulting cultures were suspended in FBS with 10% of DMSO and frozen at -150°C (two cryotubes per clone). The stabilates were later thawed and reintroduced into culture and after one passage were used for IC_{50} and MIC determination (see above paragraph **4.4.3**).

For proteomics, WT *T. gondii* ME49, and C3 and C4 clones, were cultured in HFF monolayers in T75 flasks and pellets were obtained as previously described (Müller et al., 2023). Briefly, to release tachyzoites from host cells, infected cells were repeatedly passed through a syringe, followed by filtration through a polycarbonate membrane (3 µm pore size) and stored on ice. Parasites were counted and centrifuged at 800 × g for 10 min at 4°C. The supernatant was removed and each of the three pellets was resuspended in 1.5 mL DMEM and divided into three aliquotes of 500 µL each. After another centrifugation step, the pellets were stored at −80°C for subsequent whole-cell shotgun mass spectrometry. For each strain, two technical and three biological replicates were analyzed.

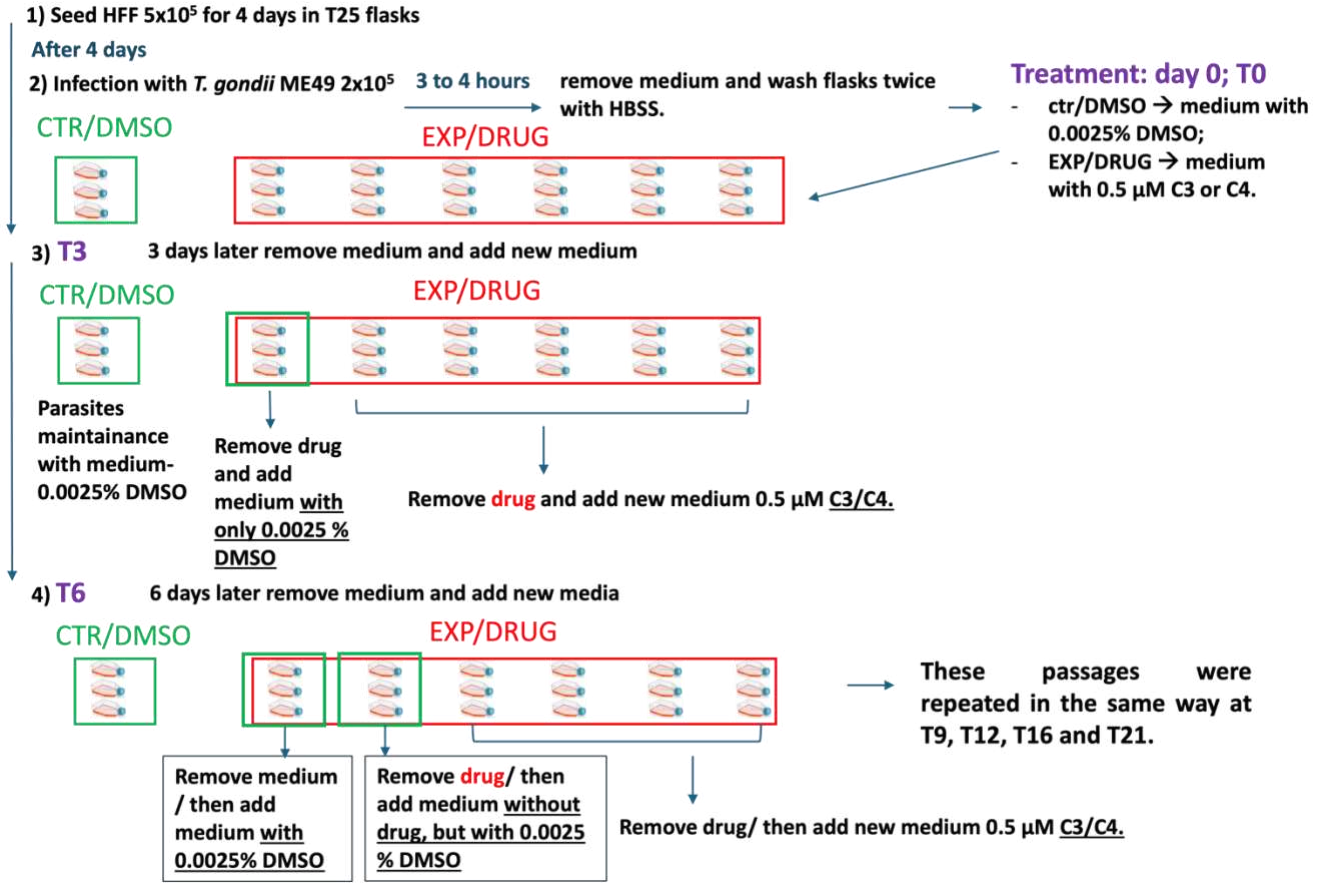

Figure 10. Experimental design of long-term *in vitro* treatment.

4.5.4 Differential Affinity Chromatography (DAC)

Differential Affinity Chromatography (DAC) was performed to identify *T. gondii* proteins binding the compounds, to identify potential drug targets.

Epoxy-activated Sepharose 6B (Merck, Darmstadt, Germany) matrices conjugated to either C3, C4 or tyrosine (as an internal control with similar chemical structure as C3 and C4 and ineffective against *T. gondii*) were prepared as previously described (Müller et al., 2007).

In brief, sepharose lyophilized (0.5 g) with a C12 spacer (Sigma, Buchs, Switzerland) were suspended in 15 mL of H_2O in a falcon tube, vortexed until dissolution occurred and centrifugated at 300 *x* g for 5 minutes, RT. Washes with H_2O were repeated twice and afterwards samples were washed once in the coupling buffer (0.1 M Na_2CO_3, adjusted with HCl to pH 9.5.) Ligands (C3, C4 and tyrosine), 10 or 20 mg each, were dissolved in 1 mL DMSO and added to the falcon tubes with 1 mL of coupling buffer. The falcon tubes were incubated for 3 days at 37 °C under slow but continuous shaking.

After the incubation, samples were washed twice with 10 mL of coupling buffer as described above, subsequently were washed once with ethanolamine (1 M, pH 9.5), and eventually were overlayed with 5 mL of ethanolamine and incubated ON at 20 °C on a shaker in the dark.

The resulting columns medium (approximately 2 mL) were then transferred to a chromatography column (e. g. Novagen, Merck, Darmstadt, Germany) and extensively washed with a solution PBS-DMSO 1:1 in order to remove unbound ligand. The resulting columns were stored in PBS containing 0.02% NaN_3 at 4°C until use. In addition, a mock column, with resin treated in the same way but without C3, C4 or tyrosine, was prepared and was used in tandem with C3, C4 or tyrosine (mock first, then compound). Frozen pellets of *T. gondii* ME49 tachyzoites were resuspended in ice-cold extraction buffer containing 1% Triton X-100 and 1% HALT proteinase inhibitor cocktail (ThermoFisher Scientific, Reinach, Switzerland), vortexed thoroughly, and were centrifuged at 10.000 *x* g for 30 min. The resulting supernatants were subjected to affinity chromatography. Bound proteins were eluted with 50 mM acetic acid (5 mL per column), lyophilized and stored at -80°C for subsequent proteomic analysis (see below).

4.5.5 Proteomics

Proteomic analyses were conducted at the Proteomics and Mass Spectrometry Core Facility, Department for BioMedical Research (DBMR), University of Bern, under the supervision of Prof. Manfred Heller as described previously (Semeraro et al., 2024).

Briefly, the DAC samples were resuspended in 10 µL solution containing 8 M urea/100 mM Tris pH 8, reduced with 0.1 M dithiothreitol (DTT) for 30 min at 37°C, alkylated with 0.5 M iodoacetamide (IAA) for 30 min at 37°C, and digested with LysC 2 hours at 37°C followed by trypsin at RT ON. The digests were analyzed by nano-liquid chromatography on a Dionex, Ultimate 3000, (ThermoFisher Scientific, Reinach, Switzerland) coupled to a timsTOF Pro (Bruker Daltonics, Bremen, Germany), through a CaptiveSpray source (Bruker, Bremen, Germany) with an endplate offset of 500 V, a drying temperature of 200°C and with the capillary voltage fixed at 1.6 kV. A volume of 2 µL from the protein digests were loaded onto a pre-column (C18 PepMap 100, 5 µm, 100A, 300 µm i.d. x 5mm length, ThermoFisher, Reinach, Switzerland) at a flow rate of 10 µL/min with 0.05% trifluoroacetic acid (TFA) in water/acetonitrile 98:2 (Merck, Buchs, Switzerland). After loading, peptides were eluted in back flush mode onto a homemade C18 CSH Waters column (1.7 µm, 130 Å, 75 µm × 20 cm) by applying a 70-minute gradient of 5% acetonitrile to 40% in water/0.1% formic acid, at a flow rate of 250 nl/min. The TimsTOF Pro was operated in data-dependent acquisition (DDA) mode using the Parallel Acquisition

SErial Fragmentation (PASEF) option. The mass range was set between 100 and 1700 m/z, with 10 PASEF scans in a mobility range between 0.7 and 1.4 V s/cm^2. The accumulation time was set to 2 ms, and the ramp time was set to 100 ms. Fragmentation was triggered at 20,000 arbitrary units (au), and peptides (up to charge 5) were fragmented using collision induced dissociation with a spread between 20 and 59 eV.

The data was searched and quantified with fragpipe (Yu et al., 2020) version 20.0 with the following parameters: database was *T. gondii* entries from uniprot (Bateman, 2019) (strain ATCC 50861, release July 2023), to which common contaminants were added; precursor and fragment mass tolerances were set to ±20 ppm and ±0.05 Da, respectively; protein digestion was set to trypsin, with a maximum of three missed cleavages; variable modifications allowed were oxidation on methionine and protein N-terminal acetylation; carbamidomethylation of cysteines was given as fixed modification; the minimum number of matched fragments was set to five; validation was done with Percolator (MSBooster enabled); protein inference was done with Protein Prophet, and results filtered at 1% False Discovery Rate (FDR) for protein level. Quantification was done without match between runs. Protein groups identified by only 1 peptide were removed from the list of positively identified proteins.

Next to fragpipe's measure of quantification (FragI), MaxLFQ values were reported by the software. Top3 (Silva et al., 2006) values were calculated as the sum of the three most intense peptide forms for each protein, having first normalized the peptide forms by variance stabilization normalization (vsn) (Huber et al., 2002). After filtering off contaminants, both the peptide forms and the FragI and MaxLFQ were re-normalized by vsn. In order the calculate consistent log2 fold change, missing values were replaced at the protein level by the lowest value of the corresponding sample. Ibaq values were calculated as described (Schwanhüusser et al., 2011). The empirical cumulative distribution of the log2 fold changes was obtained from the ecdf function of the R base package.

For the analysis of the adapted tachyzoites, three technical and three biological replicates were subjected to whole-cell shotgun mass spectrometry. Cell pellets were re-suspended in 8 M urea/100 mM Tris-HCl pH. Proteins were reduced and alkylated as described elsewhere (Braga-Lagache et al., 2016). Samples were diluted by addition of 1:10-volume of 50 mM Tris/HCl pH 8.0 before protein precipitation with 5 volumes of cold (-20°C) acetone over night at -20 °C. Proteins were pelleted by centrifugation at 16'000 *x*g for 10 min at 4°C and the acetone supernatant was discarded. Pellets were dried in ambient air for 15 min and stored at -20°C until use. Proteins were re-dissolved in 8 M urea/50 mM Tris-HCl pH 8 and protein content determined by bicinchoninic acid (BCA) assay after 1:10 (v/v) dilution with water. Urea was then diluted to 1.6 M by addition of 20 mM Tris-HCl pH 8/2 mM calcium

dichloride before digestion of the proteins with trypsin over-night at room temperature. Digestions were stopped by adding 1:20-volume of 20% (v/v) tri-fluoroacetic acid (TFA, Fluka). The digests underwent nano-liquid chromatography analysis using a Nano Elute2 (Bruker Daltonics, Bremen, Germany) connected to a timsTOF HT (Bruker Daltonics, Bremen, Germany), via a CaptiveSpray source (Bruker, Bremen, Germany). The analysis was conducted with an endplate offset of 500 V, a drying temperature of 200°C, and with the capillary voltage fixed at 1.6 kV. For the chromatographic separation, a volume of 5 µL corresponding to 500 ng protein digest was loaded onto a pre-column (C18 PepMap 100, 5 µm, 100A, 300 µm i.d. x 5 mm length, ThermoFisher) and subsequently eluted in back flush mode onto a Bruker 10 cm pulled emitter column (ionOpticks) (1.9 µm, 75 µm) by applying a 30 minute gradient of 5% acetonitrile to 30% in water/0.1% formic acid, at a flow rate of 500 nl/min. The timsTOF HT was operated either in DDA or data-independent acquisition (DIA) mode using the Parallel Acquisition SErial Fragmentation (PASEF) mode. For the DDA method, the mass range was set between 100 and 1700 m/z, with 8 PASEF scans between 0.75 and 1.35 V s/cm2. The accumulation and ramp time were set to 100 ms. Fragmentation was triggered at 15,000 arbitrary units (au), and peptides (up to charge 5) were fragmented using collision induced dissociation with a spread between 20 and 75 eV.

The dia-PASEF acquisition method was set with 47 isolation windows of 26 m/z width, including an overlap of 1 m/z. Isolation windows were associated with ion mobility range between 0.7 to 1.45V s/cm^2. TIMS accumulation and separation were both set at 100 ms.

The DDA data were used to produce a spectral library with fragpipe (Yu et al., 2020) version 20.0 with the following parameters: database was *T. gondii* ME49 from the Eukaryotic Pathogen, Vector and Host Informatics Resource (Alvarez-Jarreta et al., 2024)(release 55), to which common contaminants were added; precursor and fragment mass tolerances were set to ±20 ppm and ±0.05 Da, respectively; protein digestion was set to trypsin, with a maximum of three missed cleavages; variable modifications allowed were oxidation on methionine and protein N-terminal acetylation; carbamidomethylation of cysteines was given as fixed modification; the minimum number of matched fragments was set to 5; validation was done with Percolator (MSBooster enabled); filtering was done at 1% FDR for protein level.

DIA data was analyzed by Spectronaut version 18.1.230626.50606 (Biognosis) with factory settings and the spectral library as described above, excluding single hit proteins. Potential contaminants were then removed for further analysis. Missing Spectronaut protein intensity values were imputed in the following manner: if there was at most one detection in a replicate group, then the remaining missing

values were imputed by a random draw from a Gaussian distribution of width 0.3 x sample standard deviation and shifted left from the sample mean mu by 2.5 x sample standard deviation; all other missing values were replaced by the Maximum Likelihood Estimation method (Silver et al., 2009) for differential expression tests using the moderated T-test (Kammers et al., 2015). For multiple test correction, the R tool fdrtool (Strimmer, 2008) was applied. Significance criteria using 20 imputation cycles were applied as described in Ref. (Uldry et al., 2022) (paragraph 4.9), imposing a minimum log2 fold change of ≥ 0.58 in absolute value, and a maximum adjusted *p*-value of 0.05 (the latter value reachable at asymptotically high log2 fold changes).

For each drug, three technical and three biological replicates were subjected to whole-cell shotgun mass spectrometry.

4.6 Evaluation of the effect of thiosemicarbazones on host immune cells and evaluation of the toxicity in a model organism

Before proceeding with *in vivo* experiments involving these compounds, it is essential to further investigate their potential side effects, particularly on the immune system and embryonic development. Given that mice are commonly used as model organisms for studying toxoplasmosis, an *in vitro* viability assay on murine splenocytes was conducted after treatment with thiosemicarbazones, to assess any potential immunosuppressive effects.

Additionally, the zebrafish embryo development test was performed to simulate congenital toxoplasmosis in a model organism and evaluate any potential damage to embryonic development following treatment.

4.6.1 Assessment of viability of murine splenocytes after treatment with C3 and C4 *in vitro* (AlamarBlue)

To perform this *in vitro* assay, spleens were aseptically collected from mice under the hood after the euthanasia. Splenocytes were isolated from the spleens as previously described (Păunescu et al., 2021). Shortly, the spleens were immersed immediately into 5 mL of RPMI 1640 with 10% FCS, penicillin/streptomycin 1%, glutamine 2mM and β-mercaptoethanol 55 µM in a 50 mL Falcon tube. The spleens were then disaggregated through a cell strainer of 40 µm using the top of a syringe and collecting the flow through in a 50 mL Falcon. The filter was washed with 10-15 mL of media. Samples were centrifuged at 1250 rpm, for 10-15 minutes at 4°C. Supernatant was discarded, the cell pellets

were resuspended in 3-4 mL of red blood cell lysis 1X and incubated for 4-5 minutes at RT. At this point at least 20 mL of medium was added to neutralize the lysis buffer. Another centrifugation in the same condition was performed, supernatant was discarded, and pellets resuspended in 4-5 mL of media. One mL of solution was filtered again in a new Falcon Tube to remove clumps and cells were counted by Trypan Blue (live cells with intact membranes were not coloured) and seeded in 96-well plates ($5x10^4$ cells/well, 100 µl/well). The splenocytes were either left unstimulated (negative control) or stimulated with ConA (5 mg/mL) or LPS (10 mg/mL), which are known to activate immune responses. The compounds being tested were prepared in DMEM 10% FBS and added to the cultures at concentrations of 0.1, 0.5, 1 e 2 µM. Cyclosporine A (CsA) was included as a positive control for strong immunosuppressive activity. After 48 h splenocyte viability was assessed using AlamarBlue assay, see paragraph **4.3.1**.

4.6.2 Effects of C3 and C4 on early zebrafish (*Danio rerio*) embryo development

Zebrafish embryo development assay was performed as described by Anghel et al., (2020).

Briefly, at 3 h post- fertilisation (hpf), zebrafish eggs were transferred into a Petri dish containing osmosis water at the tested drugs concentration (20, 10, 1 and 0.2 µM).

From there, viable eggs were transferred into the respective 24-well plate, with one egg/well in 1 mL of the same solution. For each concentration a 24-well plate was used and it contained 20 wells with the test solution at a given concentration and 4 wells without drug as internal controls (iC). The negative control plate consisted of 20 wells containing 1 mL of osmosis water. The solvent control plate consisted of 20 wells containing 1 mL of osmosis water with 0.1% DMSO. All plates were covered with sealing foil and the embryos were maintained at 28°C. Test solution was replaced every 24 h with fresh solution. Embryos were viewed and malformations or viability changes were assessed in a blinded manner using a Nikon eclipse TS100 light microscope at 10X magnification at 24, 48, 72 and 96 hpf (hour-post-infection), with plates kept on a heating pad at 26°C during observation and medium changes. At 96 hpf, all embryos were euthanized by immersion in a solution of pre-cooled 3-101 aminobenzoic acid ethyl ester (100 µg/L; MS222; Argent Chemical Laboratories, Redmond, WA, USA) and placed at –20°C for 24 h.

At the end of the assay the impact score (Si) of the drug was calculated subtracting the mean control score (Smean) from the assay score (Sassay). The assay score was calculated using a total of 20, that represents the number of eggs in each plate per concentration of the drug (Ne), from which 1 point is subtracted for every dead embryo (Nd), while 0.5 is subtracted for each malformation of the embryo

after the treatment (Nm), including non-hatched embryos at 96 hpf. The mean control score (Smean) was calculated in the same way, but referred to the average of negative (non-treated embryos) and solvent control scores. A negative Si indicated interference, while Si ≥0 implied no interference in embryo development.

Item	Formula
$S_{neg}, S_{DMSO}, S_{assay}$	$N_e - N_d - (\frac{N_m}{2})$
S_{mean}	$\frac{(S_{neg} + S_{DMSO})}{2}$
S_i	$S_{assay} - S_{mean}$

Figure 11. Proposed algorithm for the zebrafish embryo development assay score calculation. Sneg= negative control score (no compound, no DMSO); S_{DMSO}= solvent control score (no compound, 0.01% DMSO); Sassay= assay score (score for each compound concentration); Smean = control mean score; Ne = number of embryos introduced per test item (20 per compound and concentration); Nd = number of dead embryos after 96 hpf (score –1 for each dead embryo); Nm = number of embryonal malformations observed after 96 hpf (score –0.5 for each malformation, including non-hatched embryos at 96 hpf); Si= impact score of the drug (Anghel et al., 2020).

4.7 *In vivo* efficacy of the compounds in the murine model of cerebral toxoplasmosis

Once assessed that thiosemicarbazones have a good effect *in vitro* against *T. gondii* and did not show immunosuppressive effects on the murine host splenocytes, the next step was testing the compounds *in vivo* in the murine model of cerebral toxoplasmosis. Mice are the most widely used model for studying toxoplasmosis infection, given that their immune system shares many similarities with the human one (Masopust et al., 2017), making them an effective model for understanding the pathogenesis and immune response to *T. gondii*.

4.7.1 Drug stock preparation

C3 was dissolved in DMSO and then diluted 1:10 in H_2O 15% DMSO before oral administration.

C4 was dissolved in DMSO and then diluted 1:10 in corn oil before oral administration.

Corn oil at 25% DMSO was used as control.

4.7.2 Thiosemicarbazones efficacy assessment in CD1 mice orally infected with TgShSp1 oocysts

Animal experiments were approved by the Animal Welfare Committee of the Canton of Bern, Switzerland (license BE48/2023), and mice were handled in strict accordance with practices to minimize suffering. Forty-eight female CD1 mice, 8 weeks of age, were purchased from Charles River (Sulzberg, Germany) and were maintained in a common room under controlled temperature and a 14 h/10 h light/dark cycle in the animal facility for two weeks for adaptation before the experiments.

Mice were randomly distributed into different groups: i) negative control group (C-) with non-infected (challenged with PBS) and non-treated mice (n = 2), ii) positive control group 1 (C+) with infected and non-treated mice (n = 4), iii) placebo control group (C+) with infected but non-treated drug mice (corn oil 25% DMSO was used as placebo) (n = 8) and two treatments group after infection: iv) C3 dosed at 10 mg/kg/day (n = 8), v) C4 dosed at 10 mg/kg/day (n = 8).

Infections were carried out with 120 TgShSp1 oocysts by peroral application at day 0, the C- group received PBS only. Placebo, C3 and C4 treatments were started at 3 days post infection (pi) by oral gavage at 10 mg/kg/day for 5 days.

Two additional non-infected groups of 8 mice each were included to study the *in vivo* effect of C3 and C4 treatment on spleen cells and one group of naïve mice was left as negative control (n = 2). During and following treatments all mice were monitored clinically for 4 weeks. Following euthanasia, blood, brain, eye, heart and spleens samples were collected to extract DNA and quantify parasite load.

4.7.2a DNA extraction from mice organs

DNA was extracted using the NucleoSpin DNA RapidLyse Kit (Macherey-Nagel, Oensingen, Switzerland) according to standard protocols. First, 500 µl of RNA Lysis Buffer (RLY) containing 40 µl/mL of Liquid Proteinase K was added to each sample and shredded 4 times for 45 seconds at 5.5 m/s (letting the sample rest in ice for 5 minutes after every shredding) in the Fastprep-24 rotor-stator homogenizer (MP Biomedicals Germany GmbH, Eschwege, Germany), in order to digest the organs. To activate the digestion, samples were incubated 3 h or ON at 56°C, 900 rpm. A part of the lysate from each sample (160 µl) was transferred in a new tube to go on with the DNA extraction, following the standard protocol of the kit. DNA concentrations were quantified using the Nanodrop spectrophotomer (Thermofisher Scientific, Scientific, Reinach, Switzerland) or QuantiFluor double-stranded DNA (dsDNA) system (Promega, Madison, WI, USA).

4.7.2b Parasite load quantification by Real-time PCR (529 bp gene detection)

Quantification of parasite load in the organs was carried out by a Real-time PCR following the protocol described by (Hänggeli et al., 2022) using 529 bp gene as a target, a marker commonly used for the diagnosis of toxoplasmosis, to confirm (or not) the presence of *T. gondii* DNA. Quantitative Real-time PCR was performed with the Bio-Rad CFX 96 QPCR instrument (Biorad Laboratories AG, Cressier, Switzerland) and for each reaction DNA concentrations were adjusted to 5 ng/µl, qPCR reactions were performed in a final volume of 10 µl containing 1x SensiFast master mix (Bioline, Meridian Bioscience, Cincinnati, OH, USA), 0.5 µM of reverse and forward primers, 0.1 µM of 529rpeQ-P probe, 0.3 mM dUTP, and one unit of heat-labile Uracil DNA Glycosylase (UDG). Amplification was performed in the Bio-Rad CFX 96 QPCR instrument (Biorad Laboratories AG, Cressier, Switzerland) using the following thermal profile: (1) initial incubation of 10 min at 40°C, followed by (2) denaturation step of 5 min at 95°C and (3) 40 cycles of two-step amplification (10 s at 95°C and 20 s at 62°C). For quantification, a standard curve was created based on a 10-fold serial dilution of DNA from *T. gondii*, equivalent to tachyzoites number ranging from 1 $\times 10^4$ to 1 per 4 µl. The parasite load was expressed as number of tachyzoites per 20 ng of DNA. Negative controls were inserted in each plate. Statistical analyses were performed using Microsoft Excel software package (Microsoft, Redmond, WA, USA). Comparisons of the parasite burdens between groups were conducted with the non-parametric Kruskal-Wallis test, followed by the Mann-Whitney-U test.

The oligonucleotides sequences are described in **table 3.**

Table 3. Sequence of primers and TaqMan probe designed in this study.

529rpe-F	5'-AGGAGAGATATCAGGACTGTAG-3'
529rpe-R	5'-GCGTCGTCTCGTCTAGATCG-3'
Probe 529rpeQ-P	FAM- GAGTCGGAGAGGGAGAAGATGTT- BHQ

4.7.2c Histopathology of mice brains

Mice brains from three groups (one mice per group: a positive control group and two treatment groups dosed with C3 and C4 at 10 mg/kg/day) were fixed in 10% neutral buffered formalin (NBF) for at least 48 hours. The fixed brains were dehydrated through increasing ethanol concentrations and cleared with xylene. The tissue was then embedded in paraffin, trimmed and cut into 3-5 mm thick sections using a microtome. Sections were deparaffined, rehydrated and stained with hematoxylin and eosin (H&E) for histopathological analysis under a light microscope (Bancroft and Layton, 2013).

4.*7.3* Assessment of susceptibility of murine splenocytes to C3 and C4 *in vivo*: measurement of viability and proliferation

These experiments were conducted as described by Müller et al., 2022b. Briefly, spleens from mice treated with the compounds were aseptically collected under the hood after the euthanasia. Splenocytes were isolated from the spleens and seeded in 96-well plates ($5x10^4$ cells/well). For proliferation/viability assays, splenocytes were either left unstimulated or were stimulated with Concanavalin A (ConA, 5 µg/mL), lipopolysaccharide (LPS, 10 µg/mL), ConA plus C3 or C4 (0.1–2 µM) or LPS plus C3 or C4. Experiments were done in quadruplicate in 200 µL/wells, and cultures were maintained at 37°C/5% CO_2 for 72 h. The proliferative responses of splenocytes were measured using a BrdU cell proliferation kit (QIA58, Merck Millipore, Burlington, MA, USA) according to the instructions provided by the manufacturer and absorbance measurements were done at 450/540 nm in an Hidex Sense multimode plate reader (Hidex, Turku, Finland). To measure the impact on viability, AlamarBlue assay was used (Desiatkina et al., 2022a): resazurin (0.1 mg/mL) was added and the fluorescence intensity was measured at 530/590 nm at 0, 1, 2, 3, 4 or 5 h. Differences were calculated by subtracting time point 0 values from each time point. Data are presented as mean of emission +/− SD for the indicated numbers. Data comparisons between groups were examined using a Student's t-test.

5. Results

5.1 Toxicity of thiosemicarbazones on host cells *in vitro*

5.1a AlamarBlue assay with copper complexes and their thiosemicarbazone ligands

All the compounds, including thiosemicarbazone ligands and their respective copper complexes, were tested at concentrations of 5, 10 and 20 µM on HFF, to evaluate potential cytotoxicity on the host cells. Drug concentrations that led to 50% reduction in cell viability compared to fully viable controls of cells non-treated (set to 100%) were calculated using the logit-log algorithm in Microsoft Excel®. The clustered columns in Figure 12 display the results obtained, showing that HFF maintained a high percentage of viability with all the tested treatments. No significant toxicity was detected, indicating that these compounds were safe for further testing against the parasite *T. gondii*.

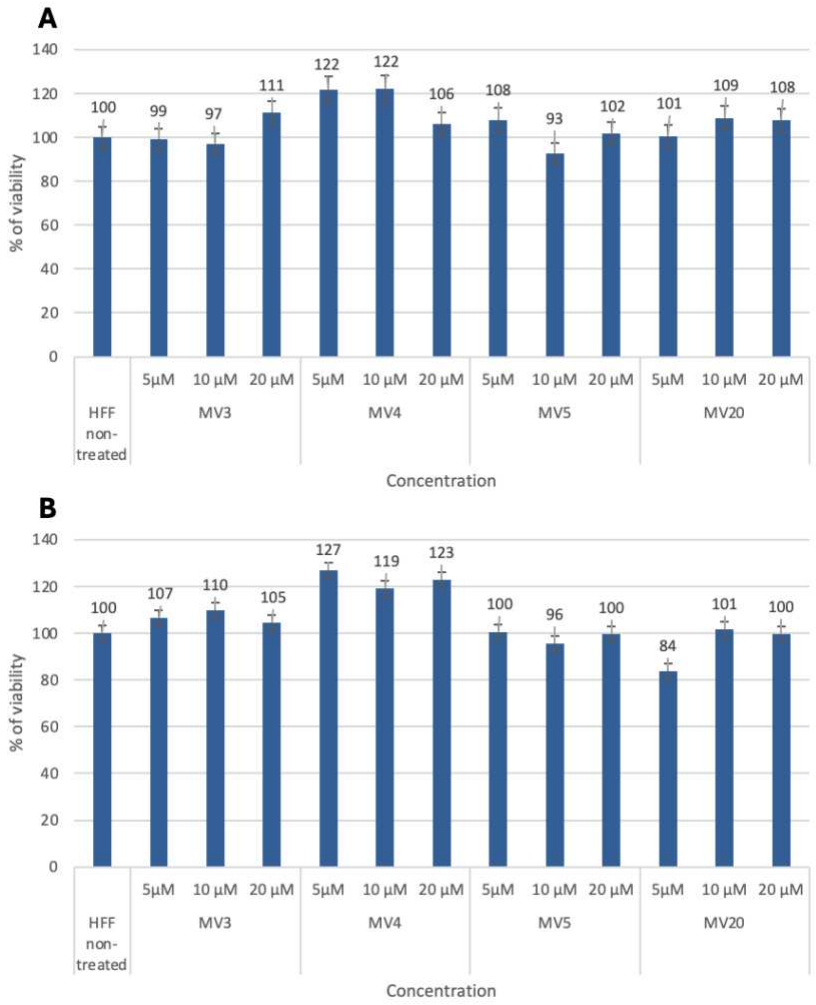

Figure 12: Clustered columns chart showing the *in vitro* activities at 5, 10 and 20 µM of the thiosemicarbazone ligands (A) and of their 4 copper complexes (B) on HFF viability, measured using AlamarBlue assay. On the x-axis, the tested concentrations are reported, while on the y-axis, the percentage of viability is shown. The percentage of viability is obtained by calculating the ratio between the mean values of each treatment and the viable non-treated controls (set to 100%), then multiplying by 100.

5.1b AlamarBlue assay with gold complexes and their thiosemicarbazone ligands

Three gold(III) complexes (C1, C2, C3) and one thiosemicarbazone ligand (C4) were tested on HFF at different concentrations, starting from 50 µM and decreasing to 0.8 µM through serial dilutions, to select compounds with low IC_{50}.

Drug concentrations that led to 50% reduction in cell viability compared to fully viable controls of cells non-treated (set to 100%) were calculated using the logit-log algorithm in Microsoft Excel®.

C1, C2 and C3 demonstrated IC_{50} values of **25.5** µM [22.3 - 29.2], **12.1** µM [10.5 – 14], **24.3** [18.1 – 32.8], respectively (In figure 13 are reported the dose *vs* response curves).

However, no reduction in HFF viability was detected with C4 at 25 µM (Table 4).

All the compounds were subsequently tested for their activity against the parasite.

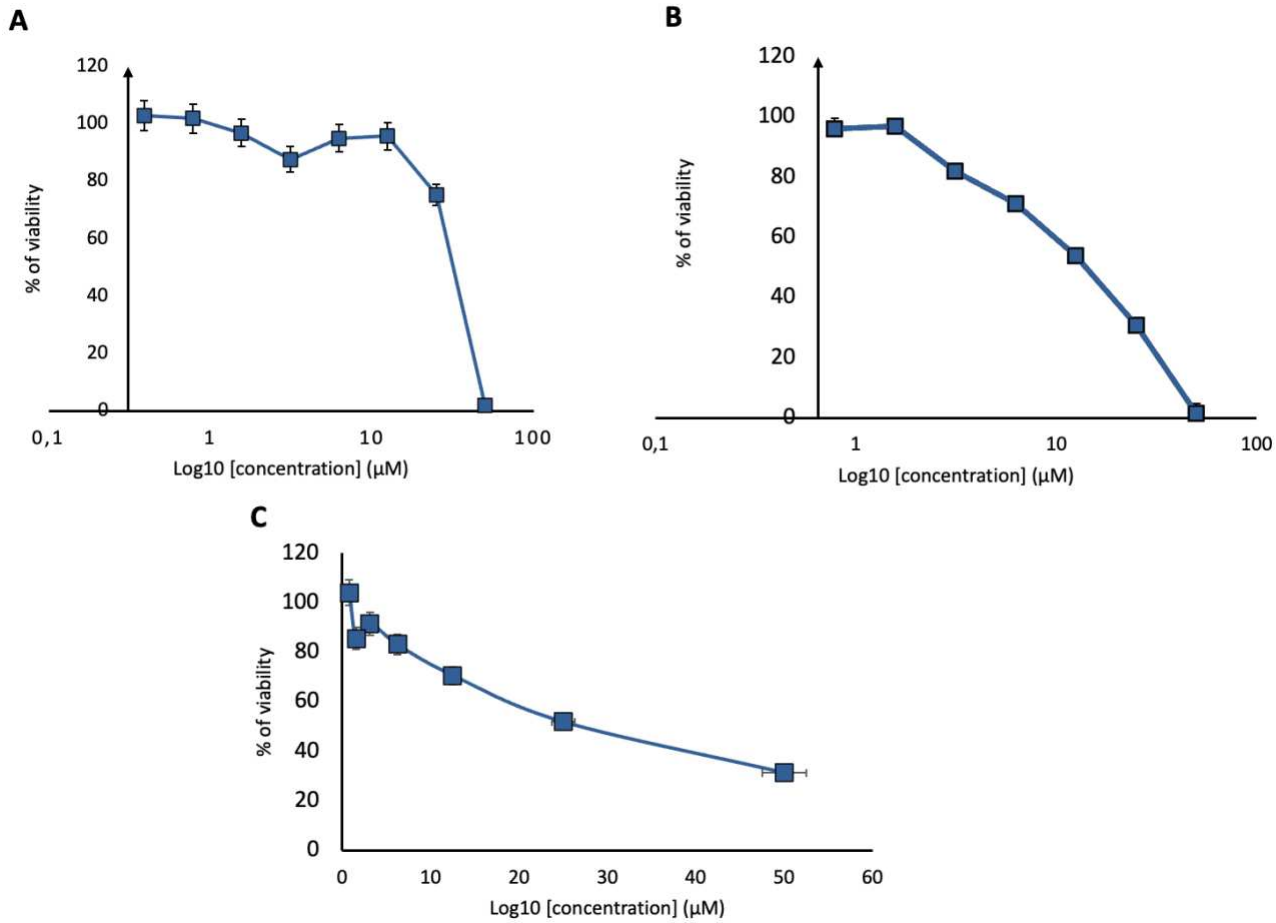

Figure 13: Dose *vs* response curves of gold complexes C1 (A), C2 (B) and C3 (C) on HFF, obtained using Alamar Blue assay. On the X-axis, the $\log_{10}$ of the tested concentrations is reported, while on the Y-axis, the percentage of viability is shown. The percentage of viability is obtained by calculating the ratio between the mean values of each treatment and the viable non-treated controls (set to 100%), then multiplying by 100.

Table 4: Results of Alamar Blue performed on HFF with C4. In the table are reported the percentages of viability of each concentration tested and the correspondent standard error (SE).

C4 activity							
Concentrations (µM)	**25**	**13**	**6**	**3**	**2**	**1**	**0,62**
% of viability	95,0	96,4	95,5	99,0	108,8	109,9	92,1
SE	2,5	3,4	4,6	2,8	1,4	1,7	2,8

5.2 *In vitro* efficacy of thiosemicarbazones on *T. gondii*

5.2a Efficacy of copper complexes and their thiosemicarbazone ligands on *T. gondii* using β-galactosidase assay

All the compounds, including thiosemicarbazone ligands and their respective copper complexes, were tested at concentrations of 5, 10, and 20 µM on *T. gondii* tachyzoites to evaluate their efficacy against

the parasite. The results, displayed in the clustered columns in Figure 14, showed no significant activity against the parasites. As a result, none of these compounds was selected for further analysis.

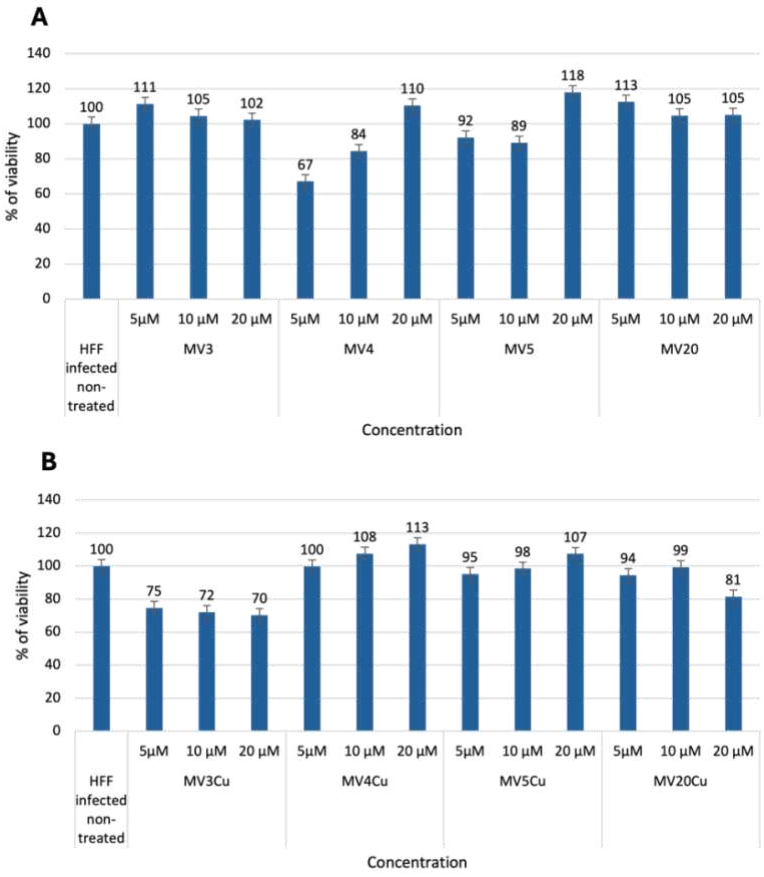

Figure 14: Clustered columns chart showing the *in vitro* activities at 5, 10 and 20 µM of the thiosemicarbazone ligands (A) and of the 4 copper compounds (B) on *T. gondii* β-gal, measured using β-galactosidase assay.

5.2b Efficacy of gold complexes on *T. gondii* using β-galactosidase assay

Three gold(III) complexes (C1, C2, C3) and one thiosemicarbazone ligand (C4) were tested on *T. gondii* at different concentrations, starting from 20 µM and decreasing to 0.3 µM through serial dilutions. Drug concentrations that led to 50% reduction in parasites viability compared to fully viable controls of infected cells non-treated (set to 100%) were calculated using the logit-log algorithm in Microsoft Excel®. C1 and C2 showed IC_{50} values against *T. gondii* of **11.5** µM [9.1 – 14.5] and **7** µM [5.5 – 8.9], respectively (shown in figure 15 through the dose *vs* response curves).

However, additional experiments were conducted with C3 and C4 at lower concentrations, as the initial testing range (20 µM to 0.3 µM) still left a high number of viable parasites, making it impossible to calculate the IC_{50}. New dilutions for these two compounds were prepared, starting from 10 µM and decreasing to concentrations in the picomolar range.

Additional experiments showed that C3 and C4 had IC_{50} values against *T. gondii* of **0.028** µM [0.027 – 0.030] and **0.030** µM [0.040 – 0.020], respectively (shown in figure 15 through the dose *vs.* response curves). Similar results were obtained when compounds were added 3 h after host cell invasion: C3 showed IC_{50} values ranging between 0.020 and 0.026 µM and C4 showed IC_{50} values ranging between 0.015 and 0.025 µM.

At this point the SI of each compound was calculated and reported in the table below:

Table 5: IC_{50} of each compound calculated on HFF and on *T. gondii* β-gal and correspondent SI.

Compounds	**IC_{50} on the parasite when added concomitantly to infection**	**IC_{50} on the parasite when added 3 h post- infection**	**IC_{50} on HFF**	**SI**
	T. gondii β-gal (µM)	*T. gondii* β-gal (µM)	Toxicity (µM)	(IC_{50} on HFF/IC_{50} on *T. gondii RH* β-gal)
C1	**11.5** [9.1 – 14.5]	/	25 [22.3 – 29.2]	2
C2	**7** [5.53 – 8.89]	/	12.1 [10.5 – 14]	1.7
C3	**0.028** [0.027 – 0.030]	**0.023** [0.020 – 0.026]	24 [18.1 – 32.8]	**240**
C4	**0.030** [0-040 – 0.020]	**0.020** [0.015 – 0.020]	>25	**>240**

Based on the results obtained, among the four compounds tested, only C3 and C4 demonstrated a promising selectivity index (SI) and a good efficacy against the parasite at very low concentrations without showing toxicity to the host cells. These findings suggested their potential as promising therapeutic candidates. Consequently, both compounds were chosen for further investigations, including studies to explore their mode of action and additional *in vitro* experiments focused on assessing their toxicity.

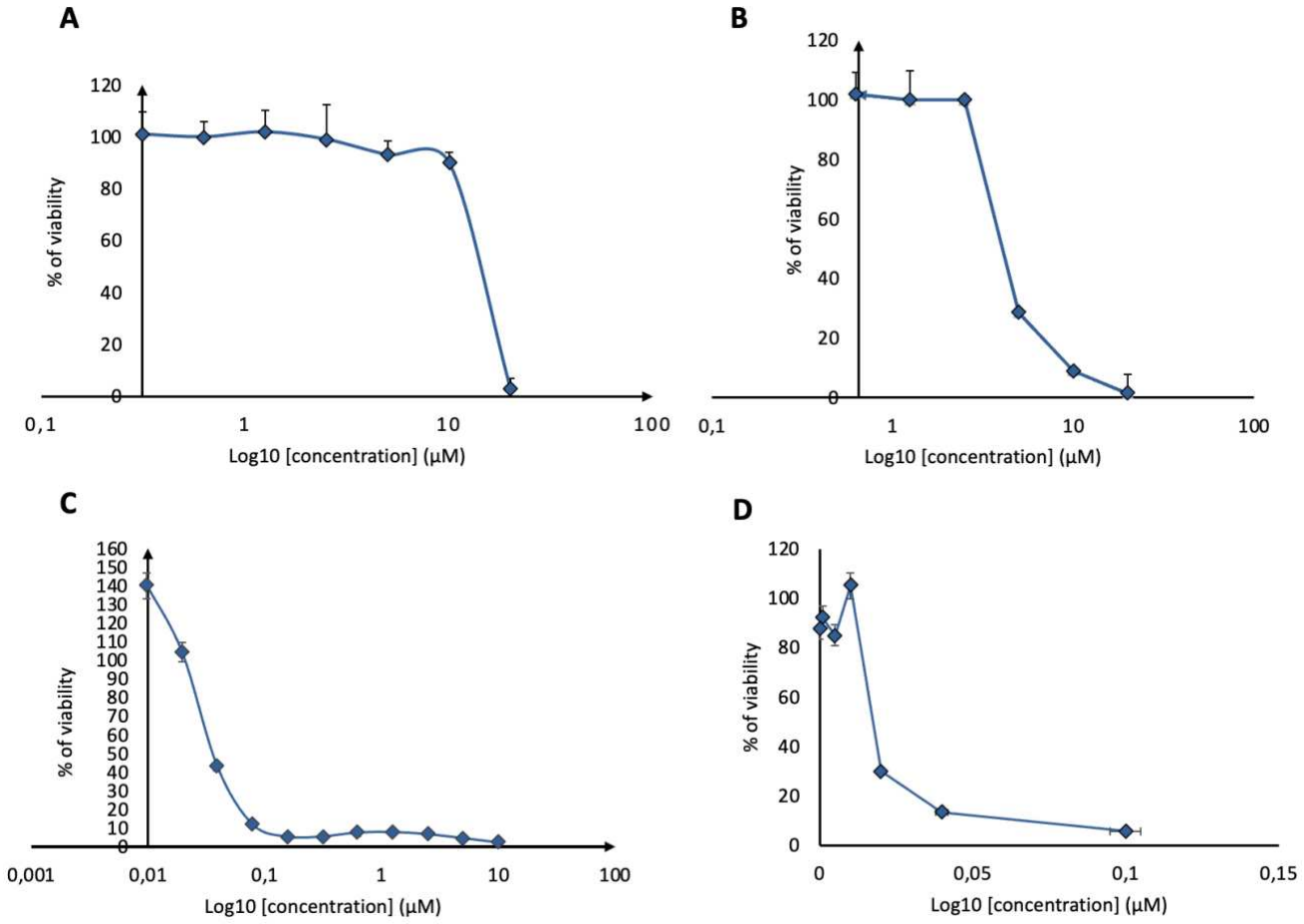

Figure 15: Dose *vs* response curves of gold complexes C1 (A), C2 (B), C3 (C) and C4 (D) on *T. gondii* β-gal, obtained measuring β-galactosidase enzyme activity (*Toxo* β-gal assay). On the x-axis, the $\log_{10}$ of the tested concentrations is reported, while on the y-axis, the percentage of viability is shown. The percentage of viability is obtained by calculating the ratio between the mean values of each treatment and the viable non-treated controls (set to 100%), then multiplying by 100.

5.2c Efficacy of gold complexes and their thiosemicarbazone ligands on *T. gondii* ME49 wild-type and adapted clones to the treatment

IC_{50} was determined first on *T. gondii* β-gal, a transgenic type I strain with RH background (see paragraph **5.2.b**).

Here results of the IC_{50} and minimum inhibitory concentration (MIC) values calculated for the type II *T. gondii* ME49 wild-type (WT) strain, in comparison to clones adapted to treatment, are reported. IC_{50} values were determined using Real-time PCR, while MICs were assessed through microscopic observation. IC_{50} values were determined by quantitative Real-time PCR and are given at 95% confidence interval (CI); LI is the "Inferior Limit" of CI and LS is the "Superior Limit" of CI. Both compounds (C3 and C4) showed similar IC_{50} values for *T. gondii* ME49 WT strain and the three clones adapted to each treatment (Figure 16), indicating that adaptation was lost after freezing/thawing

cycles, suggesting only a temporary adaptation to the drug exposure. The MIC values were also consistent across all tested strains, remaining at 25 µM (Table 6). These findings suggest that *T. gondii* did not develop permanent resistance to C3 or C4 *in vitro* but rather transiently adapted to the stress induced by the drugs through a reversible mechanism.

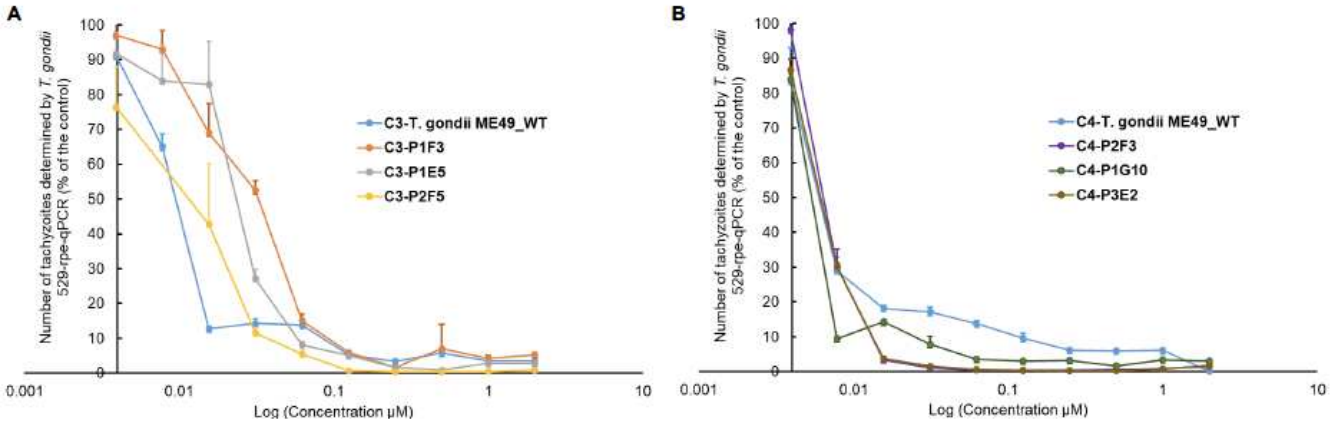

Figure 16: Dose-response curves for the compounds C3 (A) and C4 (B) against *T. gondii* ME49 WT and their respective adapted clones (three per drug) as determined by quantitative PCR.

Table 6: Half maximal inhibitory concentrations (IC_{50}) and minimal inhibitory concentration (MIC) of the gold (III) complex C3 and its C4 ligand against *T. gondii* ME49 WT tachyzoites, and three cloned strains, each derived from C3-adapted or C4-adapted *T. gondii*.

C3	**IC_{50} (nM)**	**MIC (µM)**
T. gondii ME49 wildtype (WT)	31 ([16–62)	25
P1F3	45 (28–70)	25
P1E5	90 (54–150)	25
P2F5	51 (31–84)	25
C4		
T. gondii ME49 wildtype (WT)	13 (6–27)	25
P2F3	11 (6–18)	25
P1G10	10 (4–23)	25
P3E2	6 (4–9)	25

5.3 Mechanism of action of C3 and C4 compounds

5.3a TEM results

To detect possible ultrastructural changes in tachyzoites exposed to C3 and C4, treated and untreated parasites were comparatively analyzed by transmission electron microscopy (TEM).

T. gondii ME49 tachyzoites cultured without compounds (Figure 17) went through intracellular proliferation by endodyogeny within a parasitophorous vacuole, separated from the cytoplasm by a parasitophorous vacuole membrane (PVM). Tachyzoites showed the typical hallmarks of apicomplexans including secretory organelles such as rhoptries, micronemes and dense granules and a conoid situated at the apical pole. Tachyzoites have a single mitochondrion composed of branched tubules, of which only parts are visible in any given section plane, exhibiting densely packed cristae within an electron dense matrix. Normally parasites proliferate by endoduogeny, and in rapidly dividing cultures multiple newly formed tachyzoites were often seen emerging from a residual body. At 6–12 h after initiation of drug treatments with C3 (Figure 18) and C4 (Figure 19), few but distinct changes were detectable. For instance, a large portion of parasitophorous vacuoles (> 50%) were surrounded by a multi-layered parasitophorous vacuole membrane (Figure 18A-C; Figure 19A), as opposed to the typical single membrane surrounding non-treated parasites. At these early time points, tachyzoites in C3-treated cultures, however, did not appear to be structurally altered and underwent cell division, while approximately 30% of parasites in C4 treated cultures exhibited an aberrant cytoplasmic organization, most notably with increased vacuolization and “empty spaces” forming between the nuclear membrane and the cytoplasm of tachyzoites (Figure 19C and D). At 24 h of C3 treatment, such cytoplasmic alterations were also visible occasionally in 10-20% of tachyzoites (Figure 18D and E) and slight structural disturbances such as a partially dissolved matrix could be detected in the mitochondrion in C3-treated (Figure 18D) and C4-treated (Figure 19D) tachyzoites. At 48 h, C3-treated parasites had largely recovered, and only slight alterations could be seen in some, (< 5%) of tachyzoites in C4-treated cultures. In conclusion, the changes induced by treatments with C3 and C4 were rather mild and apparently only of a transient nature.

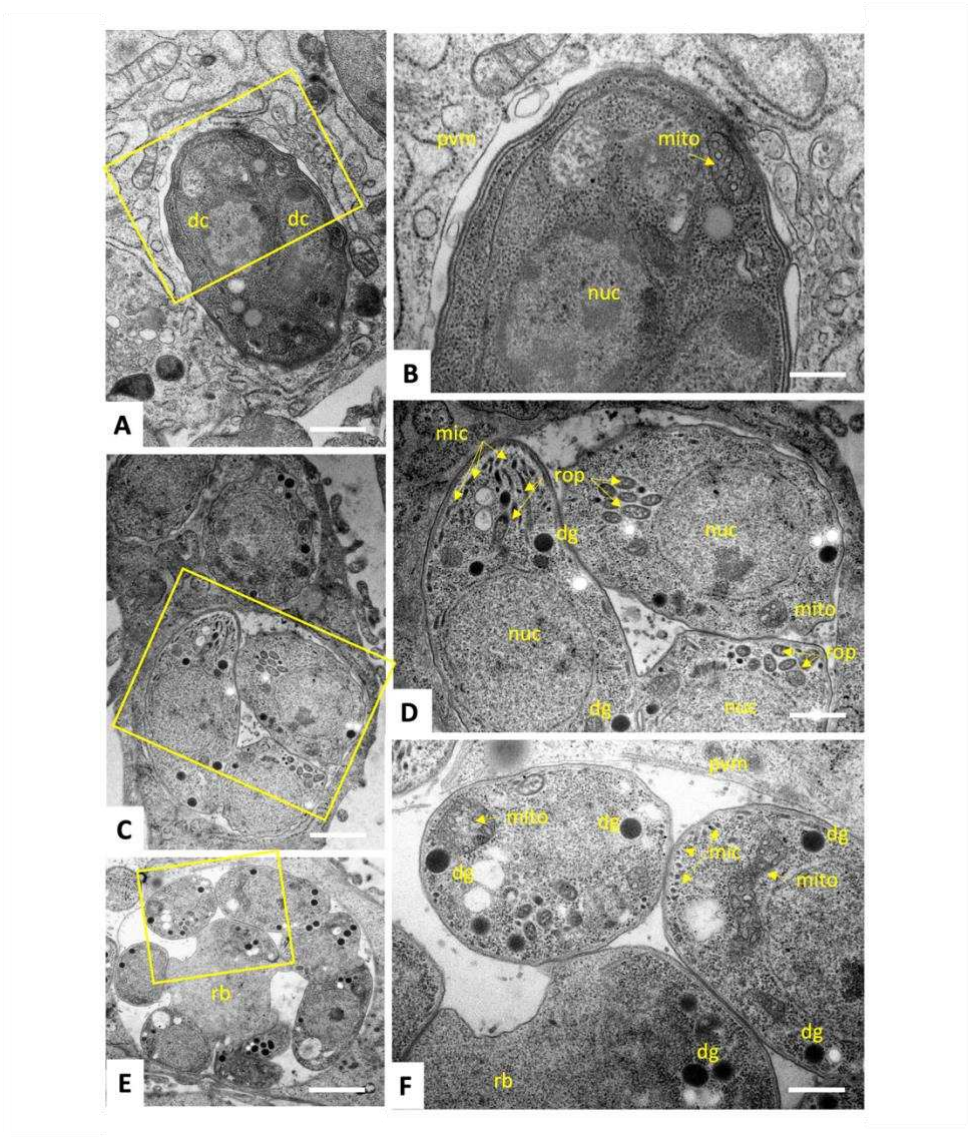

Figure 17: TEM of non-treated *T. gondii* ME49 tachyzoites (A-E) and tachyzoites treated with the positive control drug DB745. (A) A tachyzoite undergoing endodyogeny with the two emerging daughter cells (dc) at 12 h post-infection, situated within a parasitophorous vacuole. The boxed area in (A) is shown at higher magnification in (B). The vacuole is surrounded by the parasitophorous vacuole membrane (pvm). (C) A vacuole containing numerous tachyzoites at 24 h p.i., the boxed area is shown at higher magnification in (D), revealing rhoptries. (rop), dense granule (dg), micronemes (mic), the mitochondrion, and the nucleus (nuc). (E) Proliferating tachyzoites still attached to a residual body (rb) within a parasitophorous vacuole at 48 h of culture. (F) tachyzoites treated with DB745 during 48 h, showing tachyzoites (T) with severe structural alterations. Bars in A = 1 µm; B = 0.3 µm; C = 1.2 µm; D = 0.6 µm; E = 1.5 µm; F = 1.2 µm.

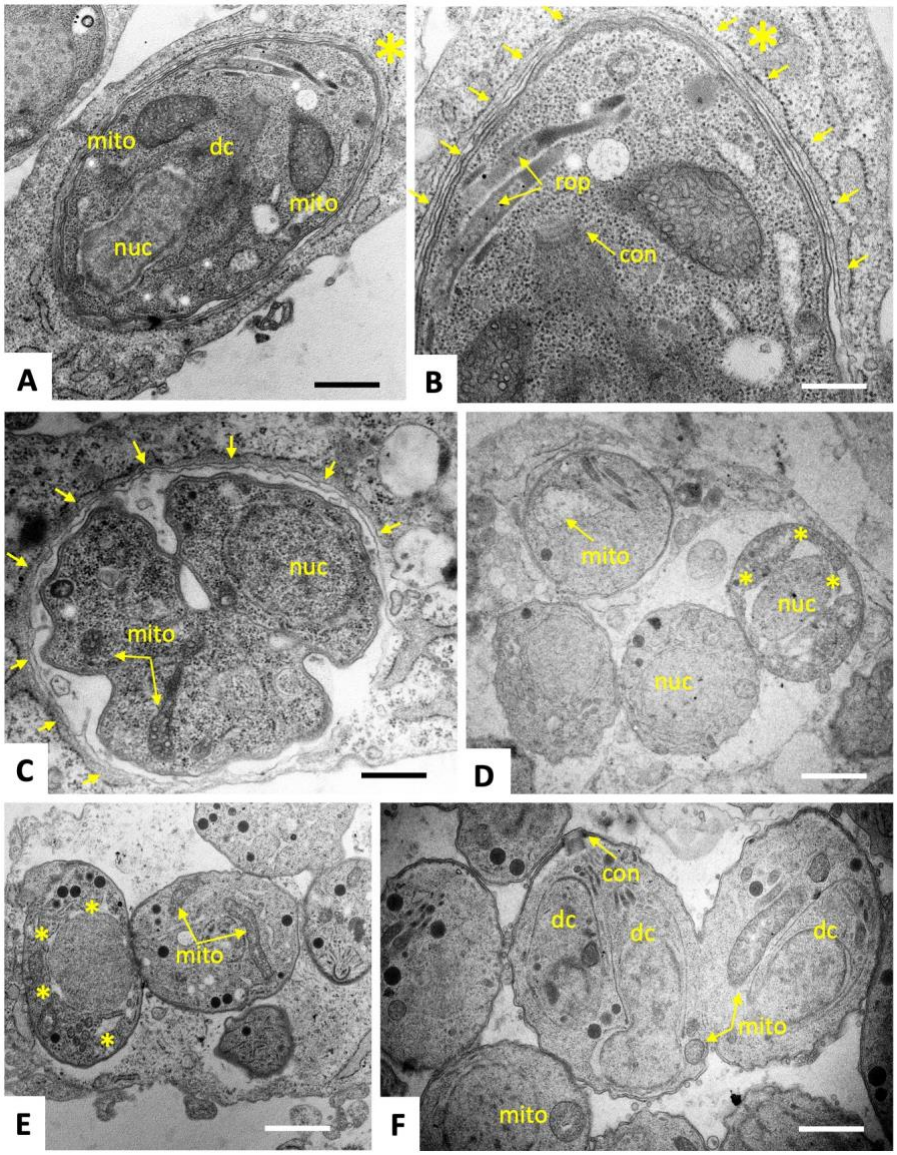

Figure 18: TEM of *T. gondii* ME49 tachyzoites grown in HFF and treated with 0.5 µM C3 during 6 – 12 h (A-C), 24 h (D, E) and 48 h (F). A tachyzoite undergoing endodyogeny with an emerging daughter cell (dc) after 6 h of treatment is depicted in (A), and the respective apical part, including the conoid of the daughter cell (con) is shown at higher magnification in (B). A large portion of the parasitophorous vacuole is surrounded by a multi-layered membrane (marked with small arrows). Similar findings were obtained after 12 h (C). At 24 h, the multilayered membrane surrounding the parasitophorous vacuole was no longer visible , but many parasites exhibited cytoplasmic alterations, leaving an empty space between the nuclear periphery and the cytoplasm, marked by asterisks (*) as shown in (D) and (E), and the matrix of the mitochondrion (mito) was partially dissolved. At 48 h, most tachyzoites had lost these ultrastructural alterations and had a normal appearance (F). Bars in A = 0.8 µm; B = 0.5 µm; C = 0.8 µm; D = 1 µm; E = 1 µm; F = 0.8 µm.

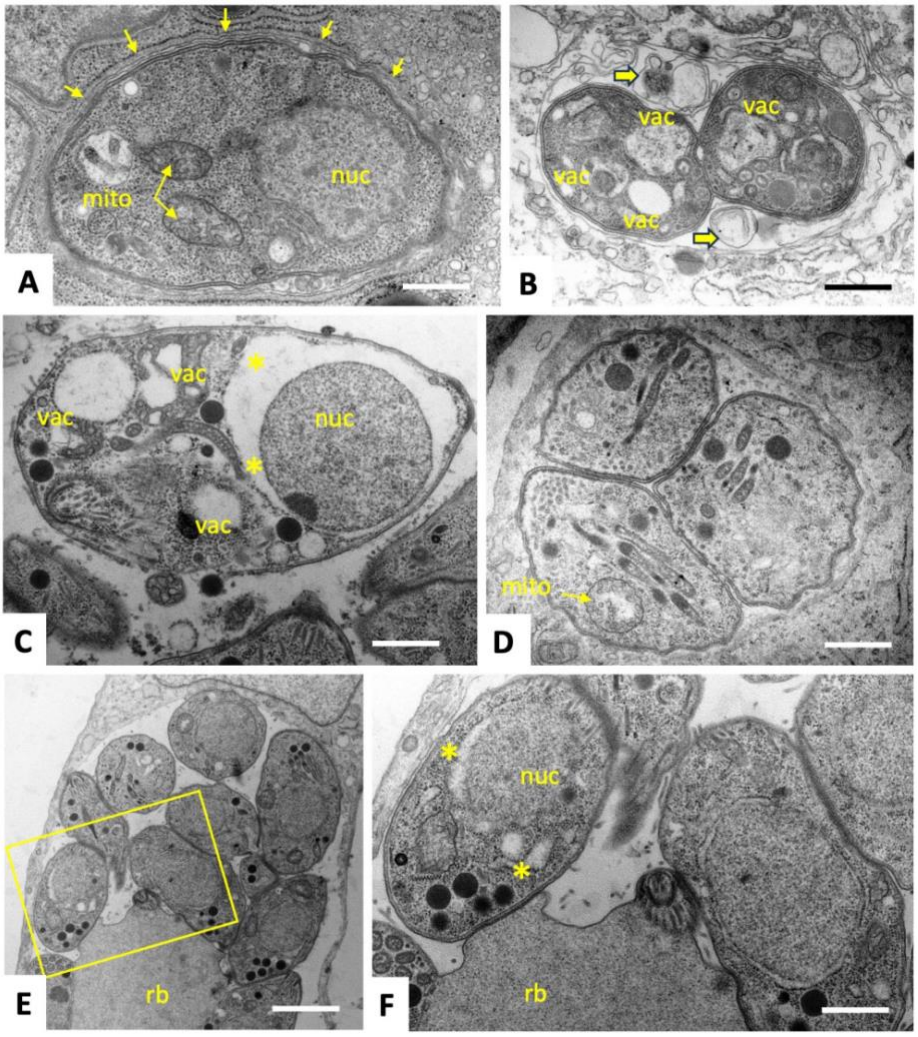

Figure 19: TEM of *T. gondii* ME49 tachyzoites grown in HFF and treated with 0.5 µM of C4 during 6h (A), 12 h (B, C), 24 h (D), and 48 h (E, F). The boxed area in (E) is depicted at higher magnification in (F). A multi-layered membrane, indicated by arrows surrounding the parasitophorous vacuole is evident after 6h of treatment (A). After 12 h of treatment (B and C), ultrastructural alterations become visible in a large number of parasites as evidenced by the accumulation of membranous components within the vacuolar space (thick arrows), increased numbers of cytoplasmic vacuoles (vac) and in some parasites a separation of the nucleus from the surrounding cytoplasm was visible (asterisks *, see C). In addition, pronounced alterations of the mitochondrial matrix (mito) were noted after 24 h (D). At 48 h after initiation of drug treatment (E, F), parasites exhibited a largely normal structural appearance, with the exception of some parasites still maintaining free spaces between nuclear membrane and cytoplasm (asterisks *). Bars in A = 0.6 µm; B = 1 µm; C = 0.5 µm; D = 0.9 µm; E = 2.2 µm; F = 0.9 µm.

5.3b TMRE Results

Since TEM suggested that treatment with C3 as well as C4 could partially impact on the ultrastructure of the mitochondrial matrix, the possibility that these compounds could alter the MMP was investigated. HFF cultures infected with *T. gondii* ME49 and uninfected cells were treated with 0.5 µM

of C3 or C4 for 3.5 h and then incubated with tetramethylrhodamine, ethyl ester (TMRE) for 30 min. The two known MMP inhibitors carbonyl cyanide 4-(trifluoromethoxy) phenylhydrazone (FCCP) and carbonyl cyanide m-chlorophenylhydrazone (CCCP) were used as positive controls.

As shown in Figure 20, TMRE uptake by mitochondria of FCCP or CCCP-treated cultures decreased by more than 80% compared to untreated cultures. Pyrimethamine (Pyr), the standard anti-*Toxoplasma* drug interfering in folate metabolism, did not impact on the MMP in tachyzoites or HFF, thus no change in TMRE uptake was noted. C4 and C3 treatments resulted in only a slight decrease of TMRE uptake in *T. gondii* ME49 infected (both of 17%) as well as uninfected HFF cultures (6% and 19%, respectively), also indicating that these compounds do not have a clear effect on the MMP.

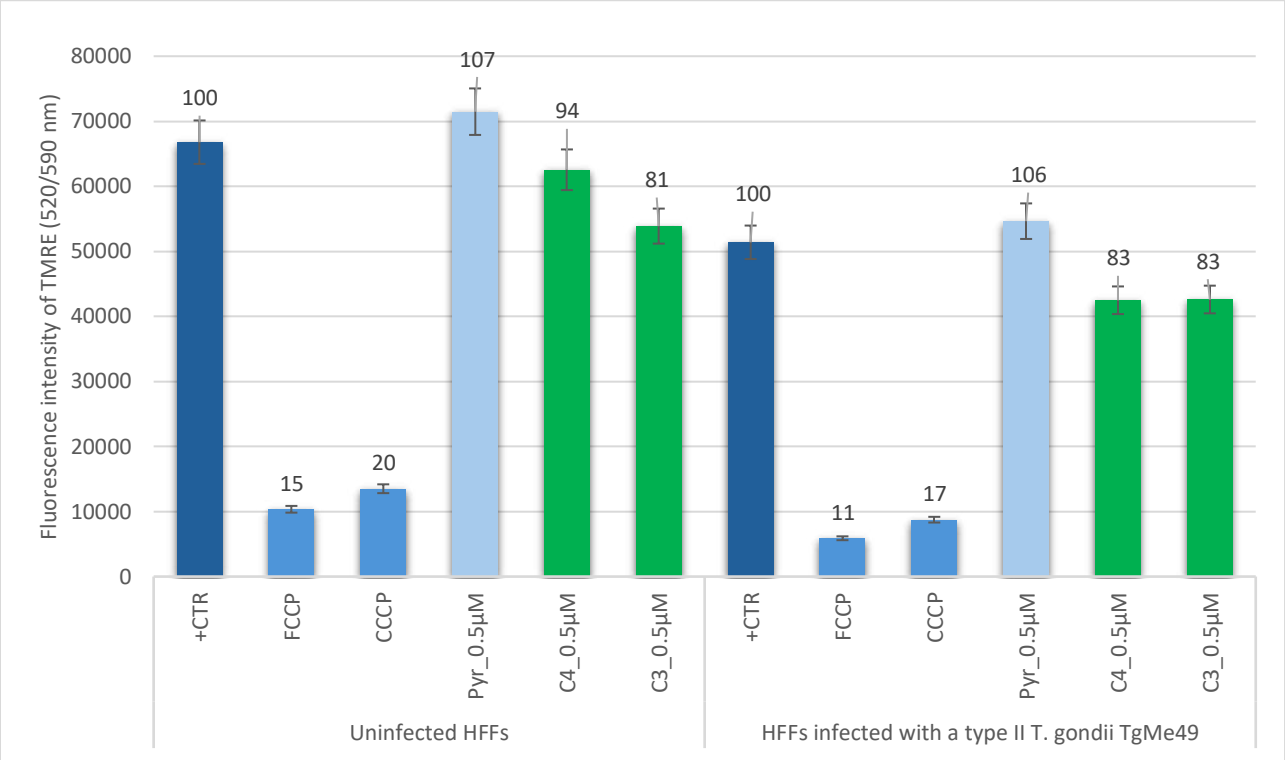

Figure 20: Measurements of the mitochondrial membrane potential by TMRE uptake in uninfected HFF and *T. gondii* infected HFF. TMRE uptake was measured in the presence or absence of either uncouplers (FCCP and CCCP), pyrimethamine (PYR) and C3 and C4. Assays were carried out in T25 tissue culture flasks, and the bars represent the mean of TMRE fluorescence. Standard deviations (SD) were calculated from three biological replicates. 100% of TMRE uptake was set for the control cells in absence of uncouplers or treatments and the corresponding percentage of TMRE fluorescence intensity is displayed on the top of each bar.

5.3c DAC results

To characterize proteins that specifically bind to either C3 and C4, or to both compounds, differential affinity chromatography (DAC) was combined with mass spectrometry (MS)-based quantitative proteomics of respective eluates. Tyrosine was included as a control compound, having a closely related

chemical structure but no effects on *T. gondii* proliferation. Overall, the analysis of the DAC eluates yielded 5137 unique peptides that were mapped to 630 *T. gondii* proteins (see Suppl. Table S1 for the full dataset) with equal intensity distribution among samples as displayed in Figure 21 A.

A total of 118 proteins were exclusively identified in the mock column eluate, whereas 512 proteins were found in proteomes obtained from eluates of the remaining three columns: C3, C4 and tyrosine. The largest proportion of the identified proteins (318/630) were exclusively C4-binding proteins, whereas only 14 proteins were exclusively C3-binding proteins (Figure 21 B). One hundred and sixty-two proteins were commonly identified in proteomes obtained from C3- and C4 columns, while only seven proteins were commonly found in the eluates of tyrosine, C3- and C4 columns (Figure 21 B). The fourteen proteins exclusively binding to the C3 column are shown in Table 7 as ranked by relative abundance. The ribosomal protein RPL27 (TGME49_262690) was the most abundant and constituted 42% of total C3-specific binding proteome (Table 7). Among the 318 proteins specifically binding to C4, the SAG-related sequence (SRS) protein SRS25 encoded by ORF TGME49_213280 was the most abundant (Table 8). A total of 11 SRS proteins were identified as specifically binding to C4, five of which were among the 20 most abundant proteins (Table 8). The hypothetical protein encoded by ORF TGME49_253690 was the second most abundant protein binding to C4 (Table 8). The ribosomal protein RPSA (ToxoDB ORF: TGME49_266060) was among the five most abundant proteins and represented 3% of the C4-specific binding proteome. A large portion (50/162; 31%) of the 162 proteins that bind to both C3 and C4 but were not found in Mock- or tyrosine-eluates, were ribosomal proteins. In Table 9, the twenty most abundant proteins which are shared between C3 and C4 columns are ranked according to their relative abundance. Most (18 out of 20) proteins commonly interacting with C3 and C4 were ribosomal proteins (Table 9).

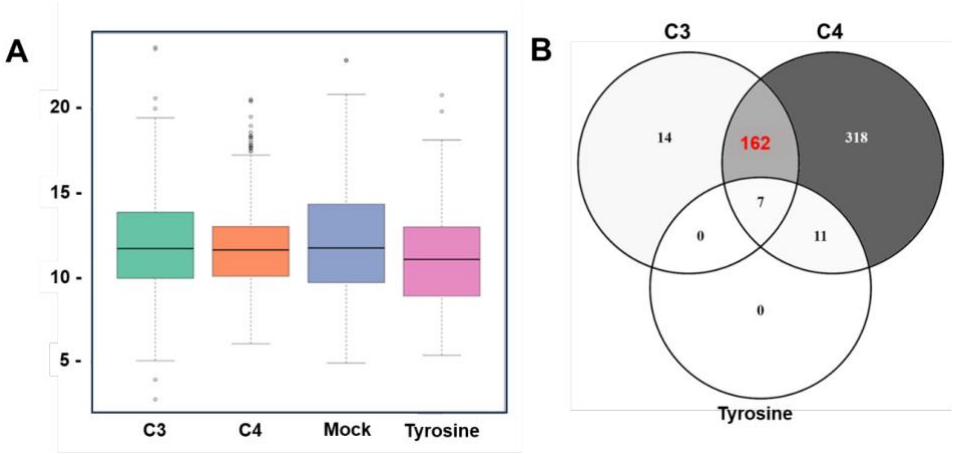

Figure 21: Identification of *Toxoplasma* proteins that bind to C3 and / or C4 by affinity chromatography coupled mass-spectrometry. **A**: box and whisker plot describing protein intensity distributions as calculated by the iBAQ (intensity Based Absolute Quantification) algorithm across eluates from C3 (gold(III) complex), C4 (salicyl-TSC ligand), mock and tyrosine columns. **B**: Venn diagram detailing the distribution of identified proteins (512) which did not bind to the mock column.

Table 7: List of the fourteen proteins specifically binding to C3 columns as identified by DAC followed by mass spectrometry. See Suppl. Table S1 for the full dataset. The relative abundances (rAbu) based on iBAQ sum up to a total of 1000000 for each sample. The proteins are listed according to their decreasing rAbu values.

ToxoDB ORF	Annotation	rAbu C3
TGME49_262690	ribosomal protein RPL27	741
TGME49_244110	nucleosome assembly protein (nap) protein	324
TGME49_309740	LSM domain-containing protein	100
TGME49_321520	hypothetical protein	91
TGME49_279390	proliferation-associated protein 2G4, putative	80
TGME49_319870	ubiquitin-conjugating enzyme subfamily protein	77
TGME49_313560	60S ribosomal protein L7a, putative	71
TGME49_248810	nuclear factor NF7	54
TGME49_231850	serine-threonine phosophatase 2C (PP2C)	51
TGME49_209170	hypothetical protein	43
TGME49_272400	casein kinase ii regulatory subunit protein	43
TGME49_227810	rhoptry kinase family protein ROP11 (incomplete catalytic triad)	35
TGME49_256050	signal recognition particle 14kd protein	28
TGME49_305340	corepressor complex CRC230	9

Table 8: List of the twenty most abundant proteins binding to C4 columns as identified by DAC followed by mass spectrometry. See Suppl. Table S1 for the full dataset. The relative abundances (rAbu) based on iBAQ sum up to a total of 1000000 for each sample. The proteins are listed according to their decreasing rAbu values.

ToxoDB ORF	Annotation	rAbu C4
TGME49_213280	SAG-related sequence SRS25	22200
TGME49_253690	hypothetical protein (putative transmembrane protein)	15804
TGME49_316710	hypothetical protein	4878
TGME49_266060	ribosomal protein RPSA	3977
TGME49_288245	hypothetical protein	2980
TGME49_231160	hypothetical protein	2724
TGME49_226570	hypothetical protein	1943
TGME49_285870	SAG-related sequence SRS20A	1652
TGME49_319560	microneme protein MIC3	1600
TGME49_289680	Ras-related protein Rab11	1461
TGME49_263630	hypothetical protein	1426
TGME49_214410	hypothetical protein	1316
TGME49_214770	small GTP binding protein rab1a, putative	1305
TGME49_225555	hypothetical protein	1284
TGME49_308020	SAG-related sequence SRS57	1218
TGME49_249900	adenine nucleotide translocator, putative	1171
TGME49_233450	SAG-related sequence SRS29A	1156
TGME49_308840	SAG-related sequence SRS51	1153
TGME49_245490	microneme protein MIC8	1126
TGME49_227920	hypothetical protein	1043

Table 9: List of the twenty most abundant common proteins binding to both C3- and C4-affinity columns as identified by DAC followed by mass spectrometry. See Suppl. Table S1 for the full dataset. The relative abundances (rAbu) based on iBAQ sum up to a total of 1000000 for each sample. The proteins are listed according to their decreasing rAbu values in the C3 dataset.

ToxoDB ORF	Annotation	rAbu C3	rAbu C4
TGME49_309810	ribosomal protein RPP2	3431	3473
TGME49_249250	ribosomal protein RPL35A	3406	214
TGME49_262670	ribosomal protein RPL18A	2651	522
TGME49_313390	ribosomal protein RPL6	2390	482
TGME49_261570	ribosomal protein RPL7A	2348	372
TGME49_205340	ribosomal protein RPS12	2026	493
TGME49_292130	ribosomal protein RPL13A	1678	447
TGME49_238070	glutaredoxin domain-containing protein	1666	332
TGME49_267060	ribosomal protein RPL14	1540	317
TGME49_320050	ribosomal protein RPL5	1492	223
TGME49_204020	ribosomal protein RPL8	1487	114
TGME49_238250	ribosomal protein RPL36	1422	517
TGME49_245680	ribosomal protein RPL21	1362	219
TGME49_260260	ribosomal protein RPP1	1354	2505
TGME49_314810	ribosomal protein RPL7	1325	666
TGME49_270380	ribosomal protein RPS13	1265	1846
TGME49_210690	ribosomal protein RPS6	1242	759
TGME49_215470	ribosomal protein RPL10A	1090	400
TGME49_218820	alba 2	1046	753
TGME49_232230	ribosomal protein RPL30	986	50

5.3d Long term treatments and generation of clones of drug adapted *T. gondii* tachyzoites

Further studies were carried out using *T. gondii* ME49 tachyzoites. While C3 and C4 treatments were highly effective in short term three-day-growth assays, treatments with both compounds at 0.5 µM for an additional four to eight days revealed that parasites quickly resumed proliferation despite continuous drug pressure. To investigate the actual drug susceptibility of such drug-adapted strains, C3 and C4-adapted tachyzoites were cloned, and three clones/drug were frozen as stabilates and stored at -150°C. Subsequently the stabilates were thawed and subjected to IC_{50} and MIC determinations and results are summarized in Table 6 and Figure 16 (see paragraph **5.2c**). For both drugs, the IC_{50} values for the *T. gondii* ME49 tachyzoites representing WT strain and the C3 and C4-adapted strains (three clones each), were in the similar range, suggesting that the effect was lost after freezing/thawing and

that parasites had only transiently adapted to increased drug concentrations. MIC values were in the same range (25 µM) for all strains tested. Taken together, these findings indicate that *T. gondii* did not develop *in vitro* resistance against C3 or C4, but only a transient adaptation to the environmental stress induced by C3 and C4, through a mechanism that was reversible.

5.3e Proteomic analysis analysis of *T. gondii* ME49 clones recovered after *in vitro* adaptation to C3 and C4

The *T. gondii* ME49 WT strain and the six clones derived from C3- and C4-treated cultures (three clones per drug) were analyzed by whole cell shotgun proteomics to identify differentially expressed (DE) proteins. As shown in suppl. Table S2, a total of 3860 proteins were identified. To reliably identify differentially expressed proteins in C3 and/or C4 treated tachyzoites *versus* non-treated WT, only those with fold change FC ≥ 1.5 (Log2FC ≥ 0.58) and those with FC ≤ 0.66 (Log2FC ≤ -0.58) were considered as significantly up- and down-regulated proteins, respectively, in treated parasites compared to WT. Thus, a total of 131 and 72 proteins were found to be differentially expressed in C3- and C4 treated cultures, respectively, compared to WT-parasites. C3-clones showed upregulation of the expression of 74 proteins and downregulation of 57 proteins compared to WT tachyzoites (Suppl. Table S2). Most of the dysregulated proteins (125/131) upon treatment with C3 were found exclusively in clone P1E5. Two proteins (TGME49_251180 and TGME49_229140) were commonly dysregulated in the three C3-clones P1F3, P1E5 and P2F5, whereas the ORF TGME49_238200 encoding for alpha/beta hydrolase fold domain-containing protein was shared between P2F5 /P1E5 (Suppl. Table S2). Table 10 presents the top 20 up- and downregulated proteins in C3-clones, ranked according to their FC. Interestingly, the upregulated ribosomal protein RPL44 encoded by ORF TGME49_203630 was also identified as a C3-binding protein (suppl. Table S1). Another upregulated protein (FC = 1.7 in P1E5/WT, see suppl. Table S2) annotated as cyst wall protein CST7 (TGME49_258870) shown in suppl. Table S2, was also identified as a C3-binding protein (suppl. Table 1). The most downregulated proteins in C3 treated clones were the putative ribosomal RNA (adenine(1779)-N(6)/adenine(1780)-N(6))dimethyltransferase encoded by the ORF TGME49_248200, and the cyst matrix protein MAG2 (TGME49_209755) (Table 10). Proteomic analyses of clones recovered from C4 treatment compared to *T. gondii* ME49 WT parasites showed that 66 proteins were upregulated (FC ≥ 1.5 (Log2FC ≥ 0.58); P ≤ 0.05) and six proteins were downregulated (FC ≤ 0.66; P ≤ 0.05). As shown in Table 11, the expression of hypothetical protein encoded by ORF TGME49_306300 was more than seven-fold higher in clone P1G10 compared to *T. gondii* ME49 WT parasites. TGME49_306300 contains a conserved domain (TIGR00927) described as a K+-dependent

Na+/Ca+ exchanger, which is reminiscent of transport and binding proteins for cations and iron carrying compounds. Three other upregulated proteins, namely the hypothetical protein (TGME49_277920), the ribosomal protein RPS27 (TGME49_217570) and the ribosomal-ubiquitin protein RPS27A (TGME49_245620) (suppl. Table S2) were also identified as C4-binding proteins by C4-affinity chromatography (suppl. Table S1) and among those the ribosomal protein RPS27A was also identified in the C3-binding fraction by affinity chromatography (suppl. Table S1). A further 11 upregulated proteins and one downregulated protein were identified in both C3- and C4- recovered parasites, in comparison to WT tachyzoites. As shown in Table 12, those proteins exhibiting the highest upregulated expression are transmembrane proteins and membrane transporters.

Table 10: List of twenty most differentially expressed proteins in clones adapted to compound C3 as compared to *T. gondii* ME49 WT strain. For upregulated (FC ≥ 1.5; P ≤ 0.05) and for downregulated (FC ≤ 0.66; P ≤ 0.05). Whole cell shotgun MS was performed on three clones per drug and three replicates per clone.

ToxoDB ORF	Product Description	C3_Clone	Fold Change (FC)
Upregulated ↑			
TGME49_258700	transporter, major facilitator family protein	P1F3	6.5
TGME49_225480	hypothetical protein	P1E5	6.4
TGME49_248140	hypothetical protein	P1E5	5.6
TGME49_262120	IQ calmodulin-binding motif domain-containing protein	P1E5	3.3
TGME49_253360	SNARE protein STX20	P1E5	3.2
TGME49_306300	hypothetical protein	P1E5	3.2
TGME49_257160	hypothetical protein	P1E5	3.1
TGME49_261740	rhoptry protein ROP47	P1E5	2.8
TGME49_293480	MoeA N-terminal region (domain I and II) domain-containing protein	P1F3	2.6
TGME49_250950	KRUF family protein	P1E5	2.5
TGME49_203630	ribosomal protein RPL44	P1E5	2.4
TGME49_315290	hypothetical protein	P1E5	2.4
TGME49_214410	hypothetical protein	P1E5	2.3
TGME49_268730	glutaredoxin 1	P1E5	2.3
TGME49_268740	hypothetical protein	P1E5	2.2
TGME49_234180	hypothetical protein	P1E5	2.1
TGME49_238200	alpha/beta hydrolase fold domain-containing protein	P2F5/P1E5	2/1.6
TGME49_219690	hypothetical protein	P1E5	2.0
TGME49_202940	hypothetical protein	P1E5	2.0
TGME49_251180	KRUF family protein	P1E5/P1F3/ P2F5	2/1.7/1. 5
Downregulated ↓			
TGME49_248200	ribosomal RNA (adenine(1779)-N(6)/adenine(1780)-N(6))-dimethyltransferase, putative	P1E5	0.1
TGME49_209755	cyst matrix protein MAG2	P1E5	0.1
TGME49_253350	hypothetical protein	P1E5	0.3
TGME49_297110	kinesin motor domain-containing protein	P1E5	0.3
TGME49_273780	SWI2/SNF2-containing protein	P1E5	0.4
TGME49_280570	SAG-related sequence SRS35A	P1E5	0.4
TGME49_272900	DNA repair protein RAD51	P1E5	0.4
TGME49_281900	SET domain containing lysine methyltransferase KMTox	P1E5	0.4
TGME49_247390	ATPase, AAA family protein	P1E5	0.4
TGME49_280390	HEAT repeat-containing protein	P1E5	0.5
TGME49_320190	SAG-related sequence SRS16B	P1E5	0.5
TGME49_318470	AP2 domain transcription factor AP2IV-4	P1E5	0.5
TGME49_297870	inner membrane complex protein IMC36	P1E5	0.5
TGME49_214970	DNA replication licensing factor, putative	P1E5	0.5
TGME49_301170	SAG-related sequence SRS19D	P1E5	0.5
TGME49_244500	Tubulin-tyrosine ligase family protein	P1E5	0.5
TGME49_290970	serine palmitoyltransferase SPT2	P1E5	0.5
TGME49_219700	DNA replication licensing factor MCM4, putative	P1E5	0.5
TGME49_237220	DNA replication licensing factor Mcm7, putative	P1E5	0.5
TGME49_262990	hypothetical protein	P1E5	0.5

Table 11: List of twenty most upregulated proteins and six downregulated proteins in clones adapted to compound C4 as compared to *T. gondii* ME49 WT strain, for upregulated (FC ≥ 1.5; p ≤ 0.05) and for downregulated (FC ≤ 0.66; p ≤ 0.05). Whole cell shotgun MS was performed on three clones per drug and three replicates per clone.

ToxoDB ORF	Product Description	C4_Clone	Fold Change (FC)
Upregulated ↑			
TGME49_306300	hypothetical protein	P1G10	7.2
TGME49_258700	transporter, major facilitator family protein	P2F3	4.2
TGME49_248140	hypothetical protein (putative transmembrane protein)	P3E2	4.1
TGME49_234980	hypothetical protein (putative transmembrane protein)	P2F3	3.8
TGME49_277740	zinc finger, C3HC4 type (RING finger) domain-containing protein	P2F3	2.8
TGME49_268860	enolase 1	P2F3	2.8
TGME49_265190	Ulp1 protease family, C-terminal catalytic domain-containing protein	P2F3	2.7
TGME49_276120	histone lysine methyltransferase, SET, putative	P2F3	2.3
TGME49_220170	hypothetical protein	P2F3	2.2
TGME49_200440	hypothetical protein	P2F3	2.2
TGME49_273060	ribosomal protein S17, putative	P2F3	2.1
TGME49_273550	hypothetical protein	P2F3	2.1
TGME49_293480	MoeA N-terminal region (domain I and II) domain-containing protein	P3E2	2
TGME49_238200	alpha/beta hydrolase fold domain-containing protein	P2F3/P1G10	2.01/1.9
TGME49_284580	ribose-phosphate diphosphokinase subfamily protein	P2F3	2
TGME49_211470	Fcf2 pre-rRNA processing protein	P2F3	2
TGME49_229260	basal complex component BCC4	P2F3	2
TGME49_226640	zinc binding protein, putative	P2F3	2
TGME49_224932	hypothetical protein	P2F3	1.9
TGME49_297220	AMP-binding enzyme domain-containing protein	P2F3	1.9
Downregulated ↓			
TGME49_309580	transporter, major facilitator family protein	P2F3	0.1
TGME49_268220	hypothetical protein	P2F3	0.2
TGME49_305870	DAD family protein	P1G10	0.4
TGME49_305610	hypothetical protein	P2F3	0.5
TGME49_229140	MaoC family domain-containing protein	P1G10	0.6
TGME49_320588	glycosyl hydrolases family 35 protein	P2F3	0.6

Table 12. List of differentially expressed proteins in C3- and C4-recovered clones as compared to *T. gondii* ME49 WT tachyzoites. Eleven proteins were upregulated (FC ≥ 1.5; $p \leq 0.05$), one was downregulated (FC ≤ 0.66; $p \leq 0.05$) in both C3 and C4 clones, and three proteins had a divergent expression between C3 and C4 clones.

Upregulated C3↑ C4 ↑	Annotation	C3_Clone	FC	C4_Clone	FC
TGME49_306300	hypothetical protein	P1E5	3.2	P1G10	7.2
TGME49_258700	transporter, major facilitator family protein	P1F3	6.5	P2F3	4.2
TGME49_248140	hypothetical protein (putative transmembrane protein)	P1E5	5.6	P3E2	4.1
TGME49_293480	MoeA N-terminal region (domain I and II) domain-containing protein	P1F3	2.6	P3E2	2.0
TGME49_238200	alpha/beta hydrolase fold domain-containing protein	P1E5/P2F5	1.62/2.03	P2F3/P1G10	2.0/1.9
TGME49_211470	Fcf2 pre-rRNA processing protein	P2F5	1.8	P2F3	2.0
TGME49_297220	AMP-binding enzyme domain-containing protein	P1E5	2.0	P2F3	1.9
TGME49_277920	hypothetical protein (putative transmembrane protein)	P1E5	2.0	P2F3	1.5
TGME49_224932	hypothetical protein (putative jmjC domain protein)	P1E5	1.6	P2F3	1.9
TGME49_269660	TFIIH basal transcription factor complex helicase XPB subunit	P1E5	1.6	P2F3	1.5
TGME49_274100	hypothetical protein	P2F5	1.5	P2F3	1.6
Downregulated C3↓ C4 ↓					
TGME49_229140	MaoC family domain-containing protein	P1F3	0.5	P1G10	0.6
Divergent C3↓ C4 ↑					
TGME49_312500	hypothetical protein	P1E5	0.6	P2F3	1.5
TGME49_315590	macro domain-containing protein	P1E5	0.6	P2F3	1.9
TGME49_242720	aspartyl protease ASP5	P1E5	0.7	P2F3	1.5

5.4 Effect C3 and C4 on the stimulation of the host immune cells and evaluation of the toxicity in a model organism

5.4a Assessment of viability of murine splenocytes after treatment with C3 and C4 *in vitro*

The effects of C3 and C4 treatments on murine immune cells were investigated *in vitro* to detect eventual immunosuppressive activity. Splenocytes, a mixed population of immune cells, were treated with ConA to stimulate T cells and LPS to stimulate B cells, with or without C3 and C4. Splenocytes stimulated with ConA or LPS were also treated with ciclosporin A (CsA) as a positive control, as it serves as an inhibitor for both types of stimulation. Their viability was measured using Alamar Blue assay. Figure 22 A shows that C3 reduced B cell viability only at 2 µM (very low concentration, not concerning),

while C4 did not affect T or B cells viability at any concentration tested (Figure 22 B). Based on these results, *in vivo* studies using a murine model of cerebral toxoplasmosis were planned to evaluate their efficacy in a more complex biological environment, paving the way for future therapeutic development.

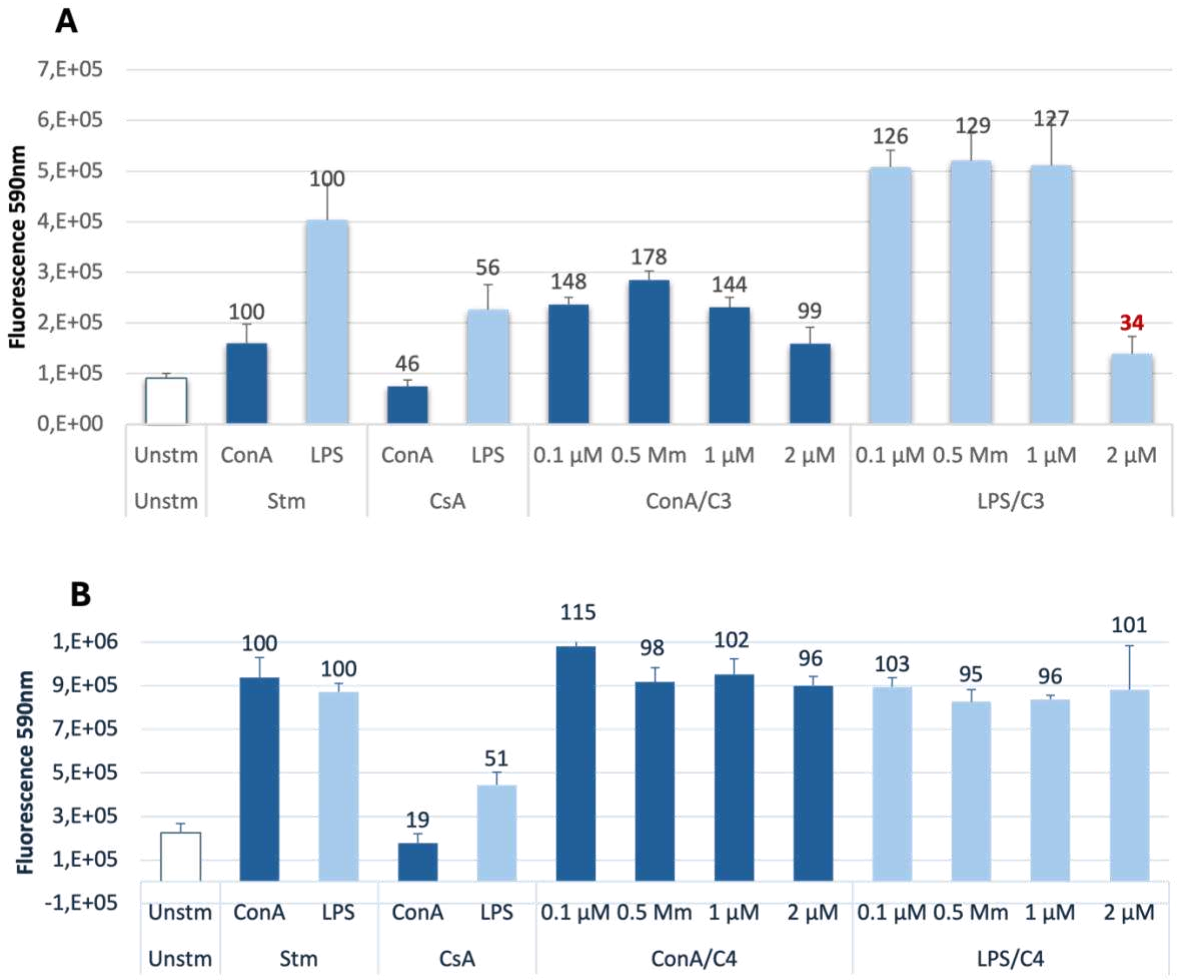

Figure 22: Effects of C3 (A) and C4 (B) on viability of murine T-cells and B-cells *in vitro.* 96-well plates were seeded with splenocytes obtained from murine spleens (2× 10^6 cells/mL, 100 µL/well), and were exposed to ConA (5 µg/mL) or LPS (10 µg/mL). C3 and C4 were added at 0.1, 0.5, 1 and 2 µM, respectively, and cultivation was carried out for 48 h at 37 °C/5% CO_2. Viability was assessed by resazurin reduction and is given as relative fluorescence units (RFU).

5.4b Effects of C3 and C4 on early zebrafish embryo development

The effects of C3 and C4 on zebrafish embryo development were assessed through daily microscopic inspection of 20 fertilized eggs per drug and concentration, cultured from 24 to 96 hours post-fertilization (hpf) with or without the compounds. This visual assessment was conducted blinded to the treatment conditions by a single expert operator. At the end of the assay, the impact score (Si) of each drug was calculated based on the observation of each concentration compared to the negative controls

(see details in Table 13). A negative Si is indicative of toxicity. Results showed that both compounds are toxic in a dose-dependent manner, causing adverse effects in early zebrafish embryo development, like malformations and death (Figure 23). C3 was shown to be toxic from 1 µM to the highest concentration tested (20 µM), while C4 was toxic at all concentrations tested. Based on these results, *in vivo* studies using a murine model of congenital toxoplasmosis were excluded.

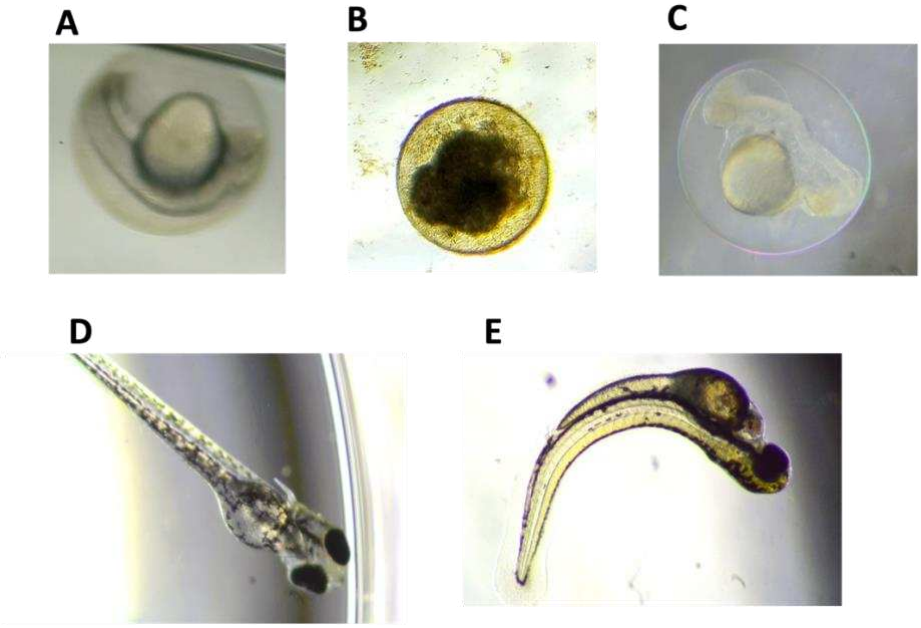

Figure 23. A) Normal zebrafish embryo 24 hpf. B) Dead zebrafish embryo after C3 treatment (24 hpf). C) Dead zebrafish embryo after C4 treatment (24hpf). D) Normal hatched embryo after 72 hpf. E) Hatched embryo with malformation (curved tail) after C4 treatment (72 hpf).

Table 13: Calculations of the scores obtained for each concentration of the compounds tested (Si.) Sneg = negative control score (no compound, no DMSO); Solvent control = solvent control score (no compound, 0.01% DMSO); Sassay, assay score (score for each compound concentration); Smean = control mean score; Si = impact score; Ne = number of embryos introduced per test item (20 per compound and concentration); Nd = number of dead embryos after 96 hpf (score –1 for each dead embryo); Nm = number of embryonal malformations observed after 96 hpf (score –0.5 for each malformation, including non-hatched embryos at 96 hpf).

Compound name	Concentration (µM)	Negative control N_e	Negative control N_d	Negative control N_m	S_{neg}	Solvent control N_e	Solvent control N_d	Solvent control N_m	$S_{solvent}$	Sblank	Compound N_e	Compound N_d	Compound N_m	S_{assay}	S_i
C3	20	20	0	6	17	20	2	4	16	16,5	20	20	0	0	-16,5
	10	20	0	6	17	20	2	4	16	16,5	20	20	0	0	-16,5
	1	20	0	6	17	20	2	4	16	16,5	20	4	16	8	-8,5
	0.2	20	0	6	17	20	2	4	16	16,5	20	0	2	19	2.5
C4	20	20	0	0	20	20	0	0	20	20	20	20	0	0	-20
	10	20	0	0	20	20	0	0	20	20	20	11	9	4,5	-15,5
	1	20	0	0	20	20	0	0	20	20	20	0	20	10	-10
	0,2	20	0	0	20	20	0	0	20	20	20	1	2	18	-2

5.5 *In vivo* efficacy of the compounds in a murine model of cerebral toxoplasmosis

5.5a Parasite load quantification by Real-time PCR

In the *in vivo* study outbred CD1 mice were experimentally infected with TgShSp1 type II oocysts. After the oral administration of 120 oocysts, C3 and C4 were administered at 10 mg/kg/day for 5 days starting at day 3 post-infection (p.i.). C3 was formulated in H_2O containing 25% DMSO and C4 in corn oil containing 10% DMSO. Neither the infection nor the treatment caused clinical signs, indicating non-toxicity at this dosage. On day 30 p.i., mice were euthanized, the brain tissue, eyes and heart were dissected, and the parasite load was determined by quantitative Real-time PCR. As shown in figure 24 A, C3 and C4 treatments did not reduce the cerebral parasite load compared to the placebo control group (p = 0.45 and p = 0.54). Similarly, figure 24 B shows no reduction in the eye parasite load compared to the control group (p = 0.90 and p = 0.78.) However, the parasite load in the heart was significantly reduced in the C4 treated group (Figure 24 C).

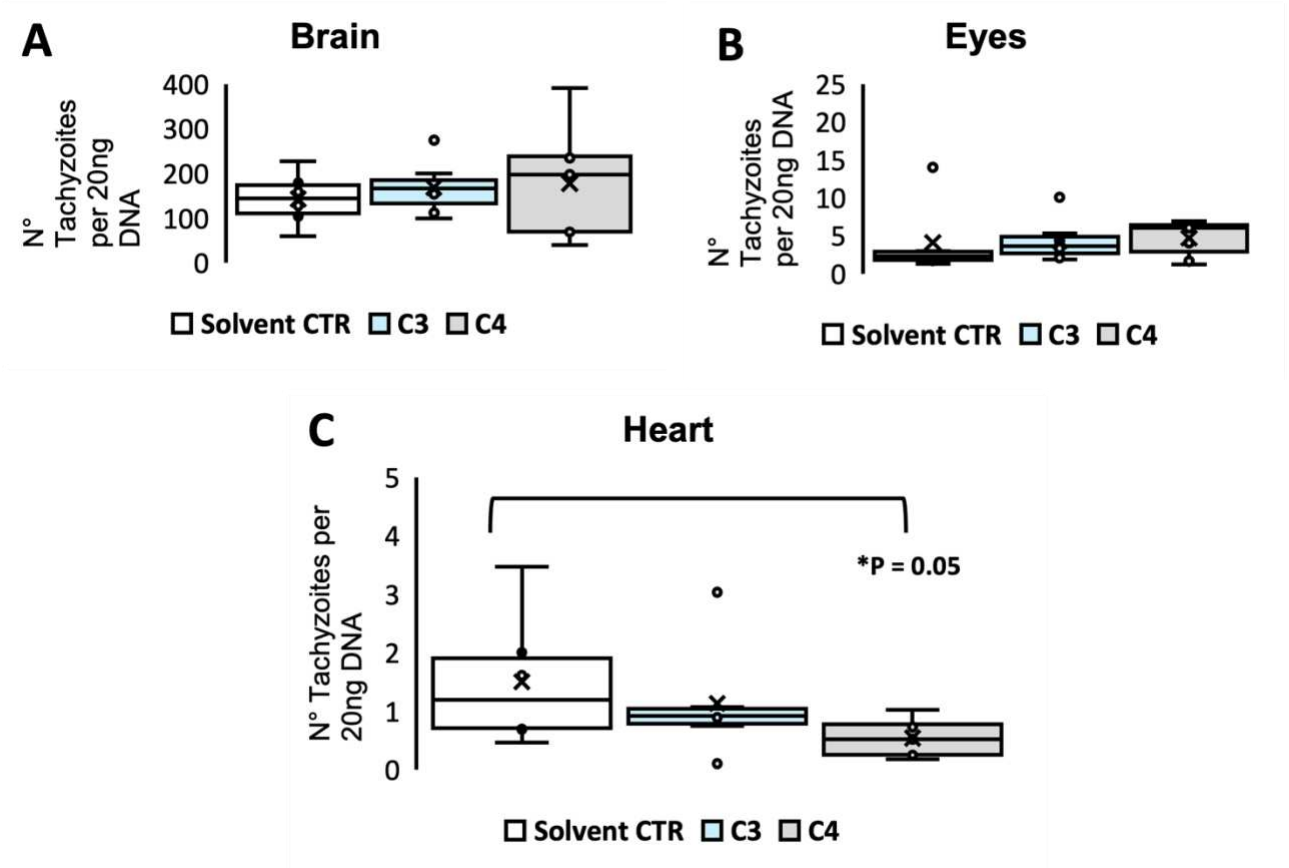

Figure 24: *In vivo* efficacy of C3 and C4 in CD1 mice experimentally infected with TgShSp1 oocysts. Box plots show the parasite load at 30 days p. i. in placebo control mice (CTR, 0.25% DMSO) and C3 and C4 treated mice. The number of parasites in 20 ng DNA extracted from brain (A), eyes (B) and heart (C) was determined using qPCR. Parasite load data are represented as box and whisker (min to max) plots with the x showing the mean per group. Statistics were obtained using Student t-test and *p*-values below 0.05 are considered statistically significant.

5.5b Histopathology of mice brains

Histopathology was conducted on mice brains from three groups of infected mice (one mice per group: a positive control group (C+) and two treatment groups dosed with C3 and C4 at 10 mg/kg/day) that were fixed in 10% neutral buffered formalin (NBF) for at least 48 hours immediately after their removal. After being processed and paraffin embedded, brains were stained with hematoxylin and eosin (H&E) for histopathological analysis under a light microscope (Figure 25). The histopathology results supported the findings from qPCR, further confirming the inefficacy of both treatments in the brain. In fact, 19 cysts per slide were found in the positive control group, 11 cysts per slide in the treatment with C3 and 16 slides in the treatment with C4 (Table 14). No tissue cysts were observed in the heart samples analyzed.

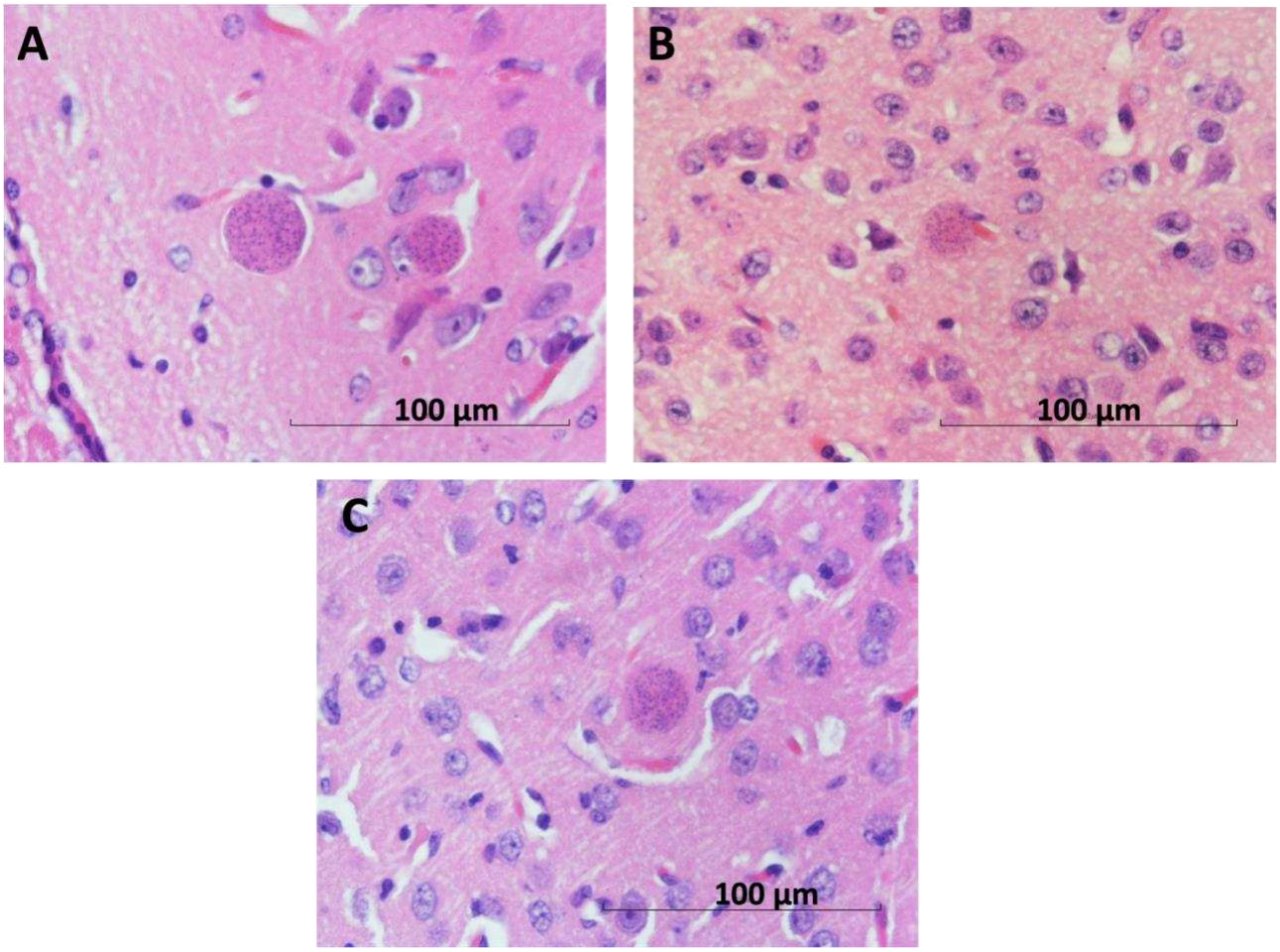

Figure 25: Tissue cysts at 40x magnification at the light microscope obtained from FFPP mice brain infected with *T. gondii*. A) Overview of cysts in mice infected and non-treated (**C+**); B) Overview of cysts in mice infected and treated with **C3**; C) Overview of cysts in mice infected and treated with **C4**.

Table 14: Comparison of results obtained from qPCR and histopathological analyses.

	No. tachyzoites per 20 ng of DNA	**No. of cysts**
C+	159	19 per slide
C3	154	11 per slide
C4	235	16 per slide

5.6 Viability and proliferation of murine splenocytes after treatment with C3 and C4 *in vivo*

5.6.1 Measurement of viability and proliferation after treatment *in vivo*

To investigate whether C3 and C4 treatments *in vivo* would have an impact on B or T cell proliferation, non-infected mice were similarly treated either with C3 and C4 or with vehicle alone, and isolated spleen cells were cultured *in vitro* and stimulated with either ConA or LPS. Viability of cells was measured using Alamar Blue assay and proliferation of cells with BrdU- ELISA.

As seen in Figure 26, C3 and C4 treatment did not affect either the viability nor the proliferative capacity of these splenocyte populations.

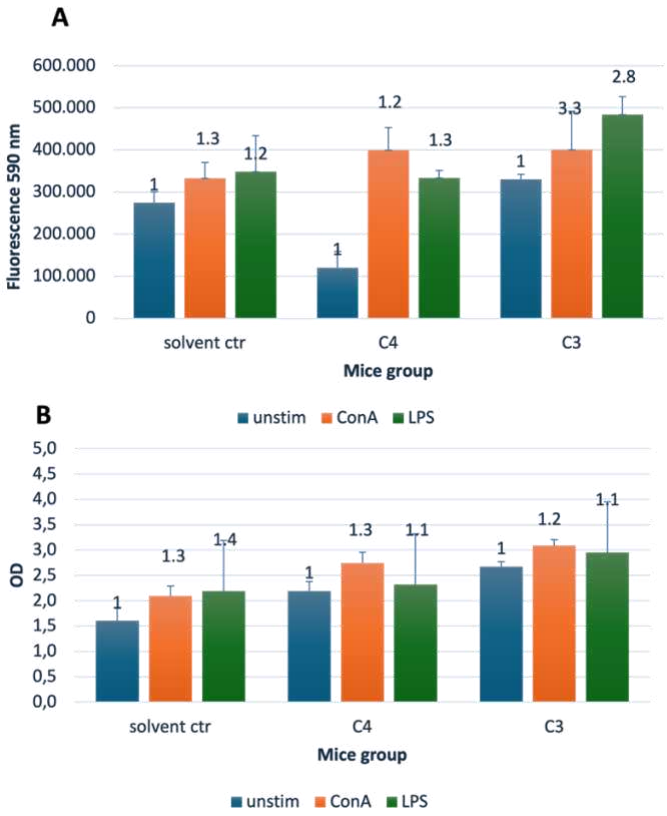

Figure 26: (A) Effects of C3 and C4 on viability of murine T-cells and B-cells *in vivo.* 96-well plates were seeded with splenocytes obtained from murine spleens (2× 10^6 cells/mL, 100 µL/well), of mice treated with C3 and C4, respectively and were exposed to ConA (5 µg/mL) or LPS (10 µg/mL) *in vitro*. Cultivation was carried out for 48 h at 37 °C/5% CO2. Viability was assessed by resazurin reduction and is given as relative fluorescence units (RFU). (B) Effects of C3 and C4 on proliferation of murine T-cells and B-cells in vivo. Stimulation was done as explained above and proliferation was measured using BrdU-ELISA.

5.6.2 Measurement of viability and proliferation after infection and treatment *in vivo*

To assess the impact of C3 and C4 treatments combined with *in vivo* infection on B and T cells proliferation, splenocytes were isolated from infected mice treated with either C3 or C4. These cells were then cultured *in vitro* and stimulated with ConA or LPS. Cell viability was measured using the Alamar Blue assay, while cell proliferation was assessed via BrdU-ELISA.

As shown in Figure 27, the combination of C3 or C4 treatment and infection did not affect either the viability or proliferative capacity of these splenocyte populations.

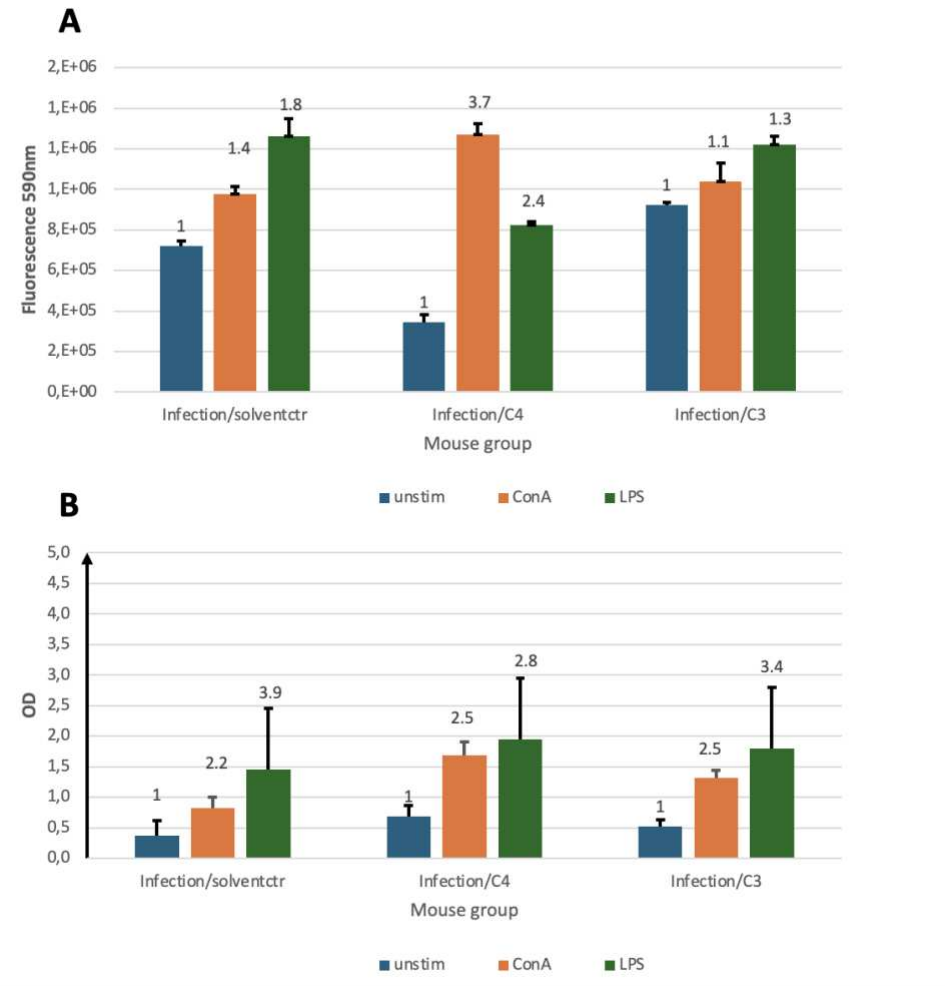

Figure 27: (A) Effects of C3 and C4 plus infection on viability of murine T-cells and B-cells *in vivo.* 96-well plates were seeded with splenocytes obtained from murine spleens (2× 10^6 cells/mL, 100 µL/well) of mice infected and treated with C3 and C4, respectively, and were exposed to ConA (5 µg/mL) or LPS (10 µg/mL) *in vitro*. Cultivation was carried out for 48 h at 37 °C/5% CO_2. Viability was assessed by resazurin reduction and is given as relative fluorescence units (RFU). (B) Effects of C3 and C4 plus infection on proliferation of murine T-cells and B-cells *in vivo*. Stimulation was done as explained above and proliferation was measured using BrdU-ELISA.

6. Discussion

In this study, various TSC ligands coordinated with different metal ions were screened for their activity against *T. gondii*. The aim was to evaluate whether metal coordination could enhance or not the antiparasitic properties of these ligands, as metal complexes have been shown to exhibit increased biological activity compared to their free ligand counterparts (Beraldo and Gambino, 2004).

Initially four TSC and their respective copper(II) complexes were tested *in vitro* for their toxicity on HFF and their activity against *T. gondii* tachyzoites. None of them exhibited cytotoxicity on host cells, nor any efficacy against the parasite, leading to their exclusion from further studies and prompting the design of new compounds.

Successively, three gold(III)–salicyl-TSC complexes (C1-C2-C3) and one salicyl-TSC compound (C4) were tested *in vitro* as well. Among these compounds, only C3 and C4 (C3 without gold) were selected for further analyses, since exhibited specific toxicity against *T. gondii* tachyzoites with IC_{50} values below 50 nM and no impairment of HFF viability at a > 500 times higher concentration. The fact that the salicyl-TSC ligand (C4) by itself was as active as the respective C3 gold(III) complex indicates that the presence of gold was not necessary to exert the anti-parasitic effect, and this is in agreement with previous studies demonstrating anti-protozoal activity for thiosemicarbazones, including *T. gondii* and *T. cruzi* (Linciano et al., 2018; Bekier et al., 2021). Since 2005, more than fifty thiosemicarbazone (TSC) derivatives have been tested against *T. gondii in vitro*, with several demonstrating promising results against the proliferative tachyzoite stage (de Aquino et al., 2008; Gomes et al., 2013; Dzitko et al., 2014; Ansari et al., 2020).

In this case, similar efficacies of the gold(III) complex C3 and its ligand C4 were noted upon the addition of the drugs concomitantly to infection but also when parasites were already intracellular. This point is very interesting because it suggests that these drugs affect intracellular parasites rather than inhibiting *T. gondii* tachyzoite entry into host cells. TEM of treated versus non-treated *T. gondii* ME49 tachyzoites was performed to investigate how intracellular tachyzoites were affected by C3 and C4 exposure. Surprisingly some effects were observed only at the early stages of treatment (6-24 h) and were slightly more pronounced upon C4 treatment. Common features seen for both C3 and C4 treatments were the build-up of several layers of membranes surrounding the parasitophorous vacuole, moderate cytoplasmic vacuolization, as well as distinct alterations in the matrix of the parasite mitochondrion. It is not clear whether the additional parasitophorous vacuole membrane material is generated by the parasite, or whether it is derived from the host. However, as there is currently no mechanism known

by which *T. gondii* could form additional lipid bilayer membranes (Sibley, 2011), it is conceivable that these membranes are host cell derived. This would imply that they lack *T. gondii* transporter proteins to acquire nutrients from the host cytoplasm, which in turn could be partially responsible for the observed cytoplasmic vacuolization as well as mitochondrial alterations. Thus, the effects of the drugs could be not directly on the tachyzoites but could be mediated, at least partially, by the host cell, potentially as attempted autophagy. This would also explain why the effect of the drug is restricted to intracellular tachyzoites. It is important to note that (i) these aberrant ultrastructural alterations were not found in all, but in a majority of tachyzoites, (ii) they were not evident in the controls, the alterations occurred only transiently, with most parasites returning to their original ultrastructural characteristics after 48 h. Thus, we cannot exclude the possibility that the tachyzoites showing these ultrastructural alterations die and disappear (possibly by authophagy by the host cells) and that the non-affected tachyzoites are responsible for the observed growth during longer term treatments. In order to identify potential interaction partners of C3 and C4 in *T. gondii*, differential affinity chromatography coupled with mass spectrometry was performed. Since ribosomal proteins, with 31% relative abundance, represent by far the major proportion of C3 and C4 binding proteins, these compounds may interfere with protein biosynthesis.

In cancer cells, thiosemicarbazones, particularly those presenting a thio carbonyl (C= S) bond, have been shown to interfere specifically with the function of RLP44 receptor during the elongation step of translation, by inhibiting the crosslinking reaction between RPL44 and the periodate-oxidized tRNA (Houngue et al., 2017). Translation is one of the best investigated targets of antimicrobials. The first drugs approved against toxoplasmosis were antibiotics, including clindamycin (Hofflin and Remington, 1987) and spiramycin (Chew et al., 2012), that inhibit translation. In addition, affinity chromatography identified several quinoline-binding proteins in the closely related *Neospora caninum* that are involved in translation (Müller et al., 2022a). If inhibition of translation is the real mode of action, the effect appears to be reversible, since prolonged treatment resulted in adaptation of *T. gondii* tachyzoites to drug exposure and parasites subsequently resumed proliferation. Results from comparative examination of proteomic data from *T. gondii* ME49 WT and the six clones recovered from C3 and C4 treatments, suggest that there are three main strategies of molecular mechanisms by which tachyzoites could reverse the effect of C3 and C4-salicyl-TSC based drugs. A first strategy could be the overexpression of C3- and C4 drug targets to restore their normal levels. This is largely supported by the STRING protein-protein interaction network analysis of upregulated proteins (see suppl. Figure 1) which reveals a cluster of ribosomal proteins. In contrast, the STRING analysis of down regulated

proteins identified a network consisting of proteins involved in DNA replication and repair (see suppl. Figure 2), which then may explain the initial inhibition of proliferation seen in the presence of the compounds. A significant example of the target overexpression strategy is given by the ribosomal protein RPL44, whose expression level increased in all six clones compared to WT tachyzoites. In addition, the expression of RPS27, which binds to both C3 and C4 by affinity chromatography, was increased in C4-adapted clones. Binding of this, and various other ribosomal proteins to the compounds, suggests that they target the ribosomes and possibly interfere with protein biosynthesis. The standard procedure to confirm drug targets consists in generating either knockouts or overexpressing strains and testing their IC_{50} values in comparison to the parental cell lines. Since protein biosynthesis is essential, it is obvious that this approach cannot be performed in this special case. Moreover, the selection procedure to obtain genetically modified strains may interfere by itself with gene expression (Hänggeli et al., 2023).

It is also important to keep in mind that just because a compound can bind to a solubilized ribosomal protein in isolation, it may not have access to that same binding motif when the protein is part of the assembled ribosome, or that it would inhibit ribosomal functions. However, for spectinomycin, which is a ribosome-targeting antibiotic, it has also been shown that bacteria enhance the expression of the 16S rRNA helix 34, which is the main target. The 16S rRNA helix 34 is, on one hand, needed for translation, but will also sequester the drug when overexpressed (Gc et al., 2019).

A second possible strategy identified in the present study for developing tolerance to C3 and C4 is the upregulation of cellular efflux transporter proteins, which could lead to a reduction of intracellular C3 and C4 concentrations. The three proteins with the highest level of upregulation in adapted strains as compared to their WT, namely the hypothetical protein encoded by TGME49_306300, a putative transporter encoded by TGME49_258700, and another hypothetical protein encoded by TGME49_248140 containing two short transmembrane domains, may be involved in this strategy. However, these proteins have not been functionally characterized with respect to transport of xenobiotics, so far, and exact localization studies should be carried out to verify the localization of these proteins at the plasma membrane. In addition, another protein, the soluble N-ethylmaleimide-sensitive-factor attachment protein receptor (SNARE) protein STX20 (TGME49_253360), was upregulated in five out of the six analyzed clones. In *T. gondii*, SNAREs are involved in exocytosis at the plasma membrane (Cao et al., 2021) and it has recently been shown that *T. gondii* STX20 associates with STX1 and STX21 to form an unconventional SNARE complex which mediates exocytosis at the plasma membrane and vesicular fusion at the apical annuli (Fu et al., 2023). Furthermore, it is well

known that bacteria upregulate the expression of porins and efflux pumps in response to most ribosome-targeting antibiotics (Fernández and Hancock, 2012; Ayaz et al., 2017; Jiao et al., 2023). Thirdly, proteomics analyses indicate that *T. gondii* responded to C3 and C4 treatments by metabolization, degradation or modification of C3 and C4, e.g. via upregulated oxidases, dehydrogenases or hydroxylases, similar to that previously reported for tetracycline (Rudra et al., 2018). Four of the six clones adapted to either C3 or C4 exhibited an upregulated expression of the alpha/beta hydrolase fold domain-containing protein (TGME49_238200). The functions of these enzymes in *T. gondii* are, however, unknown. Rapid adaption of *T. gondii* to elevated drug concentrations *in vitro* has also been described for other compounds, including decoquinate- and artemisinin-derivatives (Ramseier et al., 2021; Müller et al., 2023), bumped kinase inhibitors (Imhof et al., 2021), ruthenium-based compounds (Barna et al., 2013) and pentamidine derivatives (Kropf et al., 2012) and has also been reported in other apicomplexans including *N. caninum* tachyzoites treated with endochin-like quinolones (Anghel et al., 2018) and *Besnoitia besnoiti* tachyzoites treated with buparvaquone (Müller et al., 2019b). Overall, this suggests that the emergence of adapted/resistant parasites following long-term drug treatment *in vitro* is not uncommon, as has also previously occurred with sulfonamides (Aspinall et al., 2002; Doliwa et al., 2013), although the mechanism of decreased drug susceptibility in the latter case was based on mutations in the gene sequences that encode the drug target, specifically enzymes involved in the folate pathway. Similar IC_{50} and MIC values were observed for both compounds using clones recovered after C3 and C4-adaptation and regrowth after freezing, as well as for WT *T. gondii*. Results showed that the adaptation to these drugs was only a transient feature and was lost in absence of drugs after one cycle of cryopreservation. Consequently, the six clones regained similar drug susceptibilities as the WT parasites but could quickly readjust once drugs were added back to the culture medium. These results highlight the considerable phenotypic plasticity in *T. gondii*, which is often mediated by epigenetic changes, allowing the parasite to respond, in time, to environmental stress, including drugs (Leggett et al., 2013). Moreover, differentially expressed proteins of clone P1E5 belonging to the epigenetic machinery (Dixon et al., 2010) such as the SWI2/SNF2-containing protein (TGME49_273780) and the lysine-methyltransferase encoded by TGME49_281900 suggest the involvement of epigenetic mechanisms in the adaptation of this clone. The fact that the repressor of bradyzoite-specific genes ApiAP2IV-4 (TGME49_318470) (Radke et al., 2018) is one of the upregulated proteins of the same clone indicates a link between developmental regulation and drug adaptation. Furthermore, the fact that varying differentially expressed protein patterns are found in different clones suggests alternative modes of adaptation which are equally

effective, similar to what has been observed in different strains of nitro drug-resistant *Giardia lamblia* strains (Müller et al., 2019a). Interestingly, a higher number of differentially expressed proteins were identified in clones resistant to C3 than in clones resistant to C4. This may be due to the presence of a gold ion causing oxidative stress and thereby stimulating a variety of responses such as transport or metabolization (Barbasz and Oćwieja, 2016; Scaccaglia et al., 2024). Moreover, the degree of dysregulation of SAG1-related sequence (SRS) proteins varied among C3 and C4 clones, and the list of SRSs binding to C3 and / or C4 in affinity chromatography did not correlate with the list of differentially expressed SRSs. In fact, eleven SRS proteins were identified in affinity chromatography eluates from C4-columns, with SRS25 being the most abundant protein binding to C4. However, none of these SRSs showed a changed expression in C4-derived clones. In contrast, none of the SRSs was identified among proteins binding to C3, while a cluster of six SRSs was differentially expressed in C3 adapted clones with 5/6 being downregulated. Taken together, these results suggest that SRS25 binds to C4, but is not acting as a target, and that the differential expression of the six SRSs in clones recovered from C3 treatment is likely an arbitrary event. This hypothesis is largely supported by the fact that SRSs expression pattern in *in vitro* maintained tachyzoites is rather random (Theisen and Boothroyd, 2022). Consistent with this, we also found a significant difference in SRS expression patterns between individual SRS29B knock-out clones of *T. gondii* RH (Hänggeli et al., 2023). In conclusion, our results *in vitro* strongly suggest that the gold(III) complex (C3) and its salicyl-TSC ligand (C4) interfere with translation in *T. gondii* by targeting ribosomal proteins. The rapid adaptation to salicyl-TSC based drugs is likely mediated by different mechanisms such as upregulation of some of the target proteins, enhanced cellular efflux function and possibly drug inactivation/metabolism rather than by downregulation of targets essential for cellular maintenance. Adaptation, however, was reversible, and tolerance to these drugs was rapidly lost in their absence. The phenomenon described herein is distinct from drug resistance, which implies either introducing mutations in a drug target or stable epigenetic changes altering the expression. Nevertheless, this transient adaptation illustrates how these intracellular parasites can rapidly deal with environmental changes and displays the outstanding plasticity of the gene expression pattern of *T. gondii.* Future studies should determine whether related mechanisms could apply to other TSCs and also other drug classes that have shown inhibitory effects on parasite survival. DAC and proteomic analysis of drug treated parasites undertaken here represent an interesting starting point, and further validation of the proposed mechanisms is needed in the future to dissect this transient adaptive feature displayed by *T. gondii* tachyzoites.

After confirming the compounds' efficacy *in vitro*, their potential side effects, particularly regarding their impact on host immune cells and embryonic development, were examined.

Regarding the impact on immune cells, C3 only reduced B cells viability at 2 µM, which is not concerning as such low concentrations are rarely used *in vivo*. In contrast, C4 did not affect the viability of either T or B cells at any concentration tested. Based on these findings, *in vivo* studies using a murine model of cerebral toxoplasmosis were initiated to evaluate their efficacy in a more complex biological environment, laying the groundwork for future therapeutic development. *T. gondii* tissue cysts are commonly studied in the murine model, as mice naturally become infected in the wild with the majority of tissue cysts present in the brain (Dubey et al., 1998).

However, both compounds exhibited toxicity in the zebrafish embryo development model at all concentrations tested, leading to the exclusion of further studies in the congenital murine model of toxoplasmosis.

The *in vivo* efficacy of the compounds in the murine model of cerebral toxoplasmosis was assessed by performing Real-time PCR on DNA extracted from the brain, heart and eyes of the mice post-euthanasia. The analysis targeted the 529 bp gene of *T. gondii*, comparing parasite loads between infected, untreated mice and those treated with compounds C3 and C4.

The results showed that neither compound was effective in reducing the parasite burden in the brain and in the eyes. This lack of efficacy is likely due to the inability of these compounds, similarly to many other drugs tested for toxoplasmosis, to cross the blood-brain barrier (BBB). For instance, despite its significant tissue penetration, spiramycin shows poor ability to cross the BBB and fails to reach effective concentrations in the brain. This is due to the presence of efflux transporters such as multidrug-resistant protein 2 (Mrp2) and P-glycoprotein, which actively transport spiramycin out of the brain, as it is a substrate for these proteins (Tian et al., 2007; Grover and Benet, 2009). A similar mechanism was observed with our compounds, which were throwed out from the parasites via membrane transport proteins.

Nevertheless, a significant decrease in the parasite burden was observed in the hearts of mice treated with C4, even though the infection rate in this organ at the time of euthanasia was very low (even in the infected and untreated control group). This variability is likely due to differences in the timing of parasitic spread, which can be influenced by factors such as the route of administration of the parasites and the strain of *T. gondii* used for infection (Chiebao et al., 2021).

In synthesis, few differences were observed between C3 and C4 in this study. However, C4 demonstrated some distinct advantages. Notably, C4 showed no toxicity towards HFF even at

concentrations exceeding 25 µM, whereas C3 exhibited some degree of toxicity at 25 µM. Furthermore, unlike C3, C4 did not display any immunosuppressive effects on murine splenocytes at any concentration tested *in vitro*. Another significant finding was that C4 exhibited interactions with 318 binding proteins, compared to only 14 proteins for C3, suggesting that C4 has broader activity and potentially more targets within *T. gondii*, which may contribute to its increased efficacy. While, as previously discussed, a higher number of differentially expressed proteins were identified in clones resistant to C3 compared to those resistant to C4. This difference may be attributed to the presence of the gold ion in C3, which induces oxidative stress, thereby triggering a range of responses, including increased transport or metabolism-related processes. Safety of both compounds was confirmed when toxicity was measured on splenocytes after treatment *in vivo*.

The addition of metals does not always enhance the activity of TSCs. For example, one study on murine and human tumor cells reported that the ligands and their Cu(II), Ni(II), Zn(II), and Cd(II) complexes exhibited similar activity in leukemia and lymphoma cell lines in suspension (Hall et al., 2000).

These differences highlight that C4 is potentially a more promising candidate for further therapeutic development compared to C3, despite the limitations shared by both compounds.

Furthermore, since efficacy against parasite burden was observed only in the heart, further studies should explore alternative routes of administration that could improve the compounds' activity, together with evaluation of pharmacokinetics to better understand their metabolism and optimize their therapeutic potential.

It would also be interesting to test these compounds in combination with standard drug treatments, such as sulfadiazine or pyrimethamine (Konstantinovic et al., 2019), to enhance treatment efficacy.

Artemisone and artemiside, for example, have been reported as partially active in a murine model of reactivated toxoplasmosis. However, even though these two compounds controlled the initial phases of reactivated infection, mice died within 25 days after treatment was discontinued, indicating that the parasite was not fully eradicated (Dunay et al., 2009). More recently, it has been reported that artemisone combined with a bumped kinase inhibitor showed synergistic effects *in vitro* against *T. gondii* (Schlange et al., 2023). This combination improved the efficacy against the parasites and reduced the toxicity compared to when the molecule was used alone.

The parasitostatic activity of C3 and C4 observed in the present study could open the door to their possible use alongside other molecules that can act synergistically. Temporarily inhibiting parasite proliferation could enhance the efficacy of drugs like pyrimethamine, which on its own is not highly

effective. However, when used in synergy, it may yield better results, with lower side effects and reduced dosages.

Among the problems related to the current protocols for toxoplasmosis is the high concentration needed to be effective on *T. gondii* and consequently to the severe side effects that treated subjects might show (as hematological side effects). Combination therapies are an interesting approach usable to increase efficacy, reduce toxicity, and avoid the development of drug resistance phenomenon, already been experimented against other infectious diseases, and C3 and C4 might be part of this future approach (Andrews et al., 2014; Sun et al., 2016).

Another way to improve compounds' efficacy could be the use of nanoparticles as delivery drug systems, since it has been demonstrated that the use of drug-coupled nanoparticles greatly increases drug concentration in the brain, helping to overcome the BBB (Ha et al., 2019). When mice were treated with 100 mg/kg of oral atovaquone nanosuspensions (ANS) with sodium dodecyl sulfate (SDS) during the acute phase of toxoplasmosis, a significant increase in drug concentration was observed in both the serum and brain compared to the standard oral formulation. Additionally, there was a reduction in parasite load and inflammatory foci, demonstrating that this formulation enhances the drug's bioavailability, as well as its antiparasitic and anti-inflammatory effects (Shubar et al., 2011).

In addition, there are reports suggesting that inorganic nanoparticles (NPs), such as magnetic and metal NPs, as well as quantum dot-coated particles, can aid in crossing the blood-brain barrier (BBB) (Aguilera et al., 2019; Nosrati et al., 2019). Metals and magnetic NPs, considered inert materials, can enhance contrast-to-noise ratios and improve resolution in imaging applications. Examples include gold (Bittner et al., 2019), silver (Khan et al., 2019), and other metals which have been used as contrast agents in computed tomography (CT) imaging. These metals are also being explored for the development of multifunctional drug delivery systems that can cross the BBB and enable *in vivo* imaging to trace drugs within brain tissue (Aryal et al., 2019).

In conclusion, *T. gondii*, the parasite responsible for toxoplasmosis, continues to pose significant challenges in treatment. Current therapies manage acute infections but are limited by incomplete parasite eradication and adverse side effects. Moreover, much remains unknown about the parasite-host interactions, as *T. gondii* secretes effectors that manipulate various host cellular functions to promote its growth and differentiation into a persistent stage within host tissues. Identifying new secreted effectors and understanding their mechanisms of action are crucial steps in gaining deeper insights into the parasite's virulence and pathogenicity.

Indeed, ongoing research is focusing on the development of new compounds, such as thiosemicarbazones and other small molecules, which have shown potential in laboratory studies. Furthermore, high-throughput genomic and proteomic analyses are being utilized to identify key parasite genes and proteins that could serve as therapeutic targets. The goal is to discover essential proteins involved in *T. gondii*'s survival, replication and cyst formation, which may lead to the development of innovative treatments.

These new drugs could offer improved efficacy, reduced toxicity and broader action, addressing the limitations of existing treatments. This underscores the importance of research to identify more effective therapeutic options.

7. References

Abdullahi, S.A., Unuah, N.Z, Nordin, N., Basir, R., Nasir, W.M., Alapid, A.A., et al. (2020). Phytochemicals and Potential Therapeutic Targets on *Toxoplasma gondii* Parasite. *Mini-Reviews in Medicinal Chemistry* 20, 739–753. doi: 10.2174/1389557519666191029105736.

Adan, A., Kiraz, Y., and Baran, Y. (2016). Cell Proliferation and Cytotoxicity Assays. *Curr Pharm Biotechnol* 17, 1213–1221. doi: 10.2174/1389201017666160808160513.

Aguilera, G., Berry, C. C., West, R. M., Gonzalez-Monterrubio, E., Angulo-Molina, A., Arias-Carrión, Ó., et al. (2019). Carboxymethyl cellulose coated magnetic nanoparticles transport across a human lung microvascular endothelial cell model of the blood-brain barrier. *Nanoscale Adv* 1, 671–685. doi: 10.1039/c8na00010g.

Aguirre, A. A., Longcore, T., Barbieri, M., Dabritz, H., Hill, D., Klein, P. N., et al. (2019). The One Health Approach to Toxoplasmosis: Epidemiology, Control, and Prevention Strategies. *EcoHealth 2019 16:2* 16, 378–390. doi: 10.1007/S10393-019-01405-7.

Ajzenberg, D., Collinet, F., Mercier, A., Vignoles, P., and Dardé, M.-L. (2010). Genotyping of *Toxoplasma gondii* Isolates with 15 Microsatellite Markers in a Single Multiplex PCR Assay. *J Clin Microbiol* 48, 4641–4645. doi: 10.1128/JCM.01152-10.

Alday, P. H., and Doggett, J. S. (2017). Drugs in development for toxoplasmosis: advances, challenges, and current status. *Drug Des Devel Ther* 11, 273–293. doi: 10.2147/DDDT.S60973.

Aldebert, D., Durand, F., Mercier, C., Brenier-Pinchart, M. P., Cesbron-Delauw, M. F., and Pelloux, H. (2007). *Toxoplasma gondii* triggers secretion of interleukin-12 but low level of interleukin-10 from the THP-1 human monocytic cell line. *Cytokine* 37, 206–211. doi: 10.1016/J.CYTO.2007.03.012.

Almeida, C. M., Pedro, P. H., Nascimento, É. C. M., Martins, J. B. L., Chagas, M. A. S., Fujimori, M., et al. (2022). Organometallic gold (III) and platinum (II) complexes with thiosemicarbazone: Structural behavior, anticancer activity, and molecular docking. *Appl Organomet Chem* 36. doi: 10.1002/aoc.6761.

Almeria, S., and Dubey, J. P. (2021). Foodborne transmission of *Toxoplasma gondii* infection in the last decade. An overview. *Res Vet Sci* 135, 371–385. doi: 10.1016/j.rvsc.2020.10.019.

Alnuqaydan, A. M., Almutary, A., Bhat, G. R., Mir, T. A., Wani, S. I., Rather, M. Y., et al. (2022). Evaluation of the Cytotoxic, Anti-Inflammatory, and Immunomodulatory Effects of Withaferin A (WA) against Lipopolysaccharide (LPS)-Induced Inflammation in Immune Cells Derived from BALB/c Mice. *Pharmaceutics* 14, 1256. doi: 10.3390/PHARMACEUTICS14061256.

Alvarez-Jarreta, J., Amos, B., Aurrecoechea, C., Bah, S., Barba, M., Barreto, A., et al. (2024). VEuPathDB: the eukaryotic pathogen, vector and host bioinformatics resource center in 2023. *Nucleic Acids Res* 52, D808–D816. doi: 10.1093/nar/gkad1003.

Andrade, R. M., Chaparro, J. D., Capparelli, E., and Reed, S. L. (2014). Auranofin Is Highly Efficacious against *Toxoplasma gondii In Vitro* and in an *In Vivo* Experimental Model of Acute Toxoplasmosis. *PLoS Negl Trop Dis* 8. doi: 10.1371/journal.pntd.0002973.

Andrews, K. T., Fisher, G., and Skinner-Adams, T. S. (2014). Drug repurposing and human parasitic protozoan diseases. *Int J Parasitol Drugs Drug Resist* 4, 95–111. doi: 10.1016/j.ijpddr.2014.02.002.

Anghel, N., Balmer, V., Müller, J., Winzer, P., Aguado-Martinez, A., Roozbehani, M., et al. (2018). Endochin-like quinolones exhibit promising efficacy against *Neospora Caninum in vitro* and in experimentally infected pregnant mice. *Front Vet Sci* 5. doi: 10.3389/fvets.2018.00285.

Anghel, N., Winzer, P. A., Imhof, D., Müller, J., Langa, X., Rieder, J., et al. (2020). Comparative assessment of the effects of bumped kinase inhibitors on early zebrafish embryo development and pregnancy in mice. *Int J Antimicrob Agents* 56. doi: 10.1016/j.ijantimicag.2020.106099.

Anghel, N., Müller, J., Serricchio, M., Jelk, J., Bütikofer, P., Boubaker, G., et al. (2021). Cellular and molecular targets of nucleotide-tagged trithiolato-bridged arene ruthenium complexes in the protozoan parasites *Toxoplasma gondii* and *Trypanosoma brucei*. *Int J Mol Sci* 22. doi: 10.3390/ijms221910787.

Ansari, M., Montazeri, M., Daryani, A., Farshadfar, K., and Emami, S. (2020). Synthesis and *in vitro* anti-*Toxoplasma gondii* activity of a new series of aryloxyacetophenone thiosemicarbazones. *Mol Divers* 24, 1223–1234. doi: 10.1007/s11030-019-09986-9.

Aryal, M., Papademetriou, I., Zhang, Y. Z., Power, C., McDannold, N., and Porter, T. (2019). MRI Monitoring and Quantification of Ultrasound-Mediated Delivery of Liposomes Dually Labeled with Gadolinium and Fluorophore through the Blood-Brain Barrier. *Ultrasound Med Biol* 45, 1733–1742. doi: 10.1016/j.ultrasmedbio.2019.02.024.

Aspinall, T. V, Joynson, D. H. M., Guy, E., Hyde, J. E., and Sims, P. F. G. (2002). The Molecular Basis of Sulfonamide Resistance in *Toxoplasma gondii* and Implications for the Clinical Management of Toxoplasmosis. *J Infect Dis* 185, 1637–43. doi: 10.1086/340577.

Attias, M., Teixeira, D. E., Benchimol, M., Vommaro, R. C., Crepaldi, P. H., and De Souza, W. (2020). The life-cycle of *Toxoplasma gondii* reviewed using animations. *Parasit Vectors* 13. doi: 10.1186/s13071-020-04445-z.

Augusto, L., Wek, R. C., and Sullivan, W. J. (2021). Host sensing and signal transduction during *Toxoplasma* stage conversion. *Mol Microbiol* 115, 839–848. doi: 10.1111/mmi.14634.

Ayaz, M., Subhan, F. , Sadiq, A. , Ullah, F. , Ahmed, J. , and Sewell, R. D. (2017). Cellular efflux transporters and the potential role of natural products in combating efflux mediated drug resistance. *Frontiers in Bioscience, Landmark* 22, 732–756. doi: 10.2741/4513.

Bacci, C., Vismarra, A., Mangia, C., Bonardi, S., Bruini, I., Genchi, M., et al. (2015). Detection of *Toxoplasma gondii* in free-range, organic pigs in Italy using serological and molecular methods. *Int J Food Microbiol* 202, 54–56. doi: 10.1016/J.IJFOODMICRO.2015.03.002.

Bancroft, J.D. and Layton, C. (2013). “The Hematoxylin and Eosin” In *Theory & Practice of Histological Techniques*, 7th Edition, Churchill Livingstone of Elsevier, Philadelphia, 10-11: 172-214. doi:10.1016/B978-0-7020-4226-3.00010-X.

Barbasz, A., and Oćwieja, M. (2016). Gold nanoparticles and ions – friends or foes? As they are seen by human cells U-937 and HL-60. *J Exp Nanosci* 11, 564–580. doi: 10.1080/17458080.2015.1096024.

Barna, F., Debache, K., Vock, C. A., Küster, T., and Hemphill, A. (2013). *In Vitro* effects of novel ruthenium complexes in *Neospora caninum* and *Toxoplasma gondii* tachyzoites. *Antimicrob Agents Chemother* 57, 5747–5754. doi: 10.1128/AAC.02446-12.

Bateman, A. (2019). UniProt: A worldwide hub of protein knowledge. *Nucleic Acids Res* 47, D506–D515. doi: 10.1093/nar/gky1049.

Behnke, M. S., Khan, A., Lauron, E. J., Jimah, J. R., Wang, Q., Tolia, N. H., et al. (2015). Rhoptry Proteins ROP5 and ROP18 Are Major Murine Virulence Factors in Genetically Divergent South American Strains of *Toxoplasma gondii*. *PLoS Genet* 11. doi: 10.1371/journal.pgen.1005434.

Bekier, A., Węglińska, L., Paneth, A., Paneth, P., and Dzitko, K. (2021). 4-Arylthiosemicarbazide derivatives as a new class of tyrosinase inhibitors and anti-*Toxoplasma gondii* agents. *J Enzyme Inhib Med Chem* 36, 1145–1164. doi: 10.1080/14756366.2021.1931164.

Benmerzouga, I., Checkley, L. A., Ferdig, M. T., Arrizabalaga, G., Wek, R. C., and Sullivan, W. J. (2015). Guanabenz repurposed as an antiparasitic with activity against acute and latent toxoplasmosis. *Antimicrob Agents Chemother* 59, 6939–6945. doi: 10.1128/AAC.01683-15/ASSET/F49BDDD7-C1FE-4DBB-B6A4-C11653FF2244/ASSETS/GRAPHIC/ZAC0111545250005.JPEG.

Beraldo, H., and Gambino, D. (2004). The Wide Pharmacological Versatility of Semicarbazones, Thiosemicarbazones and Their Metal Complexes. *Mini-Reviews in Medicinal Chemistry* 4. doi: 10.2174/1389557043487484.

Bier, N. S., Stollberg, K., Mayer-Scholl, A., Johne, A., Nöckler, K., and Richter, M. (2020). Seroprevalence of *Toxoplasma gondii* in wild boar and deer in Brandenburg, Germany. *Zoonoses Public Health* 67, 601–606. doi: 10.1111/ZPH.12702.

Bittner, A., Ducray, A. D., Widmer, H. R., Stoffel, M. H., and Mevissen, M. (2019). Effects of gold and PCL- or PLLA-coated silica nanoparticles on brain endothelial cells and the blood-brain barrier. *Beilstein Journal of Nanotechnology* 10, 941–954. doi: 10.3762/BJNANO.10.95.

Błaszkowska, J., and Góralska, K. (2014). Parasites and fungi as a threat for prenatal and postnatal human development. *Annals of parasitology*, *60*(4), 225–234.

Boubaker, G., Bernal, A., Vigneswaran, A., Imhof, D., de Sousa, M. C. F., Hänggeli, K. P. A., et al. (2024). In vitro and in vivo activities of a trithiolato-diRuthenium complex conjugated with sulfadoxine against the apicomplexan parasite *Toxoplasma gondii*. *Int J Parasitol Drugs Drug Resist* 25. doi: 10.1016/j.ijpddr.2024.100544.

Braga-Lagache, S., Buchs, N., Iacovache, M. I., Zuber, B., Jackson, C. B., and Heller, M. (2016). Robust label-free, quantitative profiling of circulating plasma microparticle (MP) associated proteins. *Molecular and Cellular Proteomics* 15, 3640–3652. doi: 10.1074/mcp.M116.060491.

Brito, R. M. de M., de Lima Bessa, G., Bastilho, A. L., Dantas-Torres, F., de Andrade-Neto, V. F., Bueno, L. L., et al. (2023). Genetic diversity of *Toxoplasma gondii* in South America: occurrence, immunity, and fate of infection. *Parasit Vectors* 16. doi: 10.1186/s13071-023-06080-w.

Buxton, D., and Innes, E. A. (1995). A commercial vaccine for ovine toxoplasmosis. *Parasitology* 110 Suppl, S11–S16. doi: 10.1017/S003118200000144X.

Cai, Y., Yu, Y., Wang, Y., Zhang, Y., Luo, Q., Yu, L., et al. (2020). The role of macrophage reprogramming induced by GRA15II, a polypeptide effector molecule of *Toxoplasma gondii*, in liver diseases in model mice. *Cell Mol Immunol* 17, 788–790. doi: 10.1038/s41423-020-0422-y.

Cañón-Franco, W. A., López-Orozco, N., Gómez-Marín, J. E., and Dubey, J. P. (2014). An overview of seventy years of research (1944 - 2014) on toxoplasmosis in Colombia, South America. *Parasit Vectors* 7. doi: 10.1186/1756-3305-7-427.

Cao, S., Yang, J., Fu, J., Chen, H., and Jia, H. (2021). The dissection of SNAREs reveals key factors for vesicular trafficking to the endosome-like compartment and apicoplast via the secretory system in *Toxoplasma gondii. mBio* 12. doi: 10.1128/mBio.01380-21.

Carme, B., Demar, M., Ajzenberg, D., & Dardé, M. L. (2009). Severe acquired toxoplasmosis caused by wild cycle of *Toxoplasma gondii*, French Guiana. *Emerging infectious diseases*, *15*(4), 656–658. doi:10.3201/eid1504.081306.

Carter, C. J. (2013). Toxoplasmosis and Polygenic Disease Susceptibility Genes: Extensive *Toxoplasma gondii* Host/Pathogen Interactome Enrichment in Nine Psychiatric or Neurological Disorders. *J Pathog* 2013, 1–29. doi: 10.1155/2013/965046.

Cerávolo, I. P., Chaves, A. C. L., Bonjardim, C. A., Sibley, D., Romanha, A. J., and Gazzinelli, R. T. (1999). Replication of *Toxoplasma gondii*, but not *Trypanosoma cruzi*, is regulated in human fibroblasts activated with gamma interferon: Requirement of a functional JAK/STAT pathway. *Infect Immun* 67, 2233–2240. doi: 10.1128/IAI.67.5.2233-2240.1999.

Chew, W. K., Segarra, I., Ambu, S., and Mak, J. W. (2012). Significant reduction of brain cysts caused by *Toxoplasma gondii* after treatment with spiramycin coadministered with metronidazole in a mouse model of chronic toxoplasmosis. *Antimicrob Agents Chemother* 56, 1762–1768. doi: 10.1128/AAC.05183-11.

Chiebao, D. P., Bartley, P. M., Chianini, F., Black, L. E., Burrells, A., Pena, H. F. J., et al. (2021). Early immune responses and parasite tissue distribution in mice experimentally infected with oocysts of either archetypal or non-archetypal genotypes of *Toxoplasma gondii*. *Parasitology* 148, 464–476. doi: 10.1017/S0031182020002346.

Cole, R. A., Lindsay, D. S., Howe, D. K., Roderick, C. L., Dubey, J. P., Thomas, N. J., & Baeten, L. A. (2000). Biological and molecular characterizations of *Toxoplasma gondii* strains obtained from southern sea otters (*Enhydra lutris nereis*). *The Journal of parasitology*, *86*(3), 526–530. doi:10.1645/0022-3395(2000)086[0526:BAMCOT]2.0.CO;2.

Conrad, P. A., Miller, M. A., Kreuder, C., James, E. R., Mazet, J., Dabritz, H., et al. (2005). Transmission of *Toxoplasma*: clues from the study of sea otters as sentinels of *Toxoplasma gondii* flow into the marine environment. *Int J Parasitol* 35, 1155–1168. doi: 10.1016/J.IJPARA.2005.07.002.

Cook, A. J., Gilbert, R. E., Buffolano, W., Zufferey, J., Petersen, E., Jenum, P. A., Foulon, W., Semprini, A. E., & Dunn, D. T. (2000). Sources of *toxoplasma* infection in pregnant women: European multicentre case-control study. European Research Network on Congenital Toxoplasmosis. *BMJ (Clinical research ed.)*, *321*(7254), 142–147. doi: 10.1136/bmj.321.7254.142.

Costa, J. M., Pautas, C., Ernault, P., Foulet, F., Cordonnier, C., & Bretagne, S. (2000). Real-time PCR for diagnosis and follow-up of *Toxoplasma* reactivation after allogeneic stem cell transplantation using fluorescence resonance energy transfer hybridization probes. *Journal of clinical microbiology*, *38*(8), 2929–2932. doi: 10.1128/JCM.38.8.2929-2932.2000.

de Aquino, T. M., Liesen, A. P., da Silva, R. E. A., Lima, V. T., Carvalho, C. S., de Faria, A. R., et al. (2008). Synthesis, anti-*Toxoplasma gondii* and antimicrobial activities of benzaldehyde 4-phenyl-3-thiosemicarbazones and 2-[(phenylmethylene)hydrazono]-4-oxo-3-phenyl-5-thiazolidineacetic acids. *Bioorg Med Chem* 16, 446–456. doi: 10.1016/j.bmc.2007.09.025.

de-la-Torre, A., Sauer, A., Pfaff, A. W., Bourcier, T., Brunet, J., Speeg-Schatz, C., et al. (2013). Severe South American Ocular Toxoplasmosis Is Associated with Decreased Ifn-γ/Il-17a and Increased Il-6/Il-13 Intraocular Levels. *PLoS Negl Trop Dis* 7. doi: 10.1371/journal.pntd.0002541.

Deng, H., Huang, X., Jin, C., Jin, C. M., and Quan, Z. S. (2020). Synthesis, *in vitro* and *in vivo* biological evaluation of dihydroartemisinin derivatives with potential anti-*Toxoplasma gondii* agents. *Bioorg Chem* 94, 103467. doi: 10.1016/J.BIOORG.2019.103467.

Desiatkina, O., Boubaker, G., Anghel, N., Amdouni, Y., Hemphill, A., Furrer, J., et al. (2022a). Synthesis, Photophysical Properties and Biological Evaluation of New Conjugates BODIPY: Dinuclear Trithiolato-Bridged Ruthenium(II)-Arene Complexes. *ChemBioChem* 23. doi: 10.1002/cbic.202200536.

Desiatkina, O., Mösching, M., Anghel, N., Boubaker, G., Amdouni, Y., Hemphill, A., et al. (2022b). New Nucleic Base-Tethered Trithiolato-Bridged Dinuclear Ruthenium(II)-Arene Compounds: Synthesis and Antiparasitic Activity. *Molecules* 27. doi: 10.3390/molecules27238173.

Dixon, S. E., Stilger, K. L., Elias, E. V., Naguleswaran, A., and Sullivan, W. J. (2010). A decade of epigenetic research in *Toxoplasma gondii*. *Mol Biochem Parasitol* 173, 1–9. doi: 10.1016/j.molbiopara.2010.05.001.

Djurkovic-Djakovic, O., Milenković, V., Nikolić, A., Bobić, B., and Grujić, J. (2002). Efficacy of atovaquone combined with clindamycin against murine infection with a cystogenic (Me49) strain of *Toxoplasma gondii*. *Journal of Antimicrobial Chemotherapy* 50, 981–987. doi: 10.1093/JAC/DKF251.

Doggett, J. S., Nilsen, A., Forquer, I., Wegmann, K. W., Jones-Brando, L., Yolken, R. H., et al. (2012). Endochin-like quinolones are highly efficacious against acute and latent experimental toxoplasmosis. *Proc Natl Acad Sci U S A* 109, 15936–15941. doi: 10.1073/PNAS.1208069109.

Doggett, J. S., Ojo, K. K., Fan, E., Maly, D. J., and Van Voorhis, W. C. (2014). Bumped kinase inhibitor 1294 treats established *Toxoplasma gondii* infection. *Antimicrob Agents Chemother* 58, 3547–3549. doi: 10.1128/AAC.01823-13.

Doliwa, C., Escotte-Binet, S., Aubert, D., Velard, F., Schmid, A., Geers, R., et al. (2013). Induction of sulfadiazine resistance *in vitro* in *Toxoplasma gondii*. *Exp Parasitol* 133, 131–136. doi: 10.1016/j.exppara.2012.11.019.

Dominelli, B., Correia, J. D. G., and Kühn, F. E. (2018). Medicinal Applications of Gold(I/III)-Based Complexes Bearing N-Heterocyclic Carbene and Phosphine Ligands. *J Organomet Chem* 866, 153–164. doi: 10.1016/j.jorganchem.2018.04.023.

Dou, Z., and Carruthers, V. B. (2011). Cathepsin proteases in *Toxoplasma gondii*. *Adv Exp Med Biol* 712, 49–61. doi: 10.1007/978-1-4419-8414-2_4.

Dubey, J.P., and Frenkel J. K. (1972). Cyst-Induced Toxoplasmosis in Cats. *J Protozool* 19(1), 155–177.

Dubey, J. P. (1997). Bradyzoite-induced murine toxoplasmosis: Stage conversion, pathogenesis, and tissue cyst formation in mice fed bradyzoites of different strains of *Toxoplasma gondii*. *Journal of Eukaryotic Microbiology* 44, 592–602. doi: 10.1111/j.1550-7408.1997.tb05965.x.

Dubey, J. P., Lindsay, D. S., and Speer, C. A. (1998). Structures of *Toxoplasma gondii* tachyzoites, bradyzoites, and sporozoites and biology and development of tissue cysts. *Clinical microbiology reviews*, *11*(2), 267–299. doi:10.1128/CMR.11.2.267.

Dubey, J. P. (2009). Toxoplasmosis in sheep--the last 20 years. *Vet Parasitol* 163, 1–14. doi: 10.1016/J.VETPAR.2009.02.026.

Dubey, J. P., Velmurugan, G. V., Rajendran, C., Yabsley, M. J., Thomas, N. J., Beckmen, K. B., et al. (2011). Genetic characterisation of *Toxoplasma gondii* in wildlife from North America revealed widespread and high prevalence of the fourth clonal type. *Int J Parasitol* 41, 1139–1147. doi: 10.1016/j.ijpara.2011.06.005.

Dubey, J. P., Cerqueira-Cézar, C. K., Murata, F. H. A., Kwok, O. C. H., Yang, Y. R., and Su, C. (2020). All about toxoplasmosis in cats: the last decade. *Vet Parasitol* 283, 109145. doi: 10.1016/J.VETPAR.2020.109145.

Dubey, J. P. (2021a). Toxoplasmosis of Animals and Humans, Third edition. CRC Press.

Dubey, J. P. (2021b). Outbreaks of clinical toxoplasmosis in humans: five decades of personal experience, perspectives and lessons learned. *Parasit Vectors* 14, 1–12. doi: 10.1186/S13071-021-04769-4/TABLES/3.

Dubey, J. P., Murata, F. H. A., Cerqueira-Cézar, C. K., Kwok, O. C. H., and Villena, I. (2021). Congenital toxoplasmosis in humans: An update of worldwide rate of congenital infections. *Parasitology*. doi: 10.1017/S0031182021001013.

Ducournau, C., Cantin, P., Alerte, V., Quintard, B., Popelin-Wedlarski, F., Wedlarski, R., et al. (2023). Vaccination of squirrel monkeys (*Saimiri* spp.) with nanoparticle-based *Toxoplasma gondii* antigens: new hope for captive susceptible species. *Int J Parasitol* 53, 333–346. doi: 10.1016/J.IJPARA.2023.02.003.

Dumètre, A., and Dardé, M. L. (2003). How to detect *Toxoplasma gondii* oocysts in environmental samples? *FEMS Microbiol Rev* 27, 651–661. doi: 10.1016/S0168-6445(03)00071-8.

Dunay, I. R., Wing, C. C., Haynes, R. K., and Sibley, L. D. (2009). Artemisone and artemiside control acute and reactivated toxoplasmosis in a murine model. *Antimicrob Agents Chemother* 53, 4450–4456. doi: 10.1128/AAC.00502-09.

Dunay, I. R., Gajurel, K., Dhakal, R., Liesenfeld, O., & Montoya, J. G. (2018). Treatment of Toxoplasmosis: Historical Perspective, Animal Models, and Current Clinical Practice. *Clinical microbiology reviews*, *31*(4), e00057-17. doi:10.1128/CMR.00057-17.

Dzitko, K., Paneth, A., Plech, T., Pawełczyk, J., Stączek, P., Stefańska, J., et al. (2014). 1,4-disubstituted thiosemicarbazide derivatives are potent inhibitors of *Toxoplasma gondii* proliferation. *Molecules* 19, 9926–9943. doi: 10.3390/molecules19079926.

Elmore, S. A., Jenkins, E. J., Huyvaert, K. P., Polley, L., Root, J. J., & Moore, C. G. (2012). *Toxoplasma gondii* in circumpolar people and wildlife. *Vector borne and zoonotic diseases (Larchmont, N.Y.)*, *12*(1), 1–9. doi: 10.1089/vbz.2011.0705.

Faa, G., Gerosa, C., Fanni, D., Lachowicz, J. I., and Nurchi, V. M. (2017). Gold - Old Drug with New Potentials. *Curr Med Chem* 25, 75–84. doi: 10.2174/0929867324666170330091438.

Fasquelle, F., Scuotto, A., Vreulx, A. C., Petit, T., Charpentier, T., and Betbeder, D. (2023). Nasal vaccination of six squirrel monkeys (*Saimiri sciureus*): Improved immunization protocol against *Toxoplasma gondii* with a nanoparticle-born vaccine. *Int J Parasitol Parasites Wildl* 22, 69. doi: 10.1016/J.IJPPAW.2023.09.002.

Ferguson, D. J. P., Huskinson-Markt, J., Araujot, F. G., and Remingtontt, J. S. (1994). An ultrastructural study of the effect of treatment with atovaquone in brains of mice chronically infected with the ME49 strain of *Toxoplasma gondii*. *International journal of experimental pathology*, *75*(2), 111–116.

Fernández, L., and Hancock, R. E. W. (2012). Adaptive and mutational resistance: Role of porins and efflux pumps in drug resistance. *Clin Microbiol Rev* 25, 661–681. doi: 10.1128/CMR.00043-12.

Frueh, L., Li, Y., Mather, M. W., Li, Q., Pou, S., Nilsen, A., et al. (2017). Alkoxycarbonate Ester Prodrugs of Preclinical Drug Candidate ELQ-300 for Prophylaxis and Treatment of Malaria. *ACS Infect Dis* 3, 728–735. doi: 10.1021/acsinfecdis.7b00062.

Fu, J., Zhao, L., Yang, J., Chen, H., Cao, S., and Jia, H. (2023). An unconventional SNARE complex mediates exocytosis at the plasma membrane and vesicular fusion at the apical annuli in *Toxoplasma gondii*. *PLoS Pathog* 19. doi: 10.1371/journal.ppat.1011288.

Gabriël, S., Dorny, P., Saelens, G., and Dermauw, V. (2023). Foodborne Parasites and Their Complex Life Cycles Challenging Food Safety in Different Food Chains. *Foods* 12. doi: 10.3390/foods12010142.

Gao, X., Wang, H., Wang, H., Qin, H., and Xiao, J. (2016). Land use and soil contamination with *Toxoplasma gondii* oocysts in urban areas. *Sci Total Environ* 568, 1086–1091. doi: 10.1016/J.SCITOTENV.2016.06.165.

Gazzonis, A. L., Villa, L., Riehn, K., Hamedy, A., Minazzi, S., Olivieri, E., et al. (2018). Occurrence of selected zoonotic food-borne parasites and first molecular identification of *Alaria alata* in wild boars (*Sus scrofa*) in Italy. *Parasitol Res* 117, 2207–2215. doi: 10.1007/S00436-018-5908-5/TABLES/2.

Gc, K., To, D., Jayalath, K., and Abeysirigunawardena, S. (2019). Discovery of a novel small molecular peptide that disrupts helix 34 of bacterial ribosomal RNA. *RSC Adv* 9, 40268–40276. doi: 10.1039/c9ra07812f.

Ghasemi, M., Turnbull, T., Sebastian, S., and Kempson, I. (2021). The mtt assay: Utility, limitations, pitfalls, and interpretation in bulk and single-cell analysis. *Int J Mol Sci* 22. doi: 10.3390/ijms222312827.

Gilbert, R. E., Freeman, K., Lago, E. G., Bahia-Oliveira, L. M. G., Tan, H. K., Wallon, M., et al. (2008). Ocular sequelae of congenital toxoplasmosis in Brazil compared with Europe. *PLoS Negl Trop Dis* 2. doi: 10.1371/JOURNAL.PNTD.0000277.

Gomes, M. A. G. B., Carvalho, L. P., Rocha, B. S., Oliveira, R. R., De Melo, E. J. T., and Maria, E. J. (2013). Evaluating anti-*Toxoplasma gondii* activity of new serie of phenylsemicarbazone and phenylthiosemicarbazones *in vitro*. *Med Chem Research* 22, 3574–3580. doi: 10.1007/s00044-012-0347-9.

Gov, L., Karimzadeh, A., Ueno, N., and Lodoen, M. B. (2013). Human innate immunity to *Toxoplasma gondii* is mediated by host caspase-1 and ASC and parasite GRA15. *mBio* 4. doi: 10.1128/MBIO.00255-13/ASSET/0526F1FB-E4ED-4E64-9ED8-319FF46A3418/ASSETS/GRAPHIC/MBO0041315580006.JPEG.

Gov, L., Schneider, C. A., Lima, T. S., Pandori, W., and Lodoen, M. B. (2017). NLRP3 and Potassium Efflux Drive Rapid IL-1β Release from Primary Human Monocytes during *Toxoplasma gondii* Infection. *The Journal of Immunology* 199, 2855–2864. doi: 10.4049/JIMMUNOL.1700245.

Grover, A., and Benet, L. Z. (2009). Effects of drug transporters on volume of distribution. *AAPS Journal* 11, 250–261. doi: 10.1208/s12248-009-9102-7.

Ha, S. W., Hwang, K., Jin, J., Cho, A. S., Kim, T. Y., Hwang, S. Il, et al. (2019). Ultrasound-sensitizing nanoparticle complex for overcoming the blood-brain barrier: An effective drug delivery system. *Int J Nanomedicine* 14, 3743–3752. doi: 10.2147/IJN.S193258.

Hall, I. H., Lackey, C. B., Kistler, T. D., Durham, R. W., Jr, Jouad, E. M., Khan, M., Thanh, X. D., Djebbar-Sid, S., Benali-Baitich, O., & Bouet, G. M. (2000). Cytotoxicity of copper and cobalt complexes of furfural

semicarbazone and thiosemicarbazone derivatives in murine and human tumor cell lines. *Die Pharmazie*, *55*(12), 937–941.

Hänggeli, K. P. A., Hemphill, A., Müller, N., Schimanski, B., Olias, P., Müller, J., et al. (2022). Single- and duplex TaqMan-quantitative PCR for determining the copy numbers of integrated selection markers during sitespecific mutagenesis in *Toxoplasma gondii* by CRISPR-Cas9. *PLoS One* 17. doi: 10.1371/journal.pone.0271011.

Hänggeli, K. P. A., Hemphill, A., Müller, N., Heller, M., Uldry, A. C., Braga-Lagache, S., et al. (2023). Comparative Proteomic Analysis of *Toxoplasma gondii* RH Wild-Type and Four SRS29B (SAG1) Knock-Out Clones Reveals Significant Differences between Individual Strains. *Int J Mol Sci* 24. doi: 10.3390/ijms241310454.

Hill, D. E., Chirukandoth, S., and Dubey, J. P. (2005). Biology and epidemiology of *Toxoplasma gondii* in man and animals. *Anim Health Res Rev* 6, 41–61. doi: 10.1079/ahr2005100.

Hill, D. E., and Dubey, J. P. (2013). *Toxoplasma gondii* prevalence in farm animals in the United States. *Int J Parasitol* 43, 107–113. doi: 10.1016/J.IJPARA.2012.09.012.

Hill, D.E., and Dubey, J.P. (2014). Toxoplasmosis: Reston, Va., U.S. Geological Survey Circular 1389, 84 p., 1 appendix. doi:10.3133/cir1389.

Hofflin, J. M., and Remington, J. S. (1987). Clindamycin in a Murine Model of Toxoplasmic Encephalitis. *Antimicrob Agents Chemother*, 492–496. doi: 10.1128/AAC.31.4.492.

Houngue, H.D., Aguida, B.S., Kassehin, U.C., Poupaert, J. H., Gbaguidi, F.A. & Hountondji, C. Biological evaluation of a series of thiosemicarbazones targeting the large subunit ribosomal protein eL42 from human 80s ribosomes. *MOJ Biorg Org Chem*. 2017;1(6):189-198. DOI: 10.15406/mojboc.2017.01.00034.

Huang, S. Y., Cong, W., Zhou, P., Zhou, D. H., Wu, S. M., Xu, M. J., Zou, F. C., Song, H. Q., & Zhu, X. Q. (2012). First report of genotyping of *Toxoplasma gondii* isolates from wild birds in China. *The Journal of parasitology*, *98*(3), 681–682. doi: 10.1645/GE-3038.1.

Huang, P. K., Jianping, C., Vasconcelos-Santos, D. V., Arruda, J. S. D., Dutta Majumder, P., Anthony, E., Ganesh, S. K., Biswas, J., Ling, H. S., Teoh, S. C., & Agrawal, R. (2018). Ocular Toxoplasmosis in Tropical Areas: Analysis and Outcome of 190 Patients from a Multicenter Collaborative Study. *Ocular immunology and inflammation*, *26*(8), 1289–1296. doi:10.1080/09273948.2017.1367407.

Huber, W., Von Heydebreck, A., Ultmann, H. S. ¨, Poustka, A., and Vingron, M. (2002). Variance stabilization applied to microarray data calibration and to the quantification of differential expression. *Bioinformatics (Oxford, England)*, *18 Suppl 1*, S96–S104. doi:10.1093/bioinformatics/18.suppl_1.s96.

Imhof, D., Anghel, N., Winzer, P., Balmer, V., Ramseier, J., Hänggeli, K., et al. (2021). *In vitro* activity, safety and *in vivo* efficacy of the novel bumped kinase inhibitor BKI-1748 in non-pregnant and pregnant mice experimentally infected with *Neospora caninum* tachyzoites and *Toxoplasma gondii* oocysts. *Int J Parasitol Drugs Drug Resist* 16, 90–101. doi: 10.1016/j.ijpddr.2021.05.001.

Jiao, L., Liu, Y., Yu, X. Y., Pan, X., Zhang, Y., Tu, J., et al. (2023). Ribosome biogenesis in disease: new players and therapeutic targets. *Signal Transduct Target Ther* 8. doi: 10.1038/s41392-022-01285-4.

Jin, C. M., Kaewintajuk, K., Jiang, J. H., Jeong, W. J., Kamata, M., KIM, H. S., et al. (2009). *Toxoplasma gondii*: A simple high-throughput assay for drug screening in vitro. *Exp Parasitol* 121, 132–136. doi: 10.1016/J.EXPPARA.2008.10.006.

Johnson, C. K., Tinker, M. T., Estes, J. A., Conrad, P. A., Staedler, M., Miller, M. A., et al. (2009). Prey choice and habitat use drive sea otter pathogen exposure in a resource-limited coastal system. *Proc Natl Acad Sci U S A* 106, 2242–2247. doi: 10.1073/PNAS.0806449106.

Kammers, K., Cole, R. N., Tiengwe, C., and Ruczinski, I. (2015). Detecting significant changes in protein abundance. *EuPA Open Proteom* 7, 11–19. doi: 10.1016/j.euprot.2015.02.002.

Kazemi Arababadi, M., Abdollahi, S. H., Ramezani, M., and Zare-Bidaki, M. (2024). A Review of Immunological and Neuropsychobehavioral Effects of Latent Toxoplasmosis on Humans. *Parasite Immunol* 46, e13060. doi: 10.1111/pim.13060.

Khan, A. M., Korzeniowska, B., Gorshkov, V., Tahir, M., Schrøder, H., Skytte, L., et al. (2019). Silver nanoparticle-induced expression of proteins related to oxidative stress and neurodegeneration in an in vitro human blood-brain barrier model. *Nanotoxicology* 13, 221–239. doi: 10.1080/17435390.2018.1540728.

Khan, T., Raza, S., and Lawrence, A. J. (2022). Medicinal Utility of Thiosemicarbazones with Special Reference to Mixed Ligand and Mixed Metal Complexes: A Review. *Russian Journal of Coordination Chemistry/Koordinatsionnaya Khimiya* 48, 877–895. doi: 10.1134/S1070328422600280.

Konstantinovic, N., Guegan, H., Stäjner, T., Belaz, S., and Robert-Gangneux, F. (2019). Treatment of toxoplasmosis: Current options and future perspectives. *Food Waterborne Parasitol* 15. doi: 10.1016/j.fawpar.2019.e00036.

Krchniakova, M., Paukovcekova, S., Chlapek, P., Neradil, J., Skoda, J., and Veselska, R. (2022). Thiosemicarbazones and selected tyrosine kinase inhibitors synergize in pediatric solid tumors: NDRG1 upregulation and impaired prosurvival signaling in neuroblastoma cells. *Front Pharmacol* 13. doi: 10.3389/fphar.2022.976955.

Kropf, C., Debache, K., Rampa, C., Barna, F., Schorer, M., Stephens, C. E., et al. (2012). The adaptive potential of a survival artist: Characterization of the *in vitro* interactions of *Toxoplasma gondii* tachyzoites with di-cationic compounds in human fibroblast cell cultures. *Parasitology* 139, 208–220. doi: 10.1017/S0031182011001776.

Leggett, H. C., Benmayor, R., Hodgson, D. J., and Buckling, A. (2013). Experimental evolution of adaptive phenotypic plasticity in a parasite. *Current Biology* 23, 139–142. doi: 10.1016/j.cub.2012.11.045.

Lehmann, T., Marcet, P. L., Graham, D. H., Dahl, E. R., and Dubey, J. P. (2006). Globalization and the population structure of *Toxoplasma gondii*. *PNAS* 103, 11423–11428. doi: 10.1073/pnas.0601438103.

Lima, T. S., Gov, L., and Lodoen, M. B. (2018). Evasion of human neutrophil-mediated host defense during *Toxoplasma gondii* infection. *mBio* 9. doi: 10.1128/MBIO.02027-17/SUPPL_FILE/MBO001183713SF4.PDF.

Lima, T. S., and Lodoen, M. B. (2019). Mechanisms of human innate immune evasion by *Toxoplasma gondii. Front Cell Infect Microbiol* 9. doi: 10.3389/fcimb.2019.00103.

Linciano, P., Moraes, C. B., Alcantara, L. M., Franco, C. H., Pascoalino, B., Freitas-Junior, L. H., et al. (2018). Aryl thiosemicarbazones for the treatment of trypanosomatidic infections. *Eur J Med Chem* 146, 423–434. doi: 10.1016/j.ejmech.2018.01.043.

Lindsay, D. S., and Dubey, J. P. (2020). Neosporosis, Toxoplasmosis, and Sarcocystosis in Ruminants: An Update. *Veterinary Clinics of North America - Food Animal Practice* 36, 205–222. doi: 10.1016/j.cvfa.2019.11.004.

Liu, Y., Lu, Y., Xu, Z., Ma, X., Chen, X., and Liu, W. (2022). Repurposing of the gold drug auranofin and a review of its derivatives as antibacterial therapeutics. *Drug Discov Today* 27, 1961–1973. doi: 10.1016/j.drudis.2022.02.010.

Loo, C. S. N., Lam, N. S. K., Yu, D., Su, X. Z., and Lu, F. (2017). Artemisinin and its derivatives in treating protozoan infections beyond malaria. *Pharmacol Res* 117, 192–217. doi: 10.1016/J.PHRS.2016.11.012.

Lourido, S., Shuman, J., Zhang, C., Shokat, K. M., Hui, R., and Sibley, L. D. (2010). Calcium-dependent protein kinase 1 is an essential regulator of exocytosis in Toxoplasma. *Nature 2010,* 465, 359–362. doi: 10.1038/nature09022.

Lourido, S., Jeschke, G. R., Turk, B. E., and Sibley, L. D. (2013). Exploiting the unique ATP-binding pocket of toxoplasma calcium-dependent protein kinase 1 to identify its substrates. *ACS Chem Biol* 8, 1155–1162. doi: 10.1021/CB400115Y.

Lüder, C. G. K., Lang, T., Beuerle, B., and Gross, U. (1998). Down-regulation of MHC class II molecules and inability to up-regulate class I molecules in murine macrophages after infection with *Toxoplasma gondii*. *Clin Exp Immunol*. doi: 10.1046/j.1365-2249.1998.00594.x.

Lüder, C. G. K. (2024). IFNs in host defence and parasite immune evasion during *Toxoplasma gondii* infections. *Front Immunol* 15. doi: 10.3389/fimmu.2024.1356216.

Martins-Duarte, E. S., Dubar, F., Lawton, P., Da Silva, C. F., Soeiro, M. D. N. C., De Souza, W., et al. (2015). Ciprofloxacin derivatives affect parasite cell division and increase the survival of mice infected with *Toxoplasma gondii*. *PLoS One* 10. doi: 10.1371/journal.pone.0125705.

Masopust, D., Sivula, C. P., and Jameson, S. C. (2017). Of Mice, Dirty Mice, and Men: Using Mice To Understand Human Immunology. *The Journal of Immunology* 199, 383–388. doi: 10.4049/jimmunol.1700453.

Mateus-Pinilla, N. E., Dubey, J. P., Choromanski, L., & Weigel, R. M. (1999). A field trial of the effectiveness of a feline *Toxoplasma gondii* vaccine in reducing *T. gondii* exposure for swine. *The Journal of parasitology*, *85*(5), 855–860.

McFadden, D. C., Seeber, F., and Boothroyd, J. C. (1997). Use of *Toxoplasma gondii* expressing beta-galactosidase for colorimetric assessment of drug activity *in vitro*. *Antimicrob Agents Chemother* 41, 1849–1853. doi: 10.1128/AAC.41.9.1849.

Mcfadden, D. C., Tomavo, S., Berry, E. A., Boothroyd, J. C., and Boothroyd, J. C. (2000). Characterization of cytochrome b from *Toxoplasma gondii* and Q o domain mutations as a mechanism of atovaquone-resistance. *Molecular and biochemical parasitology*, *108*(1), 1–12. doi: 10.1016/s0166-6851(00)00184-5.

Mercier, A., Devillard, S., Ngoubangoye, B., Bonnabau, H., Bañuls, A. L., Durand, P., et al. (2010). Additional haplogroups of *Toxoplasma gondii* out of Africa: Population structure and mouse-virulence of strains from Gabon. *PLoS Negl Trop Dis* 4. doi: 10.1371/journal.pntd.0000876.

Meshnick, S. R., Berry, E. A., Nett, J., Kazanjian, P., and Trumpower, B. (2001). The interaction of atovaquone with the *P. carinii* cytochrome bc1 complex. *J Eukaryot Microbiol* Suppl. doi: 10.1111/J.1550-7408.2001.TB00505.X.

Molina, D. A., Ramos, G. A., Zamora-Vélez, A., Gallego-López, G. M., Rocha-Roa, C., Gómez-Marin, J. E., et al. (2021). *In vitro* evaluation of new 4-thiazolidinones on invasion and growth of *Toxoplasma gondii*. *Int J Parasitol Drugs Drug Resist* 16, 129–139. doi: 10.1016/J.IJPDDR.2021.05.004.

Montazeri, M., Mehrzadi, S., Sharif, M., Sarvi, S., Tanzifi, A., Aghayan, S. A., et al. (2018). Drug resistance in *Toxoplasma gondii*. *Front Microbiol* 9. doi: 10.3389/fmicb.2018.02587.

Mose, J. M., Kagira, J. M., Kamau, D. M., Maina, N. W., Ngotho, M., and Karanja, S. M. (2020). A Review on the Present Advances on Studies of Toxoplasmosis in Eastern Africa. *Biomed Res Int* 2020. doi: 10.1155/2020/7135268.

Mosmann, T. (1983). Rapid colorimetric assay for cellular growth and survival: application to proliferation and cytotoxicity assays. *J Immunol Methods* 65, 55–63. doi: 10.1016/0022-1759(83)90303-4.

Müller, J., Wastling, J., Sanderson, S., Müller, N., and Hemphill, A. (2007). A novel *Giardia lamblia* nitroreductase, G1NR1, interacts with nitazoxanide and other thiazolides. *Antimicrob Agents Chemother* 51, 1979–1986. doi: 10.1128/AAC.01548-06.

Müller, J., Braga, S., Heller, M., and Müller, N. (2019a). Resistance formation to nitro drugs in *Giardia lamblia*: No common markers identified by comparative proteomics. *Int J Parasitol Drugs Drug Resist* 9, 112–119. doi: 10.1016/j.ijpddr.2019.03.002.

Müller, J., Manser, V., and Hemphill, A. (2019b). *In vitro* treatment of *Besnoitia besnoiti* with the naphtoquinone buparvaquone results in marked inhibition of tachyzoite proliferation, mitochondrial alterations and rapid adaptation of tachyzoites to increased drug concentrations. *Parasitology* 146, 112–120. doi: 10.1017/S0031182018000975.

Müller, J., Anghel, N., Imhof, D., Hänggeli, K., Uldry, A. C., Braga-Lagache, S., et al. (2022a). Common Molecular Targets of a Quinolone Based Bumped Kinase Inhibitor in *Neospora caninum* and *Danio rerio*. *Int J Mol Sci* 23. doi: 10.3390/ijms23042381.

Müller, J., Boubaker, G., Imhof, D., Hänggeli, K., Haudenschild, N., Uldry, A. C., et al. (2022b). Differential Affinity Chromatography Coupled to Mass Spectrometry: A Suitable Tool to Identify Common Binding Proteins of a Broad-Range Antimicrobial Peptide Derived from Leucinostatin. *Biomedicines* 10. doi: 10.3390/biomedicines10112675.

Müller, J., Schlange, C., Heller, M., Uldry, A. C., Braga-Lagache, S., Haynes, R. K., et al. (2023). Proteomic characterization of *Toxoplasma gondii* ME49 derived strains resistant to the artemisinin derivatives artemiside and artemisone implies potential mode of action independent of ROS formation. *Int J Parasitol Drugs Drug Resist* 21, 1–12. doi: 10.1016/j.ijpddr.2022.11.005.

Müller, J., Boubaker, G., Müller, N., Uldry, A. C., Braga-Lagache, S., Heller, M., et al. (2024). Investigating Antiprotozoal Chemotherapies with Novel Proteomic Tools—Chances and Limitations: A Critical Review. *Int J Mol Sci* 25. doi: 10.3390/ijms25136903.

Müller, J., and Hemphill, A. (2024). *In vitro* screening technologies for the discovery and development of novel drugs against *Toxoplasma gondii*. *Expert Opin Drug Discov* 19, 97–109. doi: 10.1080/17460441.2023.2276349.

Narasimhan, J., Joyce, B. R., Naguleswaran, A., Smith, A. T., Livingston, M. R., Dixon, S. E., et al. (2008). Translation regulation by eukaryotic initiation factor-2 kinases in the development of latent cysts in *Toxoplasma gondii*. *Journal of Biological Chemistry* 283, 16591–16601. doi: 10.1074/jbc.M800681200.

Nosrati, H., Tarantash, M., Bochani, S., Charmi, J., Bagheri, Z., Fridoni, M., et al. (2019). Glutathione (GSH) Peptide Conjugated Magnetic Nanoparticles As Blood-Brain Barrier Shuttle for MRI-Monitored Brain Delivery of Paclitaxel. *ACS Biomater Sci Eng* 5, 1677–1685. doi: 10.1021/acsbiomaterials.8b01420.

Ojo, K. K., Eastman, R. T., Vidadala, R., Zhang, Z., Rivas, K. L., Choi, R., et al. (2014). A specific inhibitor of PfCDPK4 blocks malaria transmission: chemical-genetic validation. *J Infect Dis* 209, 275–284. doi: 10.1093/INFDIS/JIT522.

Păunescu, E., Boubaker, G., Desiatkina, O., Anghel, N., Amdouni, Y., Hemphill, A., et al. (2021). The quest of the best – A SAR study of trithiolato-bridged dinuclear Ruthenium(II)-Arene compounds presenting antiparasitic properties. *Eur J Med Chem* 222. doi: 10.1016/j.ejmech.2021.113610.

Pelosi, G. (2010). Thiosemicarbazone Metal Complexes: From Structure to Activity. *The Open Crystallography Journal* 3, 16–28.

Perry, S. W., Norman, J. P., Barbieri, J., Brown, E. B., and Gelbard, H. A. (2011). Mitochondrial membrane potential probes and the proton gradient: A practical usage guide. *Biotechniques* 50, 98–115. doi: 10.2144/000113610.

Pfefferkorn, E. R. (1984). Interferon γ blocks the growth of *Toxoplasma gondii* in human fibroblasts by inducing the host cells to degrade tryptophan. *Proc Natl Acad Sci U S A* 81, 908–912. doi: 10.1073/PNAS.81.3.908.

Pfefferkorn, E. R., Borotz, S. E., & Nothnagel, R. F. (1992). *Toxoplasma gondii*: Characterization of a Mutant Resistant to Sulfonamides. *Experimental parasitology*, *74*(3), 261–270. doi:10.1016/0014-4894(92)90149-5.

Piketty, C., Derouin, F., Rouveix, B., and Pocidalo, J. J. (1990). *In vivo* assessment of antimicrobial agents against *Toxoplasma gondii* by quantification of parasites in the blood, lungs, and brain of infected mice. *Antimicrob Agents Chemother* 34, 1467–1472. doi: 10.1128/AAC.34.8.1467.

Pinto-Ferreira, F., Caldart, E. T., Pasquali, A. K. S., Mitsuka-Breganó, R., Freire, R. L., and Navarro, I. T. (2019). Patterns of transmission and sources of infection in outbreaks of human toxoplasmosis. *Emerg Infect Dis* 25, 2177–2182. doi: 10.3201/eid2512.181565.

Porter, S. B., & Sande, M. A. (1992). Toxoplasmosis of the central nervous system in the acquired immunodeficiency syndrome. *The New England journal of medicine*, *327*(23), 1643–1648. doi: 10.1056/NEJM199212033272306.

Radke, J. B., Worth, D., Hong, D., Huang, S., Sullivan, W. J., Wilson, E. H., et al. (2018). Transcriptional repression by ApiAP2 factors is central to chronic toxoplasmosis. *PLoS Pathog* 14. doi: 10.1371/journal.ppat.1007035.

Ramakrishnan, C., Maier, S., Walker, R. A., Rehrauer, H., Joekel, D. E., Winiger, R. R., et al. (2019). An experimental genetically attenuated live vaccine to prevent transmission of *Toxoplasma gondii* by cats. *Sci Rep*. doi: 10.1038/s41598-018-37671-8.

Ramseier, J., Imhof, D., Anghel, N., Hänggeli, K., Beteck, R. M., Balmer, V., et al. (2021). Assessment of the activity of decoquinate and its quinoline- o-carbamate derivatives against *Toxoplasma gondii in vitro* and in pregnant mice infected with *T. gondii* oocysts. *Molecules* 26. doi: 10.3390/molecules26216393.

Rastogi, S., Xue, Y., Quake, S. R., and Boothroyd, J. C. (2020). Differential impacts on host transcription by ROP and GRA effectors from the intracellular parasite *Toxoplasma gondii*. *mBio* 11, 1–26. doi: 10.1128/MBIO.00182-20.

Rengifo-Herrera, C., Ortega-Mora, L. M., Álvarez-García, G., Gómez-Bautista, M., García-Párraga, D., García-Peña, F. J., et al. (2012). Detection of *Toxoplasma gondii* antibodies in Antarctic pinnipeds. *Vet Parasitol* 190, 259–262. doi: 10.1016/J.VETPAR.2012.05.020.

Reynolds, M. G., Oh, J., and Roos, D. S. (2001). *In vitro* generation of novel pyrimethamine resistance mutations in the *Toxoplasma gondii* dihydrofolate reductase. *Antimicrob Agents Chemother* 45, 1271–1277. doi: 10.1128/AAC.45.4.1271-1277.2001.

Robert-Gangneux, F. (2014). It is not only the cat that did it: how to prevent and treat congenital toxoplasmosis. *J Infect* 68 Suppl 1. doi: 10.1016/J.JINF.2013.09.023.

Robert-Gangneux, F., and Dardé, M. L. (2012). Epidemiology of and diagnostic strategies for toxoplasmosis. *Clin Microbiol Rev* 25, 264–296. doi: 10.1128/CMR.05013-11.

Rosenberg, A., Luth, M. R., Winzeler, E. A., Behnke, M., and Sibley, L. D. (2019). Evolution of resistance in vitro reveals mechanisms of artemisinin activity in *Toxoplasma gondii*. *Proc Natl Acad Sci U S A* 116, 26881–26891. doi: 10.1073/PNAS.1914732116.

Rudra, P., Hurst-Hess, K., Lappierre, P., and Ghosha, P. (2018). High levels of intrinsic tetracycline resistance in mycobacterium abscessus are conferred by a tetracycline-modifying monooxygenase. *Antimicrob Agents Chemother* 62. doi: 10.1128/AAC.00119-18.

Rutaganira, F. U., Barks, J., Dhason, M. S., Wang, Q., Lopez, M. S., Long, S., et al. (2017). Inhibition of Calcium Dependent Protein Kinase 1 (CDPK1) by Pyrazolopyrimidine Analogs Decreases Establishment and Reoccurrence of Central Nervous System Disease by *Toxoplasma gondii*. *J Med Chem* 60, 9976–9989. doi: 10.1021/ACS.JMEDCHEM.7B01192.

Saeij J.P.J., Boyle J.P., Coller S., Taylor S., Sibley L.D., Brooke-Powell E.T., et al. (2006). Polymorphic Secreted Kinases Are Key Virulence Factors in Toxoplasmosis. *Science (New York, N.Y.)* 314, 1780–83. doi: 10.1126/science.1133690.

Saeij, J. P. J., Coller, S., Boyle, J. P., Jerome, M. E., White, M. W., and Boothroyd, J. C. (2007). *Toxoplasma* co-opts host gene expression by injection of a polymorphic kinase homologue. *Nature* 445, 324–327. doi: 10.1038/nature05395.

Sánchez-Sánchez, R., Ferre, I., Re, M., Ramos, J. J., Regidor-Cerrillo, J., Díaz, M. P., et al. (2019). Treatment with Bumped Kinase Inhibitor 1294 Is Safe and Leads to Significant Protection against Abortion and Vertical Transmission in Sheep Experimentally Infected with *Toxoplasma gondii* during Pregnancy. *Antimicrob Agents Chemother* 63. doi: 10.1128/AAC.02527-18.

Sánchez-Sánchez, R., Imhof, D., Hecker, Y. P., Ferre, I., Re, M., Moreno-Gonzalo, J., et al. (2024). An Early Treatment With BKI-1748 Exhibits Full Protection Against Abortion and Congenital Infection in Sheep Experimentally Infected With *Toxoplasma gondii*. *J Infect Dis* 229, 558–566. doi: 10.1093/INFDIS/JIAD470.

Sanjai, C., Hakkimane, S. S., Guru, B. R., and Gaonkar, S. L. (2024). A comprehensive review on anticancer evaluation techniques. *Bioorg Chem* 142, 106973. doi: 10.1016/J.BIOORG.2023.106973.

Scaccaglia, M., Pinelli, S., Manini, L., Ghezzi, B., Nicastro, M., Heinrich, J., et al. (2024). Gold(III) complexes with thiosemicarbazone ligands: insights into their cytotoxic effects on lung cancer cells. *J Inorg Biochem* 251, 112438. doi: 10.1016/j.jinorgbio.2023.112438.

Scaccaglia, M., Rega, M., Vescovi, M., Pinelli, S., Tegoni, M., Bacci, C., et al. (2022). Gallium(III)-pyridoxal thiosemicarbazone derivatives as nontoxic agents against Gram-negative bacteria. *Metallomics* 14. doi: 10.1093/mtomcs/mfac070.

Scallan, E., Hoekstra, R. M., Angulo, F. J., Tauxe, R. V., Widdowson, M. A., Roy, S. L., et al. (2011). Foodborne illness acquired in the United States--major pathogens. *Emerg Infect Dis* 17, 7–15. doi: 10.3201/EID1701.P11101.

Schlange, C., Müller, J., Imhof, D., Hänggeli, K. P. A., Boubaker, G., Ortega-Mora, L.-M., et al. (2023). Single and combination treatment of *Toxoplasma gondii* infections with a bumped kinase inhibitor and artemisone in vitro and with artemiside in experimentally infected mice. *Exp Parasitol*, 108655. doi: 10.1016/j.exppara.2023.108655.

Schlüter, D., Deckert, M., Hof, H., and Frei, A. K. (2001). *Toxoplasma gondii* Infection of Neurons Induces Neuronal Cytokine and Chemokine Production, but Gamma Interferon-and Tumor Necrosis Factor-Stimulated Neurons Fail To Inhibit the Invasion and Growth of *T. gondii*. *Infect Immun* 69, 7889–7893. doi: 10.1128/IAI.69.12.7889.

Schwanhüusser, B., Busse, D., Li, N., Dittmar, G., Schuchhardt, J., Wolf, J., et al. (2011). Global quantification of mammalian gene expression control. *Nature* 473, 337–342. doi: 10.1038/nature10098.

Seeber, F. (2000). An enzyme-release assay for the assessment of the lytic activities of complement or antimicrobial peptides on extracellular *Toxoplasma gondii*. *J Microbiol Methods* 39, 189–196. doi: 10.1016/S0167-7012(99)00117-7.

Semeraro, M., Boubaker, G., Scaccaglia, M., Müller, J., Vigneswaran, A., Hänggeli, K. P. A., et al. (2024). Transient Adaptation of *Toxoplasma gondii* to Exposure by Thiosemicarbazone Drugs That Target Ribosomal Proteins Is Associated with the Upregulated Expression of Tachyzoite Transmembrane Proteins and Transporters. *Int J Mol Sci* 25, 9067. doi: 10.3390/ijms25169067.

Shapira, S., Harb, O. S., Margarit, J., Matrajt, M., Han, J., Hoffmann, A., et al. (2005). Initiation and termination of NF-κB signaling by the intracellular protozoan parasite *Toxoplasma gondii*. *J Cell Sci* 118, 3501–3508. doi: 10.1242/JCS.02428.

Shubar, H. M., Lachenmaier, S., Heimesaat, M. M., Lohman, U., Mauludin, R., Mueller, R. H., et al. (2011). SDS-coated atovaquone nanosuspensions show improved therapeutic efficacy against experimental acquired and reactivated toxoplasmosis by improving passage of gastrointestinal and blood-brain barriers. *J Drug Target* 19, 114–124. doi: 10.3109/10611861003733995.

Shwab, E. K., Zhu, X. Q., Majumdar, D., Pena, H. F. J., Gennari, S. M., Dubey, J. P., et al. (2014). Geographical patterns of *Toxoplasma gondii* genetic diversity revealed by multilocus PCR-RFLP genotyping. *Parasitology* 141, 453–461. doi: 10.1017/S0031182013001844.

Sibley, L. D. (2003). *Toxoplasma gondii*: Perfecting an Intracellular Life Style. *Traffic*. doi: 10.1034/j.1600-0854.2003.00117.x.

Sibley L. D. (2011). Invasion and intracellular survival by protozoan parasites. *Immunological reviews*, *240*(1), 72–91. doi:10.1111/j.1600-065X.2010.00990.x.

Silva, J. C., Gorenstein, M. V., Li, G. Z., Vissers, J. P. C., and Geromanos, S. J. (2006). Absolute quantification of proteins by LCMSE: A virtue of parallel MS acquisition. *Molecular and Cellular Proteomics* 5, 144–156. doi: 10.1074/mcp.M500230-MCP200.

Silver, J. D., Ritchie, M. E., and Smyth, G. K. (2009). Microarray background correction: Maximum likelihood estimation for the normal-exponential convolution. *Biostatistics* 10, 352–363. doi: 10.1093/biostatistics/kxn042.

Smith, J. R., Ashander, L. M., Arruda, S. L., Cordeiro, C. A., Lie, S., Rochet, E., et al. (2021). Pathogenesis of ocular toxoplasmosis. *Prog Retin Eye Res* 81. doi: 10.1016/J.PRETEYERES.2020.100882.

Speer, C. A., & Dubey, J. P. (1998). Ultrastructure of early stages of infections in mice fed *Toxoplasma gondii* oocysts. *Parasitology*, *116*(1), 35–42. doi:10.1017/S0031182097001959.

Strimmer, K. (2008). A unified approach to false discovery rate estimation. *BMC Bioinformatics* 9. doi: 10.1186/1471-2105-9-303.

Sun, W., Sanderson, P. E., and Zheng, W. (2016). Drug combination therapy increases successful drug repositioning. *Drug Discov Today* 21, 1189–1195. doi: 10.1016/j.drudis.2016.05.015.

Tait, E. D., Jordan, K. A., Dupont, C. D., Harris, T. H., Gregg, B., Wilson, E. H., et al. (2010). Virulence of *Toxoplasma gondii* is associated with distinct dendritic cell responses and reduced numbers of activated CD8+ T cells. *J Immunol* 185, 1502. doi: 10.4049/JIMMUNOL.0903450.

Tartarelli, I., Tinari, A., Possenti, A., Cherchi, S., Falchi, M., Dubey, J. P., et al. (2020). During host cell traversal and cell-to-cell passage, *Toxoplasma gondii* sporozoites inhabit the parasitophorous vacuole and posteriorly release dense granule protein-associated membranous trails. *Int J Parasitol* 50, 1099–1115. doi: 10.1016/j.ijpara.2020.06.012.

Taylor S., Barragan A., Su C., Fux B., Fentress J., Tang K., et al. (2006). A Secreted Serine-Threonine Kinase Determines Virulence in the Eukaryotic Pathogen *Toxoplasma gondii*. *Science (1979)* 314, 1773–1776. doi: 10.1126/science.1135347.

Tedde, T., Marangi, M., Papini, R., Salza, S., Normanno, G., Virgilio, S., et al. (2019). *Toxoplasma gondii* and Other Zoonotic Protozoans in Mediterranean Mussel (*Mytilus galloprovincialis*) and Blue Mussel (*Mytilus edulis*): A Food Safety Concern? *J Food Prot* 82, 535–542. doi: 10.4315/0362-028X.JFP-18-157.

Tenter, A. M. (2009). *Toxoplasma gondii* in animals used for human consumption. *Memorias do Instituto Oswaldo Cruz*, *104*(2), 364–369. doi:10.1590/s0074-02762009000200033.

Theisen, T. C., and Boothroyd, J. C. (2022). Transcriptional signatures of clonally derived *Toxoplasma* tachyzoites reveal novel insights into the expression of a family of surface proteins. *PLoS One* 17. doi: 10.1371/journal.pone.0262374.

Tian, X., Li, J., Zamek-Gliszczynski, M. J., Bridges, A. S., Zhang, P., Patel, N. J., et al. (2007). Roles of P-glycoprotein, Bcrp, and Mrp2 in biliary excretion of spiramycin in mice. *Antimicrob Agents Chemother* 51, 3230–3234. doi: 10.1128/AAC.00082-07.

Timp, W., and Timp, G. (2020). Beyond mass spectrometry, the next step in proteomics. *Science advances*, *6*(2), eaax8978. doi:10.1126/sciadv.aax8978.

Torrey, E. F., & Yolken, R. H. (2013). *Toxoplasma* oocysts as a public health problem. *Trends in parasitology*, *29*(8), 380–384. doi: 10.1016/j.pt.2013.06.001.

Twigg, R. S. (1945). Oxidation-Reduction Aspects of Resazurin. *Nature 1945,* 155, 401–402. doi: 10.1038/155401a0.

Uldry, A. C., Maciel-Dominguez, A., Jornod, M., Buchs, N., Braga-Lagache, S., Brodard, J., et al. (2022). Effect of Sample Transportation on the Proteome of Human Circulating Blood Extracellular Vesicles. *Int J Mol Sci* 23. doi: 10.3390/ijms23094515.

Van Voorhis, W. C., Doggett, J. S., Parsons, M., Hulverson, M. A., Choi, R., Arnold, S. L. M., et al. (2017). Extended-spectrum antiprotozoal bumped kinase inhibitors: A review. *Exp Parasitol* 180, 71–83. doi: 10.1016/J.EXPPARA.2017.01.001.

Vidadala, R. S. R., Rivas, K. L., Ojo, K. K., Hulverson, M. A., Zambriski, J. A., Bruzual, I., et al. (2016). Development of an Orally Available and Central Nervous System (CNS) Penetrant *Toxoplasma gondii* Calcium-Dependent Protein Kinase 1 (TgCDPK1) Inhibitor with Minimal Human Ether-a-go-go-Related Gene (hERG) Activity for the Treatment of Toxoplasmosis. *J Med Chem* 59, 6531–6546. doi: 10.1021/ACS.JMEDCHEM.6B00760/SUPPL_FILE/JM6B00760_SI_002.CSV.

Virus, M. A., Ehrhorn, E. G., Lui, L. A. M., and Davis, P. H. (2021). Neurological and Neurobehavioral Disorders Associated with *Toxoplasma gondii* Infection in Humans. *J Parasitol Res* 2021. doi: 10.1155/2021/6634807.

Vismarra, A., Kramer, L., and Genchi, M. (2022). "Toxoplasmosis," in *Encyclopedia of Infection and Immunity*, (Elsevier), 724–740. doi: 10.1016/B978-0-12-818731-9.00034-3.

Walia, V., Kumar, R., and Mitra, A. (2015). Lipopolysaccharide and Concanavalin A Differentially Induce the Expression of Immune Response Genes in Caprine Monocyte Derived Macrophages. *Anim Biotechnol* 26, 298–303. doi: 10.1080/10495398.2015.1013112.

Wang, Q., and Sibley, L. D. (2020). Assays for Monitoring *Toxoplasma gondii* Infectivity in the Laboratory Mouse. *Methods Mol Biol* 2071, 99–116. doi: 10.1007/978-1-4939-9857-9_5.

Wang, Z. T., Verma, S. K., Dubey, J. P., and Sibley, L. D. (2017). The aromatic amino acid hydroxylase genes AAH1 and AAH2 in *Toxoplasma gondii* contribute to transmission in the cat. *PLoS Pathog* 13. doi: 10.1371/JOURNAL.PPAT.1006272.

White, N. J., Pukrittayakamee, S., Hien, T. T., Faiz, M. A., Mokuolu, O. A., and Dondorp, A. M. (2014). Malaria. *The Lancet* 383, 723–735. doi: 10.1016/S0140-6736(13)60024-0.

Xue, J., Jiang, W., Chen, Y., Gong, F., Wang, M., Zeng, P., et al. (2017). Thioredoxin reductase from *Toxoplasma gondii*: An essential virulence effector with antioxidant function. *FASEB Journal* 31, 4447–4457. doi: 10.1096/fj.201700008R.

Yu, F., Haynes, S. E., Teo, G. C., Avtonomov, D. M., Polasky, D. A., and Nesvizhskii, A. I. (2020). Fast Quantitative Analysis of timsTOF PASEF Data with MSFragger and IonQuant. *Molecular and Cellular Proteomics* 19, 1575–1585. doi: 10.1074/mcp.TIR120.002048.

Zarnke, R. L., Dubey, J. P., Kwok, O. C., & Ver Hoef, J. M. (1997). Serologic survey for *Toxoplasma gondii* in grizzly bears from Alaska. *Journal of wildlife diseases*, *33*(2), 267–270. doi:10.7589/0090-3558-33.2.267.

Zulpo, D. L., Headley, S. A., Biazzono, L., da Cunha, I. A. L., Igarashi, M., de Barros, L. D., et al. (2012). Oocyst shedding in cats vaccinated by the nasal and rectal routes with crude rhoptry proteins of *Toxoplasma gondii*. *Exp Parasitol* 131, 223–230. doi: 10.1016/J.EXPPARA.2012.04.006.

Zulpo, D. L., Igarashi, M., Sammi, A. S., Dos Santos, J. R., Sasse, J. P., Da Cunha, I. A. L., et al. (2017). rROP2 from *Toxoplasma gondii* as a potential vaccine against oocyst shedding in domestic cats. *Rev Bras Parasitol Vet* 26, 67–73. doi: 10.1590/S1984-29612017007.

8. Websites

1. CDC Toxoplasmosis 2024: www.cdc.gov/parasites/toxoplasmosis.
2. WHO, 2024: https://www.who.int/data/gho/data/indicators/indicator-details/GHO/foodborne-illnesses-per-100-000--2010-(median--95--uncertainty-interval).
3. EFSA-ECDC report, 2023: https://efsa.onlinelibrary.wiley.com/doi/epdf/10.2903/j.efsa.2023.8442.
4. MSD MANUAL: trimethoprim and sulfamethoxazole by Brian J. Werth, *PharmD, University of Washington School of Pharmacy Reviewed/Revised May 2024:* https://www.msdmanuals.com/professional/infectious-diseases/bacteria-and-antibacterial-medications/trimethoprim-and-sulfamethoxazole.

9. Appendix

Additional results of proteomics:

Supplementary Figure 1.

Protein-protein interaction network of proteins differentially upregulated (128 proteins) in C3- and C4-clones compared to *T. gondii* wildtype tachyzoites. A small cluster of ribosomal proteins was identified. The interaction network was created by the STRING knowledgebase and software tool from the Swiss Institute of Bioinformatics (www.expasy.org).

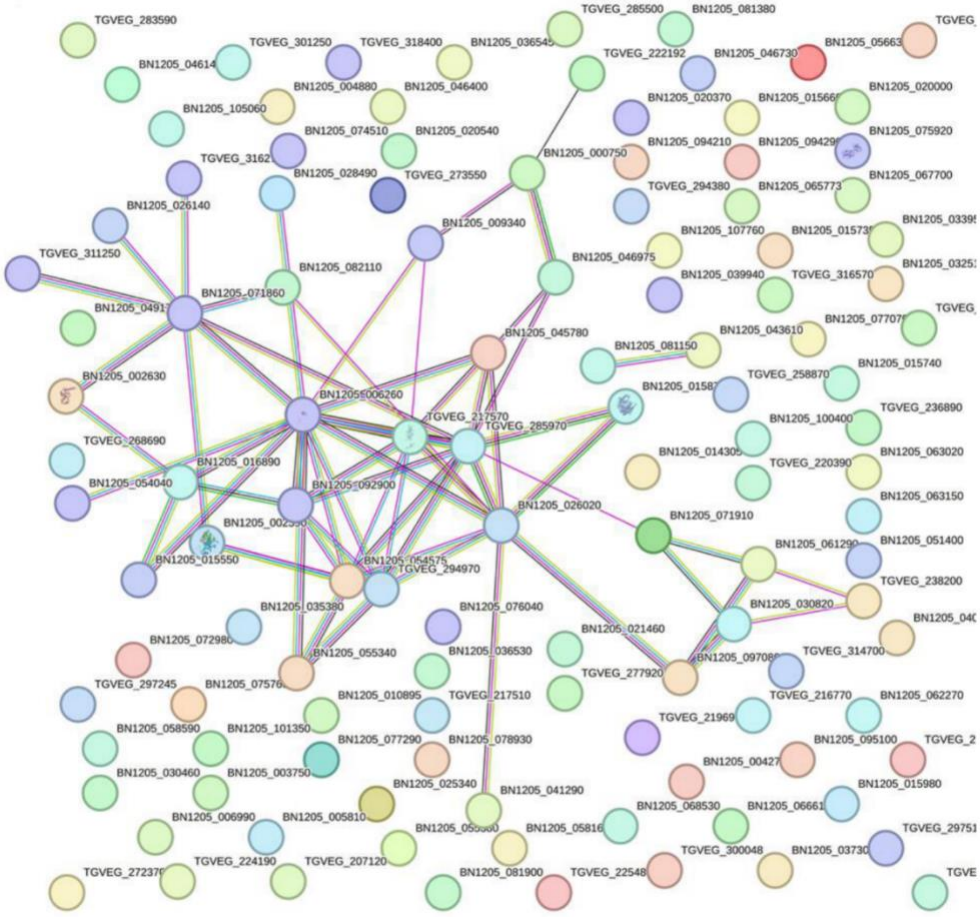

Supplementary Figure 2. Protein-protein interaction network of proteins differentially downregulated (59 proteins) in C3- and C4-clones compared to *T. gondii* wildtype tachyzoites. A unique network consisting of proteins involved in DNA replication and repair was revealed. The interaction network was created by the STRING knowledgebase and software tool from the Swiss Institute of Bioinformatics (www.expasy.org).

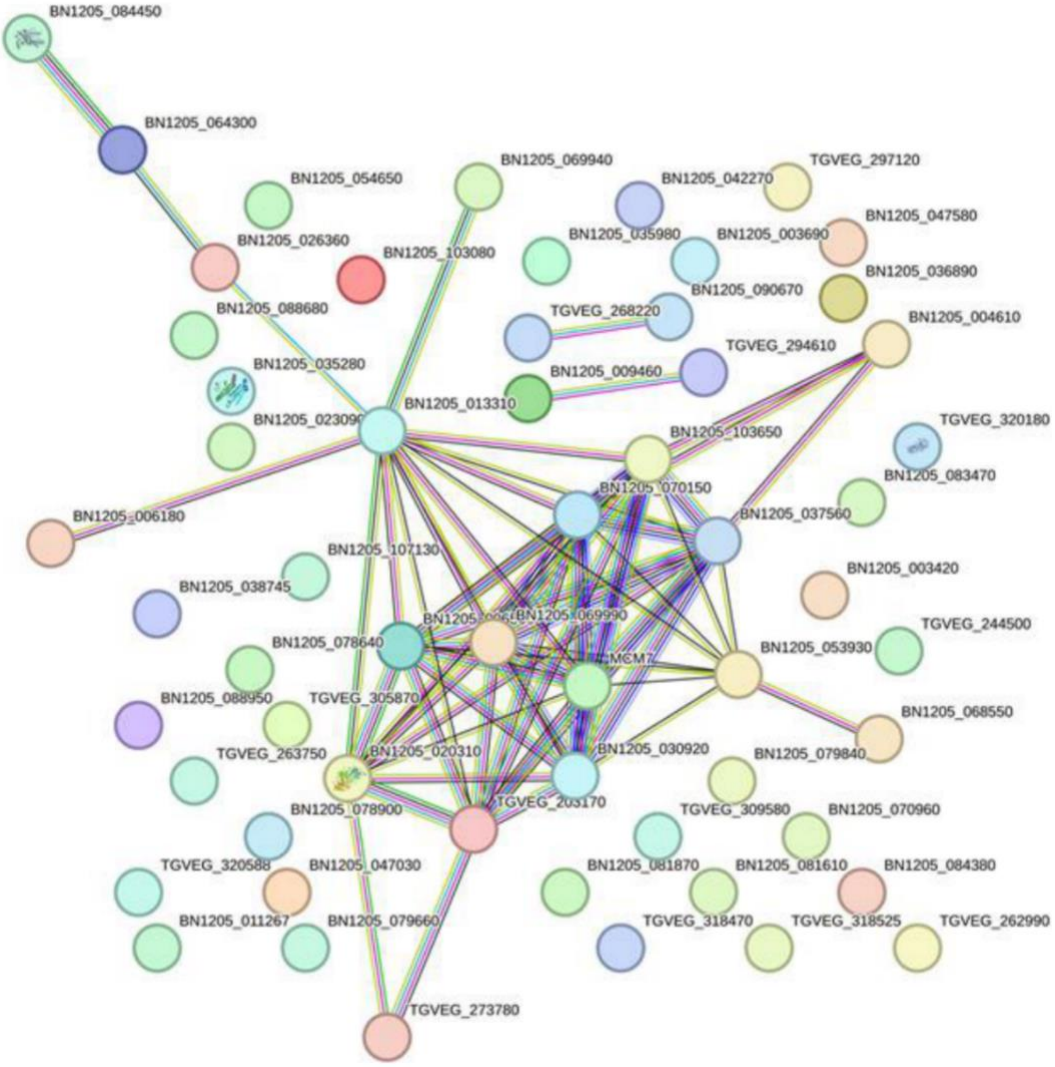

Extended results of DAC-MS and proteomics (table S1 and table S2) are available at this link:
https://univpr-my.sharepoint.com/:f:/g/personal/manuela_semeraro_unipr_it/EhA__q2jU7FKgSNKvw7w--gBoTotEYWnWjYnNfWrmApI2g?e=gX0HzO .

10. Aknowledgement

I would like to thank Dr. Mirco Scaccaglia and all the Operative Unit of Inorganic Chemistry (Department of Department of Chemistry, Life Sciences and Environmental Sustainability, University of Parma) for the synthesis of the compounds tested in this study;

Prof. Andrew Hemphill and his research group for the hospitality and the great opportunity I had to perform all of the experiments I described at his laboratory, at Institute of Parasitology (University of Bern, Switzerland);

Dr. Federico Armando and all the Operative Unit of Anatomical pathology (Department of Veterinary Medicine, University of Parma) for the histopathological analyses.

Prof. Manfred Heller and his own research group for the proteomic analyses conducted at the Proteomics and Mass Spectrometry Core Facility, (Department for BioMedical Research, University of Bern).